ENGINEERING-PDH.com
ONLINE CONTINUING EDUCATION

COLD-FORMED STEAL SEISMIC DESIGN RECOMMENDATIONS - VOL 1 OF 3

Main Category:	Civil Engineering
Sub Category:	Structural
Course #:	STR-117
Course Content:	140 pgs
PDH/CE Hours:	7

OFFICIAL COURSE/EXAM

(SEE INSTRUCTIONS ON NEXT PAGE)

WWW.ENGINEERING-PDH.COM
TOLL FREE (US & CA): 1-833-ENGR-PDH (1-833-364-7734)
SUPPORT@ENGINEERING-PDH.COM

STR-117 EXAM PREVIEW

- TAKE EXAM! -

Instructions:

- At your convenience and own pace, review the course material below. When ready, click "Take Exam!" above to complete the live graded exam. (Note it may take a few seconds for the link to pull up the exam.) You will be able to re-take the exam as many times as needed to pass.
- Upon a satisfactory completion of the course exam, which is a score of 70% or better, you will be provided with your course completion certificate. Be sure to download and print your certificates to keep for your records.

Exam Preview:

1. Ductile shear panel performance requires that the primary lateral load-resisting elements deform significantly while continuing to resist axial loads.
   a. True
   b. False
2. Each panel consists of a cold-formed steel frame with columns at the edges and single interior studs spaced __ in. on center. The top and bottom of the panels have a standard channel track.
   a. 8
   b. 12
   c. 16
   d. 24
3. According to the reference material, the plateau stress, given in Table 4-1 through Table 4-3, occurs when yielding takes place in the test specimen prior to strain hardening.
   a. True
   b. False
4. The procedure given in ASTM E 564-95, section 6.3.3 (ASTM 1995), specifies that a preload of approximately 10% of the estimated ultimate load should be applied first for _ minutes, then released for 5 minutes before reading the initial conditions.
   a. 5
   b. 10
   c. 15
   d. 20

5. The strength of even virgin ASTM A653 materials can vary significantly. According to the reference material, for Grade 50, the elongation (strain) may vary between 1 and 3 times the minimum specified (i.e., 12%), but is typically ___ times the minimum specified.
    a. 1 ¾
    b. 2 ¼
    c. 2 ½
    d. 2 ¾
6. Even with concerns about the appropriateness of the test procedures, some observations can be made from the Seattle District tests. These panels were designed for an ultimate load of __ kips.
    a. 13
    b. 20
    c. 30
    d. 40
7. According to the reference material, the widest available coiled steel sheet in the United States is 60 in.
    a. True
    b. False
8. Building codes provide response-modification coefficients, R, by which seismically induced lateral loads are divided. Design recommendations allow the use of R values between 2 and _ for light-framed walls.
    a. 3
    b. 4
    c. 7
    d. 8
9. Using able 7-1. Summary of test panel performance, which panel had the highest ultimate shear load while being tested with a monotonic load type?
    a. A2a
    b. C1a
    c. D2a (South)
    d. D2a (North)
10. According to the reference material, the HSS thickness will normally be greater than 0.125 in. and the weld thickness for the connection to the anchor will be less than the thickness of the column.
    a. True
    b. False

Contents

1 Introduction 1

1.1 Background 1
1.2 Issues in cold-formed steel design and research studies 2
1.2.1 Previous studies 3
1.2.2 Test setup issues for CFS panel design studies 5
1.2.3 Seattle District shear panel tests 8
1.3 Research problem 11
1.4 Objective 12
1.5 Approach 12
1.6 Scope 12
1.7 Mode of technology transfer 13

2 Shear Panel Configurations Considered 15

2.1 Panel A 16
2.2 Panel B 17
2.3 Panel C 18
2.4 Panel D 18
2.5 Panel E 18
2.6 Panel F 20
2.7 Panel G 20
2.8 Panel H 20

3 Shear Panel Design Philosophy and Analytical Model 23

3.1 Seismic-resistant building performance through ductile shear panel design 23
3.2 Cold-formed steel shear panel model 25

4 Material Properties and Coupon Test Results 30

4.1 Material properties 30
4.2 Coupon test results 32

5 Predicted Panel Response Based on Analytical Model and Coupon Test Results 40

5.1 Panel A1 44
5.2 Panel A2 44

5.3 Panel A3 45
5.4 Panel C1 45
5.5 Panel D1 46
5.6 Panel D2 47

6 Test Configuration, Procedures, and Instrumentation 48

6.1 Monotonic test protocol 50
6.2 Cyclic test protocol 50
6.3 Instrumentation 52

7 Performance of Test Panels 54

7.1 A1 test panel results 55
7.2 A2 test panel results 63
7.3 A3 test panel results 70
7.4 C1 test panel results 78
7.5 D1 test panel results 84
7.6 D2 test panel results 89

References 298

Appendix A: Prototype Barracks Building And Cold-Formed Steel Test Panel Drawings 303

Appendix B: Cold-Formed Steel Test Observations 317

Appendix C: Prototype Shear Panels for Cold-Formed Steel Seismic Design 330

Appendix D: Seismic Qualification Procedure and Acceptance Criteria for Other Shear Panel Configurations 332

1 Introduction

1.1 Background

Cold-formed steel partition-wall construction first emerged as a replacement for wood stud-wall construction. It is now being used extensively as the gravity- and lateral-load-resisting structural system for low-rise construction. The American Iron and Steel Institute (AISI) has published structural design guidance for cold-formed steel members. The first specification was adopted in 1946. The current specification, AISI S100-07 (AISI 2007), includes seven parts: A–General Provisions; B–Elements; C–Members; D–Structural Assemblies and Systems; E–Connections and Joints; F–Tests for Special Cases; and G–Design of Cold-Formed Steel Structural Members and Connections for Cyclic Loading (Fatigue). Section A2.3 presents steel ductility requirements; these are material requirements only, where the ratio of tensile to yield strength, $F_u/F_y \geq 1.08$, and total elongation must be at least 10% for a 2 in. gage length and 7% for an 8 in. gage length, based on coupon tests. However, the AISI specification does not include guidance to ensure that the structural system provides adequate ductility. ASCE/SEI 7-10 (ASCE 2010) gives a response-modification coefficient, R, of 6.5 for bearing wall systems, light-framed (cold-formed steel) walls sheathed with wood structural panels rated for shear resistance or steel sheets, and a value of 4 for light-framed (cold-formed steel) wall systems using flat-strap bracing. For building frame systems, light-framed (cold-formed steel) walls sheathed with wood structural panels rated for shear resistance or steel sheets, the R value is even greater, at 7. This coefficient represents the inherent over-strength, global ductility capacity, redundancy, and energy-dissipation capacity of lateral-force-resisting systems (ATC 1995, 1997). Seismically induced lateral loads are divided by this coefficient, recognizing the structure's ability to continue resisting lateral loads after yielding. Therefore, the structural system must be proportioned and detailed to ensure such a ductile response.

The U.S. Army Corps of Engineers (USACE) has observed detailing and construction practices in cold-formed steel construction that would prevent adequate ductile performance under seismic loading. Consequently, the Corps imposed a moratorium on using cold-formed steel as the primary structural system in its own construction projects. However, because cold-formed steel construction is a cost-effective approach, Headquarters, USACE, initiated an engineering study to investigate methods of cold-formed steel design and construction that will provide the required ductility. The results of that study led directly to the preparation of seismic design specifications and details for constructing shear wall panels using cold-formed steel. The first version of these ERDC-CERL design recommendations were published in 1998 in a document entitled *Design of Cold-Formed Load Bearing Steel Systems and Masonry Veneer/Steel Stud Walls* (TI 809-07, USACE 1998). Subsequently, that publication was updated with supporting studies and disseminated in two more forms. The issuance of those documents provided crucial design information that enabled the Corps to end the moratorium on cold-formed steel construction in its own projects.

The Corps of Engineers has withdrawn TI 809-07 and its successor documents in keeping with its practice of using established industry standards where feasible. However, complete documentation of the multi-year cold-formed steel studies executed for the Corps has never before been integrated and interpreted in a single ERDC-CERL technical report. This report presents in its entirety for the first time a fully updated edition of ERDC-CERL seismic design recommendations for cold-formed steel construction, including a design philosophy for ductile performance in seismic loading and complete details of all research supporting the development of the design recommendations.

1.2 Issues in cold-formed steel design and research studies

Seismic design with cold-formed steel has two problems that are inherent in the material itself: (1) its light gage thickness and (2) its strength variability. The general objective of seismic design guidance is to assure ductile building system performance in a large seismic event and elastic response in a small event or wind loading. Ductile building performance requires that selected ductile components yield while carrying loads and absorbing energy through significant plastic response. At the same time, potentially brittle failure modes, such as column buckling or connection failure, must be prevented.

The design challenge for cold-formed steel is to specify that building components—in particular, shear panel components—be proportioned relative to each other and detailed such that the ductile response is assured. In Corps CFS design, this challenge is met by designing the diagonal straps to yield and respond plastically through significant displacement in order to avoid damaging brittle connections or causing the buckling of columns.

The U.S. Army Engineer Research and Development Center, Construction Engineering Research Laboratory (ERDC-CERL) was tasked by HQUSACE to perform a comprehensive investigation for the purpose of developing, refining, and validating design guidance for cold-formed steel structures that ensures ductile performance in response to anticipated seismic loads.

1.2.1 Previous studies

Two papers documenting effective thin shear wall ductile behavior were reviewed for the present study. Both are summarized below.

A paper by Caccese, Elgaaly, and Chen (1993) claims that "tremendous post-buckling strength can be achieved in a thin plate that is restrained at its boundaries and subjected to in-plane shear."[1] Their experimental study varied two parameters: panel thickness and beam-to-column connection (moment or shear-type). Six quarter-scale specimens were tested with panel thickness ranging from 0.0299 to 0.1046 in. The panel slenderness ratios (width/thickness) varied from 1639 to 468. The test specimens were loaded cyclically with a single in-plane horizontal load (i.e., no vertical loading) at the top of the shear wall. Three panels included moment-resisting beam/column connections, and two included shear beam/column connections. The type of beam/column connection had very little influence because the infill plate was continuously welded to the beams and columns, causing the shear connection to act as a moment-resisting connection. The inelastic behavior of thin plate panels is primarily controlled by the yielding of the plates (formation of a diagonal tension field), whereas the behavior of the heavier plate panels is controlled by the column response. Earlier seismic design guidance had required that steel plate shear walls be designed not to buckle, which heavily loads and fails the columns well before the plate optimal capacity can be developed. In fact, the test results imply that panel performance significantly improves if the thin sheet is designed to allow buckling and the formation of a diagonal tension field. Optimal performance is achieved when the sheet is allowed to buckle, yield, and form the diagonal tension field cyclically, ab-

[1] A companion paper in the same journal (Elgaaly, Caccese, and Du 1993) presents mathematical models for nonlinear cyclic and dynamic finite element analysis of these panel systems.

sorbing energy hysteretically, thereby reducing amplification of building response and justifying design guidance based on acceptable R coefficients. This type of guidance will prevent more brittle connection and frame member failures while reducing amplified building response. Caccese, Elgaaly, and Chen (1993) conclude that a building could be designed using thin steel-plate shear walls so it will respond elastically to minor seismic events or high winds. Then when subjected to a severe seismic event, thin plate walls would buckle, develop the tension field, absorb energy, and protect the building gravity-load-resisting system from collapse.

Another paper documenting related work (Driver et al. 1998a[2]) describes an experimental study of a single 50% scale, four-story single-bay steel plate shear wall specimen. Infill panel thickness was 0.189 in. in the bottom two stories and 0.134 in. in the top two stories. The panel slenderness ratio in the bottom stories was 635. The specimen had moment-resisting beam-to-column connections. Gravity loads were applied at the top of the wall and equal cyclic in-plane horizontal loads were applied at each floor level. Deflections in the bottom story reached nine times the yield deflection (ductility of 9) after 20 cycles of inelastic deflections. First yielding (δ_y) occurred at 0.33 in. at the boundary of the infill plate, as well as visible buckling. The first tear occurred at 1.00 in. ($3\delta_y$) in a weld at the corner of the infill panel, but this tear did not propagate in subsequent cycles. At 1.33 in. ($4\delta_y$), local buckling occurred at the interior column flanges of the first-floor beam/column connection and at an outside flange at the base of a column. At 1.66 in. ($5\delta_y$), tears as large as 4.7 in. were seen at the top corners of the bottom panel, and these tears propagated in subsequent cycles. In this cycle, the peak maximum base shear or ultimate capacity of the panel system was reached, and the load-carrying capacity decreased gradually with each cycle of increased deflection. This shear wall system was able to maintain capacity at least up to a ductility of 5 ($5\delta_y$). Load/deflection curves from these tests show excellent hysteretic energy-dissipating performance, with very limited pinching, at deflections as great as nine times the yield deflection. This lack of pinching is primarily due to the effectiveness of the moment frame in sustaining loads when the panel tension field is unloaded. The hysteresis envelopes demonstrate this panel is both very ductile and stable, with no sudden loss of stiffness until final

[2] A companion paper in the same journal (Driver et al. 1998b) describes the development of analytical tools for predicting the behavior of steel plate shear walls.

failure. The ability of this panel to sustain damage but maintain load by redistributing forces to other parts of the system provides excellent redundancy and hysteretic energy dissipation that will effectively prevent building collapse in very severe seismic motions. However, if failures of connections seen in these panels had occurred in cold-formed steel panels, the load capacity may have begun to drop more rapidly because the redistribution of loads may have been less effective in the thin materials.

Significantly, the shear-wall panels described in both of the papers summarized above were constructed with heavier hot-rolled frame members and infill steel plates (Caccese, Elgaaly, and Chen 1993; Driver et al. 1998a). The performance described in those papers is more difficult to achieve using panels constructed with cold-formed steel frames, given the characteristics of the lighter material as discussed above. For cold-formed steel frames, it is even more critical that design guidance ensures formation of a diagonal tension field in the thin steel sheet. Inelastic column response should be limited because of the potential for more brittle failure of the columns. The columns are made up of relatively thin studs or tubing in which the controlling failure mode can be local buckling, out-of-plane buckling or connection failures. Failure in other frame members, such as the top and bottom tracks, must also be prevented, as these can occur as brittle failure modes.

Both of the papers summarized above demonstrate that the desired ductile panel behavior can be achieved if the panel is thin enough relative to the frame, and connection capacity is sufficient to ensure the formation of a diagonal tension field in the panel.

1.2.2 Test setup issues for CFS panel design studies

For cold-formed steel wall panels, it is particularly important that gravity loading be accurately represented. The panel columns are constructed of relatively thin materials, so they are more vulnerable to local buckling than the hot-rolled frames tested in the studies cited above. The panel tests presented in Caccese, Elgaaly, and Chen (1993) did not include any net gravity loading, and neglecting that loading significantly reduces the potential for local column buckling. The panel test presented in Driver et al. (1998a) included gravity loads, but they were applied using post-tensioning rods at the columns. That should be an effective method of applying gravity loads when little axial deformation is expected, as with the heavy hot-rolled sections. When horizontal load is applied and the panel deforms significantly horizontally, the diagonal tension field will form, placing the column on the side resisting the tension field in compression. This will cause shortening in the column resisting the tension field relative to the opposite column due to axial deformation. When the columns are made using thin CFS materials, they also will be vulnerable to local buckling that will cause further shortening and redistribution to the more stiffened portion of the column cross section. The column on this face will then shorten more than the other column due to both axial deformation and local buckling. In a real building, a stiff beam above the panel will cause redistribution of gravity loads away from the shortening column. Therefore, the top beam will tend to rotate, with the compression column shortening, and the tension (or reduced compression, if post-tensioned) column lengthening. This "bending" type deformation will be even more significant for tall, narrow walls (i.e., those with a large aspect ratio). In a real building, the top beam will be restrained from rotation by the relatively stiff top beam.

In the 1990s, the American Iron and Steel Institute (AISI) sponsored a multiphase experimental project to develop design values for lightweight cold-formed steel panels. The second phase of that work included development of values for diagonal-strap and full-panel sheet steel shear panels (Serrette 1997). The discussion here specifically addresses those panels designed with steel diagonal straps. (However, it also discusses full-panel sheets acting as the primary lateral load-resisting element, which were investigated in third and fourth phases of the AISI project.) The Serrette (1997) study tested panels with both monotonic static and cyclic loading. Many of the diagonal-strap panels failed by local buckling of the columns or tracks. The columns in those specimens were all built up by fastening two studs together, web to web. The studs used to fabricate these columns include knockouts in the webs for electrical conduit penetrations, etc. These studs are particularly vulnerable to local buckling where the knockout holes are located. Furthermore, the tracks at the tops of the panels buckled when they were pulled out of plane by column failure. These modes of failure would provide little ductility or structural paths for load redistribution. Better ductile performance could have been obtained had the diagonal straps been smaller relative to the frame members, using a proportional design approach. The test report acknowledged both types of failure as premature (Serrette 1997).

The non-ductile failures documented in Serrette (1997) prevented the development of diagonal strap capacity, and the subsequent strap yielding that would provide a ductile response. That type of failure certainly will not support the ductile, energy-dissipating hysteretic performance needed to justify the ASCE 7 response modification coefficients of 4, 6.5, and 7. The hysteresis plots from the cyclic tests in Serrette (1997) demonstrate extreme pinching. In real seismic motions, after a large peak excursion, this type of panel will rack in the opposite direction with little resistance for several inches. Velocity will increase during this unrestrained motion until sudden resistance is again encountered, causing impact loading. The impact can result in very high accelerations that cause brittle failures at the connections of the lateral-load-resisting elements (diagonal straps or others). Therefore, although the plots in Serrette (1997) may show reasonable ductility, it is not an acceptable level to support a sufficiently ductile failure mode. An individual loading cycle will show very little area inside the hysteretic envelope, demonstrating that very little energy will be dissipated by the tested panel design. All full-sheet panels failed at the screw connections either by pulling through the edge of the sheet or pulling through the column studs. The screw connections again failed at a closer spacing, plus the columns failed by local buckling. As with hot-rolled structural steel designed in accordance with ANSI/AISC 360-10, ductile design of cold-formed steel should prevent failure in connections. Serrette (1997) acknowledged that the premature failure of the connections in the full-sheet configuration prevented the development of the desired tension field; similar to the diagonal-strap configuration discussed above, the full-sheet configuration resulted in severely pinched hysteresis plots.

The results of the Serrette (1997) study demonstrate the critical need for design guidance that will ensure acceptable ductile performance for CFS shear panels in light-steel construction projects managed by the Corps of Engineers. The hypothesis driving the research and design recommendations documented in the present report is that proportionate design should ensure ductile plastic yielding in the lateral-load-resisting system, which will absorb energy and redistribute forces. The use of cost-effective thinner steel makes it difficult to avoid the local buckling of column components that leads to brittle column or track failures. In order to achieve the desired ductile performance, design recommendations and test procedures should constrain out-of-plane deflections and the buckling that results from them.

1.2.3 Seattle District shear panel tests

In 1997, U.S. Army Engineer District Seattle (i.e., Seattle District) conducted strength tests on two shear wall panels that were used in the construction of a barracks building at Fort Lewis, WA (USACE 1997). The panels were tested to determine their shear strength following the cyclic load procedure specified in ASTM E 564-95, "Standard Practice for Static Load Test for Shear Resistance of Framed Walls for Buildings" (ASTM 1995). That procedure, however, is not appropriate for measuring the hysteretic behavior of structural systems. This is an important limitation because the hysteretic performance of shear wall panels is critical to determining the degree of pinching and acceptable ductility. The procedure given in ASTM E 564-95, section 6.3.3 (ASTM 1995), specifies that a preload of approximately 10% of the estimated ultimate load should be applied first for 5 minutes, then released for 5 minutes before reading the initial conditions. That step of the procedure is apparently intended to seat the panel. Any need to seat the panel in this way would indicate that the panel may rack with a very small load, suggesting that such a panel would have pinching equivalent to the initial condition offset. By design, ASTM E 564-95 does not measure this initial seating offset, so this most critical pinching measurement is not captured.

Also, this ASTM test protocol calls for loading the panels using load control with five cycles at one third, two thirds, and the full estimated ultimate load of the panel, but these increments of loading will not define the load/deflection hysteretic envelope effectively. Because the shear yield strength may be close to the ultimate load of a panel, the number of nonlinear cycles could be very small in this procedure. Therefore, this procedure is not appropriate for seismic testing where the hysteretic performance is essential to establishing values of acceptable ductility. Even in small seismic motions, the pinched hysteresis will cause the panels to deflect with almost no resistance, allowing velocity to increase until the seating deflection is overcome. At this point the lateral-load-resisting element and other panel components will be loaded with an impact, resulting in high accelerations and forces under which the panel may fail at even very low seismic motions. A well established stroke-control procedure for defining panel hysteretic performance would be much more appropriate. Two such procedures are the ATC-24 and SAC Phase 2 guidelines (ATC 1992; SAC 1997).

Even with concerns about the appropriateness of the test procedures, some observations can be made from the Seattle District tests. These panels were designed for an ultimate load of 40 kips. No gravity loads were applied in these tests. Neglecting gravity is nonconservative in relation to the columns, because the gravity-load effect will combine with the lateral-load effect to cause the columns to buckle at lower lateral loads. However, neglecting gravity should be conservative in relation to column anchors, because the greatest anchor uplift forces will occur when the lateral load is applied with no vertical load.

The Seattle District after-action report on this testing states that the test panel should exhibit ductile behavior by deflecting six times the design-load deflection (USACE 1997). Because of test equipment limitations, however, this deflection limit was not met. The report states "it was later agreed that this criteria [sic] could be modified, as the panel had exhibited adequate strength and behaved linearly to the working load (39 kips)." Because the design load was 13 kips, the desired factor of safety of 3.0 was achieved. Several assumptions underlying that conclusion must be questioned, however. First, meeting the ductility requirements should require test deflections that are at least equal to the design ductility value (6 in this case) times the yield deflection. The District evaluation assumed that test deflections could be the design ductility times the design-load deflection. Load-deflection plots for Panel 2 at the 50 kip load interval shows that panel yielding did not begin until deflections of approximately 0.6 in. were achieved. To meet the design ductility, the panel should have been deformed to deflections of at least 3.6 in. (6 x 0.6 in.), which equates to peak-to-peak deflections of 7.2 in. The panels should have been tested to deflections greater than 3.6 in. (i.e., greater than 7.2 in. peak-to-peak) to ensure that brittle failures do not occur soon after the required deflection is reached. In the final cycle, deflections only reached peak-to-peak levels of 2.3 in. (ductility of 2.0). Still, the design criteria show that ductility values, R_w, of 6.0 were used. The response modification coefficient, R, according to ASCE 7, is a measure not only of global ductility but also over-strength. As stated previously in the present report, seismically induced lateral loads are divided by this coefficient in recognition of the structural system's ability to continue resisting lateral loads after yielding. Therefore, a value of 2.0 for the ductility portion of the R coefficient can be justified based on these tests. The tests showed that these panels are significantly overdesigned because their yield strength is three times greater than their design lateral force. Because the tests were stopped prematurely due to equipment limitations, true panel over-strength (ultimate lateral capacity over yield) and ductility are not known.

A more appropriate design approach, based on the experimental results achieved, would have increased the design capacity of the panel and reduced the R coefficient, resulting in essentially the same panel design. For example, the design capacity could have been increased to 37 kips (i.e., resistance factor for tensile members or tension field of a sheet, ϕ_t, of 0.95 times the panel yield capacity of 39 kips) and the R coefficient reduced to 2.0. Since the applied seismic loads in linear analysis procedures are inversely proportional to the R coefficient, the applied loads would have increased by a factor of 3 (R reduced from 6 to 2) from 13 kips to 39 kips. Even with this very large reduction in the R coefficient, the design capacity of 37 kips is only slightly lower than the applied loads, so the impact on design would be minimal. However, had the test been carried out to larger panel deformations without loss of capacity, a larger R coefficient (greater than 2) along with the greater panel capacity could have been justified, resulting in more economical design. The design used in the Seattle (USACE 1997) study, with either the low design capacity and R coefficient of 6 or the increased capacity and reduced R coefficient, will result in almost elastic response of the building in an earthquake, as is the case with any structural system that uses a very small R coefficient. In a large earthquake, this design will result in very high accelerations and potential for extensive damage to nonstructural components that are vulnerable to larger inertia forces. A much more practical approach would be to provide the basis for justifying larger ductility values, which in this case requires conducting cyclic tests to peak-to-peak deflections of 7.2 in.

Not only should panels be tested to much greater deflections to verify higher ductility, but the resulting hysteretic envelope must not be overly pinched in order that a degree of load resistance can be maintained throughout each load cycle. To obtain such plastic behavior, the initial yielding must take place in the primary lateral-load-resisting element (i.e., steel sheet in this case), not the frame or connections, which may fail in a more brittle manner and thus lead to ultimate collapse of the shear panel system. The tops of the panels used in the Seattle study (USACE 1997) were loaded using a 3 x 6 x 3/16 in. structural tubing top beam attached to the hydraulic ram. This tube is far more flexible in bending than the beam/floor slab in the field, and therefore will not properly represent the anchorage of the tension field nor the rotational restraint for the columns.

The 50 kip limit on the hydraulic ram prevented testing to the ultimate capacity of the panels. Failure of the test fixture (base plate, panel anchorage tension rod, and structural tube top beam) also prevented testing to the ultimate capacity of the panel. Warping, or elastic buckling in the steel sheet, first occurred at the 13 kip load cycle, which should also have resulted in the development of the panel tension field. However, the hysteretic envelopes do not show a clear softening of the panel that would result from significant yielding of the steel sheet. Also, Tables 1 and 2 of the test report (USACE 1997) give values of global shear stiffness for each cycle. These stiffness values at the greatest load cycles (50 kips) are only about 20% lower than at the first load cycles (13 kips). Therefore, it is difficult to justify a yield deflection before the 0.6 in. deflection defined above as a yield deflection (corresponding to a load of 36 kips). These tests appeared to have produced limited tension-field development in the steel sheet before any failure of the frame or connections. However, the panels were simply not loaded far enough to define the hysteretic behavior. Loading was limited by failures of the tension rod anchors, test frame, and load and deflection capacity of the test ram. The result is that the Seattle test results can only justify a ductility value of 2.0. It also appears that the steel sheet was much too heavy relative to the capacity of the frame, such that the development of a significant plastic tension field was prevented. Development of tension field plastic response could have formed the basis for much greater ductility values.

1.3 Research problem

The original research problem, which was investigated and addressed in the late 1990s, was to develop and validate a design for CFS shear panels that met established standards for ductile performance under seismic loading; and then to develop and specify detailed recommendations for implementing the design. Ensuring the ductile performance of this structural system would enable USACE to lift its moratorium on cold-formed steel construction. The key requirement was to provide proportional design specifications for the behavior of the primary lateral-load-resisting elements (diagonal straps) versus the columns, and detailing guidance that ensures acceptable ductile panel performance. The proportional specifications were developed to ensure significant plastic performance of the diagonal straps before brittle failure of either the columns or connections. The recommendations include the definition of a system response-modification coefficient, R, and deflection-amplification factor, C_d. They also account for the influence of system overstrength.

1.4 Objective

The objective of this project was to compile the results of the extensive research, development, and testing program that led to the development, validation, and specifications for shear panels that provide adequate ductility to cold-formed steel buildings during a seismic event. The documentation encompasses all research activities, an updated set of detailed design recommendations derived from the research, and an example problem that illustrates how to apply the design recommendations.

1.5 Approach

This multi-year research project encompassed the following major tasks:

1. Review of related work
2. Development of a design philosophy
3. Definition of promising panel configurations
4. Development of a preliminary design model
5. Design of prototype test shear panels and development of preliminary design recommendations
6. Definition of material properties and coupon test results
7. Pretest of predicted panel response based on preliminary design model and coupon test results
8. Definition of test configuration, procedures, and instrumentation
9. Test of prototype shear panels and documentation of performance
10. Model verification testing on shake table to account for dynamic effects
11. Modification of shear panel models
12. Development of design recommendations and example design problem

1.6 Scope

The report is presented in two parts:

- Part I documents ERDC-CERL investigations that provide the technical basis for developing the CFS seismic design recommendations.
- Part II presents the seismic design recommendations (Chapter 11) and a representative seismic design problem to illustrate how the recommendations are applied (Chapter 12).

The key requirement for these recommendations is to provide proportional design criteria for the behavior of the primary lateral-load-resisting elements (diagonal straps) versus the columns, and detailing recommendations that will ensure acceptable ductile panel performance. The proportional recommendations should ensure significant plastic performance of the diagonal straps before brittle failure of either columns or connections. These recommendations include the definition of a system response modification coefficient, R, and deflection amplification factor, C_d. It also accounts for the influence of system over-strength.

The recommendations presented in Chapter 11 assume that the shear panels are adequately anchored to floor diaphragms above and below. Initially, panel anchorage was outside the scope of this study, and anchorage design was not an issue in the test panels. After initial prototype panel testing, however, it became clear that panel system performance could be improved with the proper anchorage configuration. Therefore, improved prototype shear panel configurations including anchorage details were tested, and anchorage design recommendations were written. To ensure a continuous load path for multiple-story buildings, shear panels installed above the ground floor must have shear panels installed at every story level below. It is also assumed that the diaphragms are sufficient to transfer loads between various shear panels located at a given floor level. The panels must be located such that the center of stiffness and center of mass align with each other in both horizontal directions.

Three levels of seismic design recommendations are provided:

1. Tabular data for prototype shear panels in terms of the maximum story shear and maximum and minimum gravity load. These terms are defined in Chapter 11, and the shear panel configurations and data are provided in Appendix C.
2. Detailed seismic design recommendations using shear panels with diagonal straps as the primary lateral-load-resisting element. These recommendations are provided in Chapter 11, and an example problem illustrating the recommendations is given in Chapter 12.
3. A test procedure and acceptance criteria for other shear panel configurations, which are provided in Appendix D.

1.7 Mode of technology transfer

The design recommendations presented in Chapter 11 would be appropriate to consider for incorporation into a future AISI standard on seismic design for light steel construction systems.

The spreadsheet program used in the example problem presented in Chapter 12 will be made available through the Network for Earthquake Engineering Simulation (NEES) Data Repository (http://nees.org/warehouse), a centralized resource for sharing and publishing earthquake engineering research data from experimental and numerical studies. The spreadsheet can be used as a shear-panel design-assistance tool.

2 Shear Panel Configurations Considered

Several shear panel configurations were considered. Only configurations using conventional building materials were given serious consideration in this program. Future studies that investigate the use of composite panels and other innovative materials, and evaluating their use in a similar manner as the conventional materials here, were contemplated but not investigated. Each panel consists of a cold-formed steel frame with columns at the edges and single interior studs spaced 16 in. on center. The top and bottom of the panels have a standard channel track. Table 2-1 shows a matrix of the panel configuration variables considered. The first variable is the column construction, where columns built up with studs and single structural tubes were considered. The second variable is the primary lateral load-resisting element, where diagonal steel straps and full panel steel sheets were considered. The last variable is the panel fastening system, where self-tapping screws and welded connections were considered. Input was gathered from the cold-formed steel industry on constructability and cost-effectiveness for each configuration so that the developed recommendations would focus on the most practical configurations. The following discussion of each configuration includes the feedback from industry.

The design of each panel configuration assumed all panels were rigidly anchored to the building diaphragm above and below. This rigid anchorage would prevent out-of-plane distortions at the top and bottom track and would keep the top track horizontal. For the panels tested in this program, all panel tracks were bolted to the top and bottom beam. Anchorage design was outside the scope of the initial panel configurations, but it soon became clear that anchorage behavior would significantly influence panel performance, so later panel configurations included anchorage details.

Table 2-1. Matrix of shear panel configurations considered.

Panel Configuration	Exterior Column Construction	Lateral-load-resisting Element	Panel Fastening System	Comments
A	Built-up Studs	Diagonal Steel Straps	Self-tapping Screws	Lowest capacity diagonal strap configuration
B	Structural Tubing	Diagonal Steel Straps	Self-tapping Screws	
C	Built-up Studs	Diagonal Steel Straps	Welded	

Panel Configuration	Exterior Column Construction	Lateral-load-resisting Element	Panel Fastening System	Comments
D	Structural Tubing	Diagonal Steel Straps	Welded	Highest capacity diagonal strap configuration
E	Built-up Studs	Full Panel Steel Sheet	Self-tapping Screws	
F	Structural Tubing	Full Panel Steel Sheet	Self-tapping Screws	
G	Built-up Studs	Full Panel Steel Sheet	Welded	
H	Structural Tubing	Full Panel Steel Sheet	Welded	Highest capacity full panel sheet configuration

2.1 Panel A

This should be the lowest-cost configuration of those shown in Table 2-1. It should also be the most similar to current construction practices using cold-formed steel. This panel configuration may be constructed entirely with carpenters in the field, avoiding the need for the additional trade participation of ironworkers[3]. This assumes the built-up columns may be welded without an ironworker, because the steel is 0.125 in. or less in thickness. Columns may be built up with several studs less expensively than a single structural tube because this avoids the need for ironworkers. Built-up columns would most likely be fabricated in the shop in an automated fashion (e.g., robotic welding), leading to even more cost-effective fabrication. The columns must be built up with the studs oriented to form a closed section. This will reduce, though not eliminate, the potential for local buckling. These columns are also vulnerable to local buckling due to the utility knockouts in the stud webs. The design recommendations presented in Chapter 11 recognize and account for this vulnerability. Test panel A1, A2, and A3 drawings show details for such a column (see Appendix A for all test panel drawings). Chapter 11 provides built-up column welding recommendations to ensure composite behavior of columns. The welds are simple intermittent groove welds, sized and spaced so as to provide the shear transfer needed to develop the full bending capacity of the composite column. The diagonal strap/column connections must be detailed to develop the full yield capacity of this strap. The column anchors at both the top and bottom of the panel must be detailed to transfer the shear and possible tension load in the column to the supporting diaphragms

[3] Phone conversation between Gregory Ralph of Dietrich Industries and James Wilcoski of ERDC-CERL, January 1998.

(beams or slabs).[4] These loads originate primarily from the tensile load in the connected diagonal strap. If properly detailed, this configuration should provide a cost-effective lateral-load-resisting shear panel and it warrants further evaluation.

The A2 test panel configuration included a nested stud, laid inside and parallel to the top and bottom track on both sides of the column. This stud was welded to the columns and tracks in which they rested. The nested stud was oriented with its web against the web of the channel track. This stud was also welded to the track along the edge of channel track flange. The nested studs increased the tensile and shear capacity of the column/track/anchor connection that would be insufficient with the track alone. Construction with the nested stud does not require an ironworker because the welds are less than the 0.125 in.

The A3 test panel is similar to the A1 panel, but uses an off-the-shelf anchor.

After the panel tests, the use of a nested stud was replaced with angle iron anchors on both sides of the columns. These anchors provide the needed shear and uplift resistance, as did the nested stud. The anchors must be welded to the columns, and this weld can also be made without an ironworker because the weld thickness is less than 0.125 in. The anchors also provide a good degree of moment resistance for the column, while the nested stud provided little. This moment resistance would reduce pinching of the hysteresis when loading cyclically, which may in turn lead to an increase in R, C_d, and system overstrength of the panel.

2.2 Panel B

This configuration is similar to Panel A, except the columns are hollow structural sections (HSS). The HSS thickness will normally be greater than 0.125 in. and the weld thickness for the connection to the anchor will equal the thickness of the column. Therefore an ironworker will normally be required, resulting in a cost increase. If the HSS columns are used, requiring an ironworker, welded diagonal strap-to-column connections become

4 The column anchors for the A1, A2, and A3 test panels were designed as pinned connections, but later anchor guidance requires moment resistance (as used in C1 test panel).

more practical, which results in the Panel D configuration. Therefore, no further consideration was given to this configuration.

2.3 Panel C

This configuration is similar to Panel A with stiffened angle iron anchors, except that connections are welded. This configuration may also be more cost-effective than Panel A because of the numerous fasteners required in Panel A connections. The thickness of the stud material will be under 0.125 in., so an ironworker is not needed for either the welds at the diagonal strap-to-column or column-to-anchor connections. This configuration differs from the Panel D configuration only in that the columns are built up from studs rather than the single structural tube columns. This configuration would require more labor to weld the studs into a composite column section. However, it has an advantage over the Panel D configuration in that an ironworker is not required. Columns built up from heavy studs (e.g., 97 or 118 mil) could provide similar properties as very light HSS columns. The details for the C1 test panel are provided in Appendix A. This panel is most similar to the A2 panel, except that the connections of the diagonal straps to the columns are welded rather than screwed.

2.4 Panel D

This configuration uses HSS columns and welded connections. This panel should have the greatest capacity of the diagonal-strap configurations. The heavier thickness of the column material relative to the studs in Panel C should reduce the potential for local buckling. The welded connections should be less vulnerable to failure than the self-tapping screws, especially when subjected to the cyclic seismic load conditions. The details of Panels D1 and D2 are shown in Appendix A. The D1 panel uses nested studs to anchor the panel columns, while the D2 panel uses stiffened angle anchors. The D1 panel nested studs were intended to provide only a pinned connection for the columns that would resist the shear loads applied to the columns, while the D2 panel anchors provide a moment connection for the columns.

2.5 Panel E

This panel differs from the Panel A configuration in that a full steel sheet is used on one face of the panel for the primary lateral load-resisting element in place of the diagonal straps of Panel A. Each steel sheet configuration relies on the sheet forming a diagonal tension field orientated at a 45-degree angle to the application of load. The optimal performance of these panels will be achieved when the panel height-to-width aspect ratio is approximately 1.0. This will allow the formation of the diagonal tension field at a 45 degree angle, in a way that this field transfers loads directly into the rigid anchor to the supporting beam above and below the shear panel. If this aspect ratio much greater than 1.0, the diagonal tension field will need to be resisted by the more flexible columns. If the aspect ratio is much lower than 1.0, the diagonal tension field will need to be resisted by the top and bottom track. These tracks should not be used to carry bending load by themselves. The bending resistance could be increased somewhat by adding a nested stud or column anchors to the interior of the columns similar to the D2 panel. Using the columns to resist the tension field would require very heavy columns relative to the sheet, to meet the requirement that the lateral-load-resisting element yield before the frame. For shear panels that cannot avoid this high aspect ratio, a horizontal compression member may be added at mid-height of the panel. This compression member would essentially allow the panel to act as one panel on top of the other so that two parallel tension fields would develop, one in the lower and one in the upper portion of the panel.

The sheet connection to the frame must have the capacity to resist the full yield tension field capacity of the sheet. The widest available coiled steel sheet in the United States is 60 in., so that any panel taller than 60 in. will have an aspect ratio that exceeds 1.0 unless two sheets are used together in a single panel. Using two sheets in a single panel will require welding the panels along the full length of their joint. If the sheet is to be welded, the entire panel should also be welded, resulting in either a Panel G or H configuration. Therefore the Panel E configuration is practically limited to 60 in. in width, which would result in an aspect ratio greater than 1.0.

The high aspect ratio requires that a mid-height horizontal compression member be added. The Panel E configuration then requires enough screws to develop the full yield tension field. A preliminary design of such a panel was developed using a very thin 22 gage (30 mil) steel sheet with yield strength of 33 ksi. Screws would be required around the entire panel perimeter, plus a very dense concentration at the corners and at mid-height of the columns to develop the tension field. This preliminary design called for about 1,100 #10-16 (Teks brand) self-tapping screws, on the side of the panel with the steel sheet. A heavier sheet, a higher sheet yield strength, or a lower screw strength would have all required even more fasteners. The large numbers of required fasteners make the E configuration impractical.

2.6 Panel F

This configuration differs from Panel E in that the columns are structural tubing members. Similar to the Panel E configuration, this panel could be no wider than 60 in. and would therefore have a high aspect ratio and would require a mid-height horizontal compression member. It would also require a very large number of screws, and therefore would be impractical.

2.7 Panel G

This configuration differs from Panel E in that welded connections are used in place of the screws. Continuous welds are used to fasten the sheet to the frame, effectively developing the panel tension field. The welded connections would solve the problem of the very large numbers of fasteners. The welded connections also mean steel sheets could be welded together at the internal steel studs, so wider panels with aspect ratios smaller than 1.0 could be used. This eliminates the need for the mid-height horizontal compression member. The thickness of the stud material would be less than 0.125 in., so that an ironworker would not be needed for either the welds at the sheet-to-column or column-to-anchor connections. However, it was still assumed that the Panel H configuration could be constructed more effectively because it avoids welding built-up columns from studs. Therefore, this configuration has potential, but was not given further consideration here.

2.8 Panel H

The H configuration uses a full-panel steel sheet on one face, structural tubing columns, welded connections and anchors similar to those shown in panel D2. The steel sheet would be welded around its entire perimeter, to the columns at its sides and to the heavy tracks at the top and bottoms. The tracks would be greatly stiffened near the corners of the panel, where anchors, similar to those used in the C1 and D2 test panels (see Appendix A drawings), at the insides of the columns are against the tracks. This panel was judged to be the most practical of all steel sheet configurations for the reasons stated in the Panel E, F, and G discussion. Ideally, the panel width should be approximately equal to the panel height (aspect ratio equal to 1.0). However, the use of narrower panels with a mid-height horizontal compression member could be investigated. If detailed properly, this panel should offer greater R and C_d values, plus better system overstrength than any diagonal strap configuration. This panel differs from Panel D in that it uses a steel sheet rather than diagonal straps. Under cyclic loading, at large deflections where the Panel D straps are significantly elongated, the straps will offer little resistance soon after a peak excursion. This is because the strap that had been in tension will buckle when unloaded, but the opposite diagonal strap had itself been stretched in the other direction, so it will remain buckled until the panel deflects significantly back in the other direction. In this condition, the Panel D columns must provide almost all the lateral resistance. The Panel H steel sheet on the other hand should pick up load soon after a peak excursion. The sheet buckled perpendicular to the tension field must be forced to straighten out picking up some load in the process. The sheet should not be attached to the intermediate studs at the interior of the sheet because spot welds or other connections at these locations could shock load the welded connection to the panel columns and tracks. The test results for the D1 panel reported in Chapter 7 show that spot welds between the diagonal straps and intermediate studs failed suddenly, shock loading the connections of the strap to the columns. This shock loading took place under very low-velocity cyclic testing. In a seismic event the shock loading could be more severe because several spot welds could fail at the same time on either a diagonal strap or steel sheet. Therefore, the sheet should not be welded to the intermediate studs because when the spot welds fail they could cause brittle failure of the perimeter sheet weld connections to the frame. Also, any improved capacity from these spot welds would be minimal.

The steel sheet, welded to both the column and track in the corners, further stiffens this connection (see Caccese 1993). The unbuckling of the sheet and moment resistance of the column to anchor connection will all provide some resistance, even after a peak excursion, while the sheet is still buckled. Panel tests are needed to measure the extent of this contribution, but this effect should reduce the pinched hystereses to some extent, making the energy dissipation greater in this panel than Panel D.

The same model developed for the diagonal strap configurations (Panels A, C, and D) could be used for the Panel H configuration once a method is developed to define the width of the diagonal tension field. The diagonal tension field would develop at close to a 45-degree angle. The diagonal tension fields of panels with large aspect ratios (e.g., 50% taller than wide) would load the columns in bending. Such bending load on the columns would require very heavy columns relative to the thickness of the sheet. A more practical solution for panels with large aspect ratios is to add a mid-height compression member. A method for defining the width of the tension field was to be developed based on detailed Abaqus finite-element analysis and panel test results. However, the scope of this study did not permit testing Panel H test panels, so no further consideration was given to this configuration.

Based on the issues described for each panel above, all further panel evaluation focused on the A, C, and D configurations. These panels, plus the Panel H configuration, appear to be the most promising in terms of required ductile behavior, constructability, and cost-effectiveness.

3 Shear Panel Design Philosophy and Analytical Model

This chapter presents the design philosophy used in the development of cold-formed steel shear panel design that is presented in detail in Chapter 11. It also introduces analytical models that were used in the design of test panels.

3.1 Seismic-resistant building performance through ductile shear panel design

Design forces resulting from earthquake motions are determined partially on the basis of energy dissipation in the nonlinear range of response. Building codes provide response-modification coefficients, R, by which seismically induced lateral loads are divided. Design recommendations allow the use of R values between 2 and 7 for light-framed walls (ASCE/SEI 7-10, Table 12.2-1).

Ductile shear panel performance requires that the primary lateral load-resisting elements deform significantly while continuing to resist lateral loads. Diagonal straps perform this function for the shear panel configurations developed for detailed study. The thin tension-only diagonal straps will yield and continue to resist load as they elongate. As they are loaded cyclically, they will absorb energy hysteretically, thereby reducing amplification of building response and justifying design recommendations based on their R values. The diagonal straps must yield and elongate, within defined limits of lateral load, while other components that could fail in a brittle manner must be proportionately designed to remain elastic for the maximum loads that could be applied to them based on the diagonal strap strength. The diagonal straps effectively act a fuse to limit the loads applied to other components. This behavior will prevent damage through more brittle failures to connections and frame members while reducing amplified building response. A building can be designed to behave elastically to minor seismic events or high winds, yet respond inelastically to moderate or major seismic events in a way that protects the gravity-load-resisting system and prevents collapse. In a moderate earthquake, some plastic response may occur in the lateral-load-resisting elements, with little or no damage to the vertical or gravity-load-resisting elements. After the event, building components can be inspected and the lateral-load-resisting elements can be replaced with no disruption of or shoring of the vertical load system (columns, anchors, or diaphragms). The shear panels are constructed so that the lateral-load-resisting elements are installed last so they could be more easily replaced after a damaging earthquake.

The thin materials used in cold-formed steel construction makes them particularly vulnerable to buckling and tearing. The large material strength variability also makes achieving ductile panel system behavior difficult because one must account for this variability in proportionate design that ensures significant diagonal strap yielding before column buckling or any brittle failures in the connections. When columns are built-up with light-gage studs, the columns are particularly vulnerable to local buckling at the knockouts cut in the webs of panel studs for penetration by building utilities. Panel columns may yield after significant plastic response in the straps, but they must not buckle. Limited local buckling of the columns is acceptable after this plastic response as long as it does not result in gross section collapse.

Chapter 11 defines design recommendations that address several possible modes of failure in the diagonal strap connections to the columns. Each mode of failure must have a minimum capacity that exceeds the maximum load that may be applied to them through the diagonal straps. The shear panels are anchored to the diaphragms above and below using fasteners that are connected to these columns. Chapter 11 defines an anchor configuration that can withstand limited inelastic response itself, but other potentially brittle modes of failure must be prevented. The recommendations in Chapter 11 define each mode of failure, and the brittle ones must have a minimum capacity that exceeds the maximum loads applied to them from the diagonal straps and columns acting as a moment frame.

The simple model presented here can be represented in a spreadsheet and used as a design aid. The models developed in this work were used to design test panels. After coupon tests to measure the real material properties of test panels, the models were used to develop pre-test predictions of panel response (see Chapter 5). Then the adequacy of the models and recommendations were evaluated based on actual test panel performance.

3.2 Cold-formed steel shear panel model

Figure 3-1 provides a schematic drawing of the analytical model. This model applies to the A, C, and D shear panel configuration defined in the previous chapter. The columns in the A and C configurations are built up with cold-formed steel studs that have utility knockouts in stud webs. In the built-up columns the knockouts will be in their flanges. The thin cold-formed steel flange that was already vulnerable to local buckling is now much more vulnerable both because of the reduced area and the unsupported flange along the knockout. Tests by others demonstrate that the studs are particularly vulnerable to local buckling at the knockouts (Serrette 1997). The reduced section area and greater vulnerability to local buckling is not taken into account in the simple models developed here, but the design guidance in Chapter 11 does account for it by defining an effective column cross-section for carrying axial loads. The columns may begin to buckle locally at the knockouts, but should have the reserve capacity to redistribute the loads to other parts of the column cross-section, preventing gross column collapse.

Figure 3-1. Schematic drawing of cold-formed steel shear panel model.

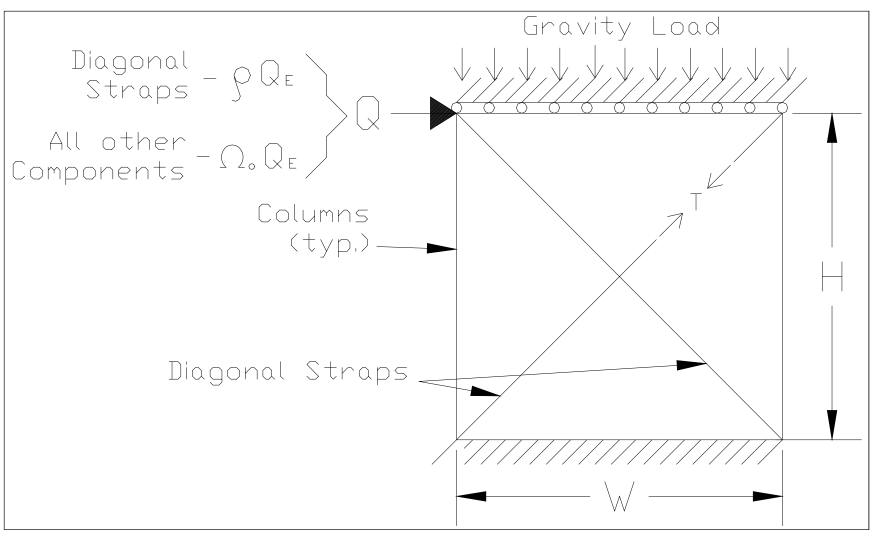

The load-deflection behavior of each shear wall panel is modeled based on spreadsheet calculations. The drawings for each test panel configuration (A1, A2, A3, C1, D1 and D2) are given in Appendix A. Each of these panels uses thin, flat diagonal-strap cross-braces as the lateral-load-resisting element. The design intent is that the diagonal straps carry the majority of the lateral load and provide for the needed panel ductility with significant plastic response. The supporting frame and connections must provide sufficient capacity to resist the resultant forces, but should remain elastic until significant strap inelastic response.

Because the diagonal straps are quite thin, they are assumed to carry load in tension only. The initial test panels (A1, A2, and D1) had the diagonal straps fastened to the intermediate panel studs at 16 in. on center, so the straps would carry a very small load in compression. The thought was that this would widen the load-versus-deformation hysteresis loops slightly, because the straps would carry very small compressive loads when the panel begins to be unloaded after a peak excursion. This small contribution from the straps acting in compression was conservatively ignored, and they were designed as tension only members. After the initial panel test it was seen that the connections to the intermediate studs had a negative influence on panel performance. At large panel deformation, these connections would suddenly fail, shock loading the diagonal straps and their connections to the columns. It was decided that this shock loading could lead to a brittle failure of an already heavily loaded strap-to-column connection. These intermediate connections were eliminated from future test panels and should not be used in actual construction.

The shear panel frame columns will provide some lateral resistance, if the columns are able to act with the slabs above and below as moment frames. The column anchors are detailed to provide moment resistance for the eccentric loading of the diagonal strap and for the full moment capacity of the columns. However, though the anchors have the full moment capacity of the columns, the anchor stiffness will be less than fully fixed. The design recommendations presented in Chapter 11 neglect the column moment frame capacity. But the model developed here and used to predict panel performance in Chapter 5 defines panel capacity based on both the diagonal straps alone and with the columns acting as a fully fixed moment frame. The actual panel capacity should be somewhere between ignoring the moment frame and assuming it is fully fixed. The moment-frame capacity of the columns is very important for widening the hystereses loops, by carrying lateral load when the panel is unloaded after a peak excursion.

The intermediate studs between the panel columns will carry a small portion of the gravity load depending on the flexural stiffness of the diaphragms. The gravity load used in this model is assumed to be only that portion carried by the columns. After large lateral deflections, the axial capacity of the intermediate studs will decrease due to the P delta effects on these very slender studs. Therefore, the axial capacity of these studs was conservatively ignored.

The following equations are used in the spreadsheet model. The lateral yield capacity of a shear panel based on the diagonal strap strength alone, Q_{sy}, is given by:

$$Q_{sy} = n_s b_s t_s F_{sy} \left(\frac{W}{\sqrt{H^2+W^2}}\right) \quad \text{(Eq 3-1)}$$

where

- n_s = the number of diagonal straps in each direction, i.e., straps on 1 or 2 faces
- b_s = the diagonal strap width
- t_s = the diagonal strap thickness
- F_{sy} = the strap yield strength
- W = the overall width of the shear panel
- H = the overall height of the panel.

The panel lateral deflection when the strap yields, δ_{sy}, is defined by:

$$\delta_{sy} = \frac{F_{sy}}{E}\sqrt{H^2+W^2}\left(\frac{\sqrt{H^2+W^2}}{W}\right) = \frac{F_{sy}}{E}\left(\frac{H^2+W^2}{W}\right) \quad \text{(Eq 3-2)}$$

where

- E = the steel modulus of elasticity.

The panel initial lateral stiffness based on the diagonal strap stiffness alone, k_{sy}, is given by:

$$k_{sy} = \frac{Q_{sy}}{\delta_{sy}} = \frac{n_s b_s t_s F_{sy}\left(\frac{W}{\sqrt{H^2+W^2}}\right)}{\frac{F_{sy}}{E}\left(\frac{H^2+W^2}{W}\right)} = n_s b_s t_s E\left(\frac{W^2}{(H^2+W^2)^{3/2}}\right) \quad \text{(Eq 3-3)}$$

The lateral stiffness of two columns fixed at both their tops and bottoms in a shear panel, k_c, is:

$$K_c = \frac{24EI_x}{H^3} \quad \text{(Eq 3-4)}$$

where

I_x = the moment of inertia of an individual column in the plane of the shear panel.

The total lateral stiffness of the shear panel before strap yielding, k_T, is:

$$k_t = k_{sy} + k_c \quad \text{(Eq 3-5)}$$

The fully fixed column lateral force at strap yielding, Q_{csy}, is:

$$Q_{csy} = k_c \delta_{sy} \quad \text{(Eq 3-6)}$$

The total panel lateral force at strap yielding, Q_{Tsy}, is:

$$Q_{T_{sy}} = Q_{sy} + Q_{csy} \quad \text{(Eq 3-7)}$$

The maximum column axial load applied to the panel columns is based on the maximum yield stress in the diagonal straps, P_{vymax}, defined below:

$$P_{vymax} = \frac{GL_{max}}{2} + F_{symax} n_s b_s t_s \left(\frac{H}{\sqrt{H^2+W^2}}\right) \quad \text{(Eq 3-8)}$$

where

GL_{max} =the maximum gravity load per shear panel, defined in detail in Chapter 11.

F_{symax} =the maximum estimated yield stress in the diagonal straps, which is defined in detail in Chapter 11.

The column design capacity is defined in Chapter 11.

The maximum estimated yield force in the diagonal straps (in the axis of the straps), P_{symax}, is:

$$P_{symax} = F_{symax} n_s b_s t_s \quad \text{(Eq 3-9)}$$

The diagonal strap-to-column connections must be designed to resist the forces defined by Equation 3-9. This equation also defines the loads applied to the panel anchors that anchor the columns to the diaphragms.

Chapter 11 provides detailed design recommendations for these connections and anchors.

The combined shear capacity of the columns and anchors must exceed the maximum shear panel horizontal seismic force P_{hymax} defined in Equation 3-10:

$$P_{hymax} = F_{symax} n_s b_s t_s \left(\frac{W}{\sqrt{H^2+W^2}}\right) \qquad \text{(Eq 3-10)}$$

This force is based on the load developed form the maximum yield strength of the diagonal straps. Chapter 11 defines the shear capacity of the columns and design of anchors to resist this load.

The shear capacity of the anchor bolts on both sides of each column must exceed the force P_{hymax} defined in Equation 3-10. Chapter 11 defines the anchor bolt shear capacity. Chapter 11 also defines applied tensile force per bolt and the several anchor design requirements for various potential modes of failure.

Chapter 11 further develops this model for cold-formed steel shear panel design purposes. Chapter 5 expands the model for that purpose to predict shear panel capacity to larger deformations where the column yields. The purpose for this is to provide a simple spreadsheet model that can be compared with cyclic test data reported in Chapter 7 and the shake table test results reported in Chapter 8. The test results in combination with comparisons with the predicted model should validate that the detailed recommendations presented in Chapter 11 can be relied upon to achieve the desired ductile behavior.

4 Material Properties and Coupon Test Results

4.1 Material properties

Actual expected yield and ultimate strength, not just design minimums, are very important for designing panels that will provide significant ductility from plastic response of the diagonal straps before damage to the panel columns or connections. Cold-formed steel suppliers may reroll materials to obtain a thinner product from a thicker one. The rerolling causes strain hardening, which may significantly increase the strength and the variability in strength. The degree of strength variability depends on the degree of strain hardening and makes design of shear panels with cold-formed steel difficult. The ratio or ultimate over yield strength (F_u/F_y) is also significantly reduced in the rerolling, and this ratio is critical if net section failure in connections is to be prevented. Also, strain hardening will significantly reduce the ductility or elongation of the material. Therefore, the recommendations here prohibit the use of rerolled materials for the diagonal straps, where the maximum yield and plastic behavior are critical. They also assume only virgin ASTM A653 or, better yet, ASTM A1003/A1003M Type H steel will be used (ASTM 2013a, 2013b).

The strength of even virgin ASTM A653 materials can vary significantly. The following information on ASTM A653 material properties was obtained from a 1995 in-house study conducted at Bethlehem Steel (Larson 1998). In this study, data were gathered from two galvanized coating lines where the conditions of the lines varied significantly so as to provide a good range of test results:

> ASTM A653 does not specify a maximum yield or tensile (ultimate) strength. Normally the concern in the high-strength end of the range is having enough ductility to form a part. A653 specifies a minimum elongation to satisfy this concern.
>
> 1) For Grade 33 (data also included Grade 40), the yield strength may vary between 1 and 2 times the minimum specified (i.e., 33 ksi), but is typically 1½ times the minimum specified.

2) For Grade 50, the yield strength may vary between 1 and 1½ times the minimum specified (i.e., 50 ksi), but is typically 1⅛ times the minimum specified.

3) For Grade 33 (data also included Grade 40), the tensile (ultimate) strength may vary between 1 and 1½ times the minimum specified (i.e., 45 ksi), but is typically 1¼ times the minimum specified.

4) For Grade 50, the tensile (ultimate) strength may vary between 1 and 1¼ times the minimum specified (i.e., 65 ksi), but is typically 11/16 times the minimum specified.

5) For Grade 33 (data also included Grade 40), the elongation (strain) may vary between 1 and 2 times the minimum specified (i.e., 20%), but is typically 1½ times the minimum specified.

6) For Grade 50, the elongation (strain) may vary between 1 and 3 times the minimum specified (i.e., 12%), but is typically 2¼ times the minimum specified.

Grade 50 would tend to significantly reduce the "over-strength" issue while providing adequate ductility. However, this information is based on an in-house Bethlehem Steel study and is not necessarily representative of the steel industry. Individual sample size (grade/coating) in this study varied from 30 to 717 coils. An individual sample may include several thicknesses for a given sample grade and coating.

Note minimum ductility requirements in AISI Specification S100-07, section A2.3.1 (AISI 2007a, 8): $F_u/F_y > 1.08$ and total elongation of at least 10% for a 2 in. gage length, based on ASTM A370 coupon test requirements (ASTM 2014b).

The section "Load and Resistance Factor Design, LRFD, Commentary on the LRFD Design Specification for Structural Steel Building" (AISC 2011), provides a good discussion on limit states and an overview of the probabilistic basis for the LRFD. The LRFD specification uses a general format given by the following equation (AISC 2011, Equation B3-1):

$$R_u \leq \emptyset R_n \qquad \text{(Eq 4-1)}$$

where

R_u = the required strength using LRFD load combinations
R_n = the nominal strength
ϕ = the resistance factor corresponding to R_n
ϕR_n = the design strength.

The left side of Equation 4-1 represents the required resistance computed by structural analysis based on the assumed loads. The right side of this equation represents a limiting structural capacity provided by the selected members or connection detail. The resistance factors, ϕ, reflect the fact that the loads, load effects on forces and moments, and the resistances can be determined to imperfect degrees of accuracy. The probabilistic basis for the LFRD attempts to define the mean and standard deviations of the load effects and resistance factors. The probability of a given limit state being reached (e.g., a material yielding or fracture occurring in a connection) is the probability that ϕR_n exceeds R_u, which is related to the mean and standard deviations of these.

The Bethlehem Steel study, excerpted above, provides some basis for the mean yield and ultimate strengths of cold-formed steel materials that can be related to certain limit states. Many of these limit states form the basis of the design provisions in Chapter 11. However, the authors are unaware of the standard deviations of these properties other than the large range of properties defined in the Bethlehem Steel study. Therefore, conservative assumptions had to be made to develop design recommendations based on this data that would prevent brittle modes of failure (limit states) by encouraging ductile modes of failure (diagonal strap yielding).

4.2 Coupon test results

To gain a better understanding of shear panel tests results, material tests were conducted on each of the primary components of the test panels. In order to design the panels it is important to know the material properties of critical panel elements such as the diagonal straps, columns, and anchor angles. Several coupons taken from these materials for each panel were tested in accordance with ASTM A370, *Standard Test Methods and Definitions for Mechanical Testing of Steel Products* (ASTM 2014b). The data obtained from each coupon are shown in Table 4-1 and Table 4-2. The results of the data were analyzed to determine average values for the yield stress, F_y, yield strain, plateau stress, ultimate stress, F_u, and strain at the ultimate stress. These average results are shown in Table 4-3.

Table 4-1. Coupon test results for the A1, A2, and A3 panels.

Material	Thickness (in.)	Yield Strain (in/in)	Yield Stress (ksi)	Plateau Stress (ksi)	Strain at Ultimate (in/in)	Ultimate Stress (ksi)	Ultimate / Yield Stress	Elongation in 2 in.	Stress at Elongation (ksi)
A1 Diagonal Strap									
Coupon 1a	0.0496	0.0013	44.21	43.23	0.183	52.04	1.18	22.0%	51.10
Coupon 1b	0.0480	0.0011	45.60	43.02	0.134	54.24	1.19	20.0%	53.80
Coupon 1c	0.0472	0.0014	45.22	44.58	0.160	54.52	1.21	21.6%	52.90
Coupon 1d	0.0476	0.0014	46.06	44.58	0.164	54.63	1.19	20.0%	54.10
A1 Strap Average	0.0481	0.0013	45.27	43.85	0.160	53.86	1.19	20.9%	52.98
A1 Column Stud									
Coupon 2a	0.0453	0.0013	43.25	43.61	0.134	53.83	1.24	20.5%	53.43
Coupon 2b	0.0469	0.0013	41.27	42.48	0.145	52.16	1.26	19.8%	46.36
Coupon 2c	0.0496	0.0013	41.38	40.05	0.166	49.36	1.19	19.9%	46.41
Coupon 2d	0.0504	0.0013	40.19	39.38	0.158	48.44	1.21	20.1%	47.98
Coupon 2e	0.0504	0.0013	40.77	39.65	0.155	48.24	1.18	20.1%	41.93
A1 Stud Average	0.0485	0.0013	41.37	41.03	0.152	50.41	1.22	20.1%	47.22
A2 Diagonal Strap									
Coupon 3a	0.0720	0.0007	31.90	N/A	0.189	49.70	1.56	21.8%	49.40
Coupon 3b	0.0720	0.0012	32.39	N/A	0.180	49.54	1.53	20.2%	49.44
Coupon 3c	0.0709	0.0009	32.47	N/A	0.211	50.78	1.56	21.7%	50.59
Coupon 3d	0.0709	0.0014	32.12	N/A	0.207	50.83	1.58	21.0%	50.43
A2 Strap Average	0.0715	0.0010	32.22	N/A	0.197	50.21	1.56	21.2%	49.97
A2 Column Stud									
Coupon 4a	0.1004	0.0017	61.04	60.17	0.117	73.78	1.21	16.9%	14.72
Coupon 4b	0.1004	0.0018	60.03	60.04	0.116	72.90	1.21	15.5%	15.87
Coupon 4c	0.1004	0.0019	58.97	60.37	0.128	73.22	1.24	17.3%	2.91
Coupon 4d	0.1004	0.0020	60.74	60.34	0.114	72.88	1.20	16.6%	0.22
A2 Stud Average	0.1004	0.0018	60.19	60.23	0.119	73.20	1.22	16.6%	8.43
A3 Diagonal Strap									
Coupon 5a	0.0433	0.0019	59.95	N/A	0.029	62.50	1.04	4.0%	60.58
Coupon 5b	0.0433	0.0021	59.86	N/A	0.035	62.34	1.04	6.9%	54.99
Coupon 5c	0.0433	0.0022	60.46	N/A	0.029	62.81	1.04	4.9%	60.19
Coupon 5d	0.0429	0.0020	60.61	N/A	0.032	63.11	1.04	13.7%	44.73
Coupon 5e	0.0429	0.0024	60.49	N/A	0.031	63.05	1.04	12.2%	45.01
Coupon 5f	0.0437	0.0029	59.85	N/A	0.028	61.95	1.04	4.6%	61.22
A3 Strap Average	0.0432	0.0023	60.20	N/A	0.031	62.63	1.04	7.7%	54.45
A3 Column Stud									
Coupon 6a	0.0555	0.0014	39.83	39.31	0.178	49.09	1.23	20.3%	48.76
Coupon 6b	0.0547	0.0014	40.04	40.20	0.182	49.94	1.25	20.4%	49.80
Coupon 6c	0.0551	0.0015	44.12	43.02	0.166	50.76	1.15	20.3%	50.58
Coupon 6d	0.0555	0.0014	42.62	41.84	0.170	50.04	1.17	20.5%	49.86
Coupon 6e	0.0551	0.0011	42.32	42.48	0.155	50.42	1.19	20.2%	50.22
A3 Stud Average	0.0552	0.0014	41.79	41.37	0.170	50.05	1.20	20.3%	49.84

Table 4-2. Coupon test results for the C1, D1, and D2 panels.

Material	Thickness (in.)	Yield Strain (in/in)	Yield Stress (ksi)	Plateau Stress (ksi)	Strain at Ultimate (in/in)	Ultimate Stress (ksi)	Ultimate / Yield Stress	Elongation in 2 in.	Stress at Elongation (ksi)
C1 Diagonal Strap									
Coupon 7a	0.0693	0.0029	79.50	N/A	0.026	80.87	1.02	11.5%	55.49
Coupon 7b	0.0673	0.0029	81.91	N/A	0.057	84.55	1.03	13.6%	61.12
Coupon 7c	0.0677	0.0027	80.82	N/A	0.025	83.07	1.03	13.2%	64.64
Coupon 7d	0.0681	0.0026	80.91	N/A	0.026	83.01	1.03	13.4%	62.97
Coupon 7e	0.0681	0.0026	81.12	N/A	0.027	83.49	1.03	12.3%	62.89
Coupon 7f	0.0681	0.0030	81.55	N/A	0.016	82.71	1.01	3.9%	80.60
C Strap Average	0.0679	0.0028	81.26	N/A	0.030	83.37	1.03	11.3%	64.62
C1 Column Stud									
Coupon 8a	0.0980	0.0020	65.90	66.29	0.078	81.53	1.24	19.3%	10.32
Coupon 8b	0.0976	0.0021	66.81	67.34	0.096	82.73	1.24	18.6%	11.10
Coupon 8d	0.0976	0.0025	65.54	66.16	0.098	81.81	1.25	17.2%	37.43
Coupon 8e	0.0980	0.0020	66.73	67.45	0.081	82.68	1.24	16.7%	7.56
Coupon 8f	0.0980	0.0021	66.18	66.84	0.085	82.18	1.24	16.1%	52.25
C1 Stud Average	0.0979	0.0021	66.23	66.82	0.088	82.18	1.24	17.6%	23.73
C1 Anchor Angle									
Coupon 9a	0.4976	0.0014	48.71	48.76	0.182	72.35	1.49	19.9%	71.39
Coupon 9b	0.4937	0.0016	51.72	51.58	0.146	74.40	1.44	20.8%	72.08
Coupon 9c	0.4929	0.0015	50.62	50.42	0.153	73.30	1.45	20.0%	72.31
C1 Angle Average	0.4948	0.0015	50.35	50.25	0.160	73.35	1.46	20.2%	71.93
D1 Diagonal Strap									
Coupon 10a	0.1079	0.0013	36.42	N/A	0.111	47.49	1.30	20.1%	46.89
Coupon 10b	0.1091	0.0012	38.03	N/A	0.131	47.70	1.25	19.8%	46.64
Coupon 10c	0.1079	0.0012	38.49	N/A	0.104	47.75	1.24	19.9%	47.11
Coupon 10d	0.1071	0.0011	37.56	N/A	0.128	47.81	1.27	20.0%	47.18
Coupon 10e	0.1079	0.0014	37.64	N/A	0.126	47.91	1.27	0.6%	39.83
D1 Strap Average	0.1080	0.0012	37.63	N/A	0.120	47.73	1.27	16.1%	45.53
D2 Diagonal Strap									
Coupon 11a	0.1004	0.0014	54.97	55.07	0.149	72.26	1.31	20.9%	70.61
Coupon 11b	0.1000	0.0016	54.96	55.69	0.137	73.22	1.33	20.5%	56.35
Coupon 11c	0.0996	0.0015	55.70	55.98	0.153	73.36	1.32	20.2%	71.91
Coupon 11d	0.0996	0.0018	55.43	55.39	0.164	72.69	1.31	21.6%	71.60
Coupon 11e	0.0992	0.0021	56.18	56.10	0.141	73.20	1.30	21.4%	72.27
Coupon 11f	0.1004	0.0010	55.82	56.02	0.144	73.14	1.31	21.3%	70.55
D2 Strap Average	0.0998	0.0016	55.62	55.71	0.148	73.12	1.31	21.0%	68.88
D2 Column HSS									
Coupon 12a	0.1705	0.0012	49.85	N/A	0.116	63.14	1.27	13.5%	62.51
Coupon 12b	0.172	0.0012	54.45	N/A	0.138	65.33	1.20	20.3%	64.65
Coupon 12c	0.1740	0.0017	48.42	N/A	0.149	64.32	1.33	19.1%	63.11
Coupon 12d	0.1724	0.0016	48.89	N/A	0.159	64.30	1.32	23.3%	63.28
Coupon 12e	0.1728	0.0018	48.88	N/A	0.154	64.30	1.32	20.0%	63.06
D2 Column HSS	0.1724	0.0015	50.10	N/A	0.143	64.28	1.29	19.2%	63.32
D2 Anchor Angle									
Coupon 13a	0.4886	0.0011	50.08	49.85	0.130	72.66	1.45	19.9%	71.71
Coupon 13b	0.4909	0.0013	50.44	50.49	0.151	73.46	1.46	17.6%	72.61
Coupon 13c	0.4898	0.0014	49.44	49.76	0.146	72.58	1.47	18.8%	72.06
D2 Angle Average	0.4898	0.0013	49.98	50.03	0.142	72.90	1.46	18.8%	72.13

Table 4-3. Average coupon test results for all panel types.

Material	Thickness (in.)	Yield Strain (in/in)	Yield Stress (ksi)	Plateau Stress (ksi)	Strain at Ultimate (in/in)	Ultimate Stress (ksi)	Ultimate / Yield Stress	Elongation in 2 in.	Stress at Elongation (ksi)
A1 Diagonal Strap	0.0481	0.0013	45.27	43.85	0.160	53.86	1.19	20.9%	52.98
A1 Column Stud	0.0485	0.0013	41.37	41.03	0.152	50.41	1.22	20.1%	47.22
A2 Diagonal Strap	0.0715	0.0010	32.22	N/A	0.197	50.21	1.56	21.2%	49.97
A2 Column Stud	0.1004	0.0018	60.19	60.23	0.119	73.20	1.22	16.6%	8.43
A3 Diagonal Strap	0.0432	0.0023	60.20	N/A	0.031	62.63	1.04	7.7%	54.45
A3 Column Stud	0.0552	0.0014	41.79	41.37	0.170	50.05	1.20	20.3%	49.84
C1 Diagonal Strap	0.0679	0.0028	81.26	N/A	0.030	83.37	1.03	11.3%	64.62
C1 Column Stud	0.0979	0.0021	66.23	66.82	0.088	82.18	1.24	17.6%	23.73
C1 Anchor Angle	0.4948	0.0015	50.35	50.25	0.160	73.35	1.46	20.2%	71.93
D1 Diagonal Strap	0.1080	0.0012	37.63	N/A	0.120	47.73	1.27	16.1%	45.53
D2 Diagonal Strap	0.0998	0.0016	55.62	55.71	0.148	73.12	1.31	21.0%	68.88
D2 Column HSS	0.1724	0.0015	50.10	N/A	0.143	64.28	1.29	19.2%	63.32
D2 Anchor Angle	0.4898	0.0013	49.98	50.03	0.142	72.90	1.46	18.8%	72.13

The material properties are defined in ASTM A370 (ASTM 2014b). Yield stress and strain were found using a 0.2% offset method. After finding the intersection of the 0.2% offset line and the stress-strain curve, the value of strain was offset by subtracting 0.2% from the intersection point. The result is a bilinear plot that is an accurate representation of the real stress-strain relationship. The plateau stress, given in Table 4-1 through Table 4-3, occurs when necking takes place in the test specimen prior to strain hardening. Necking of the specimen produces an increase in strain at a nearly constant stress, thereby forming a plateau on the curve. To find a value for the plateau stress, the average of the stress was taken from the point where the necking starts to the point where strain hardening begins. The values for ultimate stress and strain at the ultimate stress were obtained by finding the maximum value of stress and the corresponding strain at that stress. The material properties obtained and shown in Table 4-1 through Table 4-3 provide a fairly complete description of the material behavior of each coupon.

Figure 4-1 through Figure 4-6 plot the stress versus strain for the most representative coupons of each material. For example, after analyzing all of the data obtained from the tests conducted on the A1 diagonal strap specimens, the curve labeled “A1 Diagonal Strap” in Figure 4-1 was chosen as the most representative for that particular material. The “A1 Diagonal Strap” curve corresponds to the actual curve of coupon 1c from Table 4-1. Although some of the coupon results varied, one could expect a typical panel element to behave as shown in Figure 4-1 through Figure 4-6. Figure 4-1 plots the coupon test results for all the materials used in the A configuration panels. Figure 4-2 plots the same coupon data, but zooms in on the small strain region of up to 0.04 in./in., clearly showing material yielding and initial strain hardening. This region of small strains is of greatest interest because the test panels must reach large lateral deflections of 9.6 in. before the strap strains reach 0.04 in./in. Figure 4-3 and Figure 4-4 show similar plots for the C1 panel materials. Figure 4-5 and Figure 4-6 show these plots for the D configuration panels.

Table 4-1 and Table 4-2 show that A3 and C1 diagonal straps do not meet the required 1.08 ratio of ultimate over yield strength and the A3 straps do not meet the 10% elongation requirement for ASTM A 1003/A 1003M high-ductility steel (ASTM 2013b). The lack of a plateau in the stress-versus-strain plot and lack of increase in stress beyond yield for the A3 and C1 straps shown in Figure 4-1 and Figure 4-3 show they were strain hardened. The A2 straps may also have been somewhat strain hardened based on a lack of a plateau in Figure 4-1. Coupon tests of the A3, C1, and D2 strap materials were conducted before designing their test panels so that the panels could be designed where strap strength was equal to the maximum strength in accordance with the Bethlehem Steel study. For example, the measured yield strength of the A3 strap was 60.1 ksi, and the panel was designed as if the strap specified design strength was 30 ksi, as if Grade 33 material had been specified (see panel A3 strap specification in Figure A-7).

Table 4-3 shows the material thickness, yield strain, yield stress (F_y), ultimate stress (F_u), ratio of ultimate over yield stress, and elongation within the 2 in. coupon gage length for all the primary materials used in the cold-formed steel test panels except the D1 column hollow structural section, HSS.

Figure 4-1. Coupon test results for the A1, A2, and A3 panels.

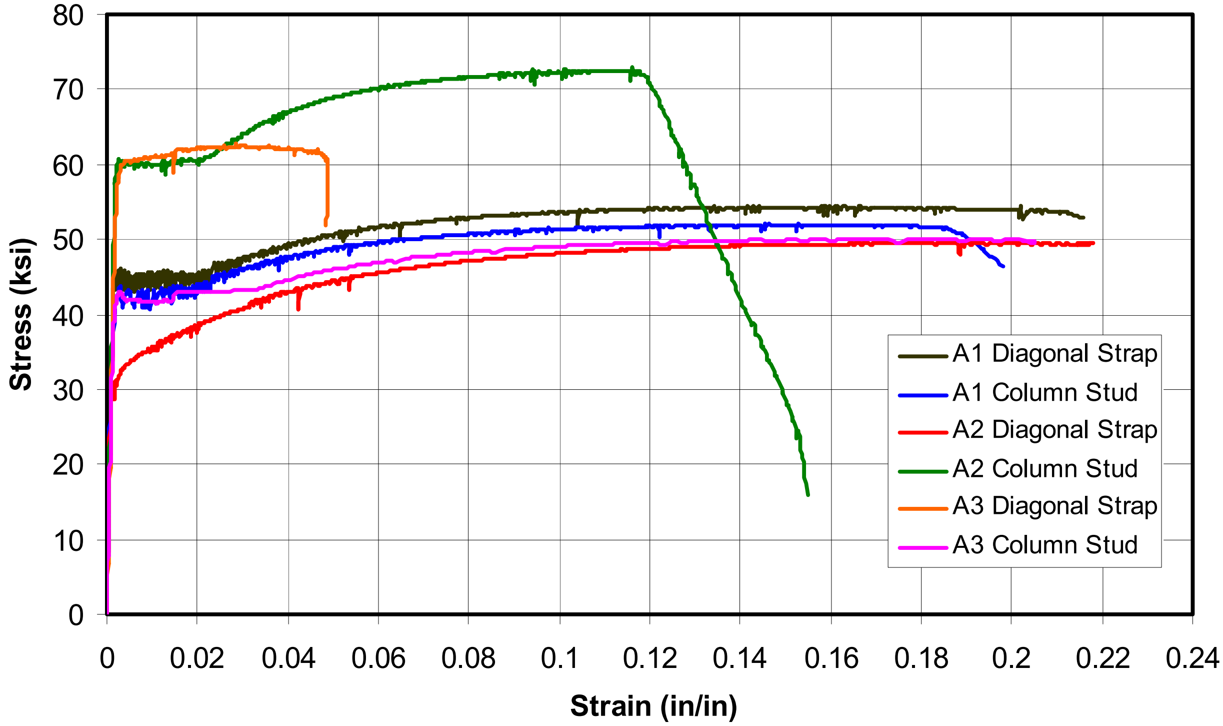

Figure 4-2. Coupon test results at small strains for the A1, A2, and A3 panels.

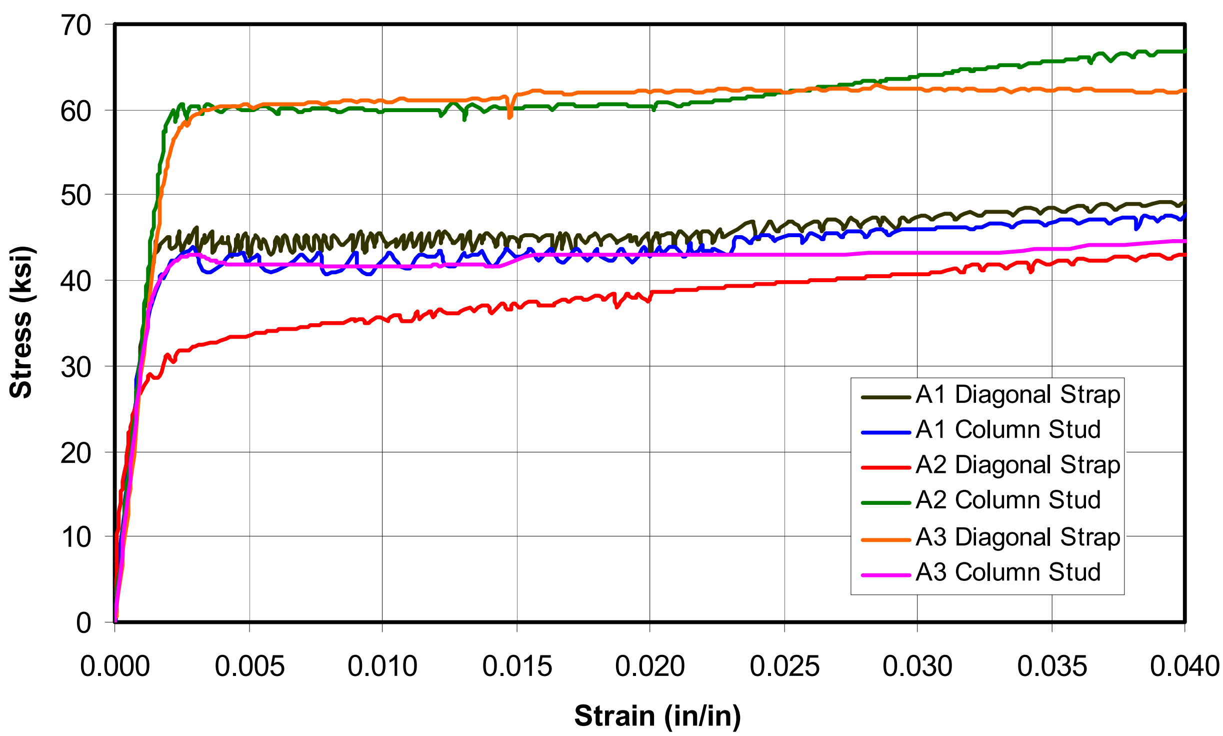

Figure 4-3. Coupon test results for the C1 panels.

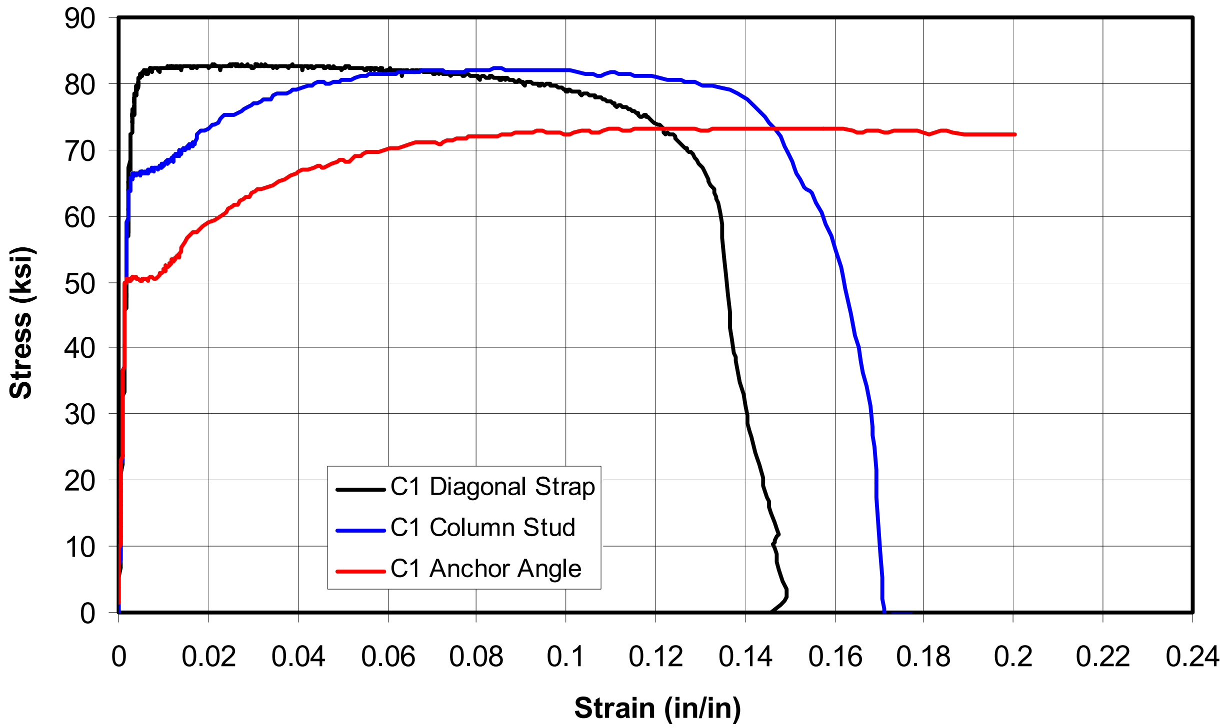

Figure 4-4. Coupon test results at small strains for the C1 panels.

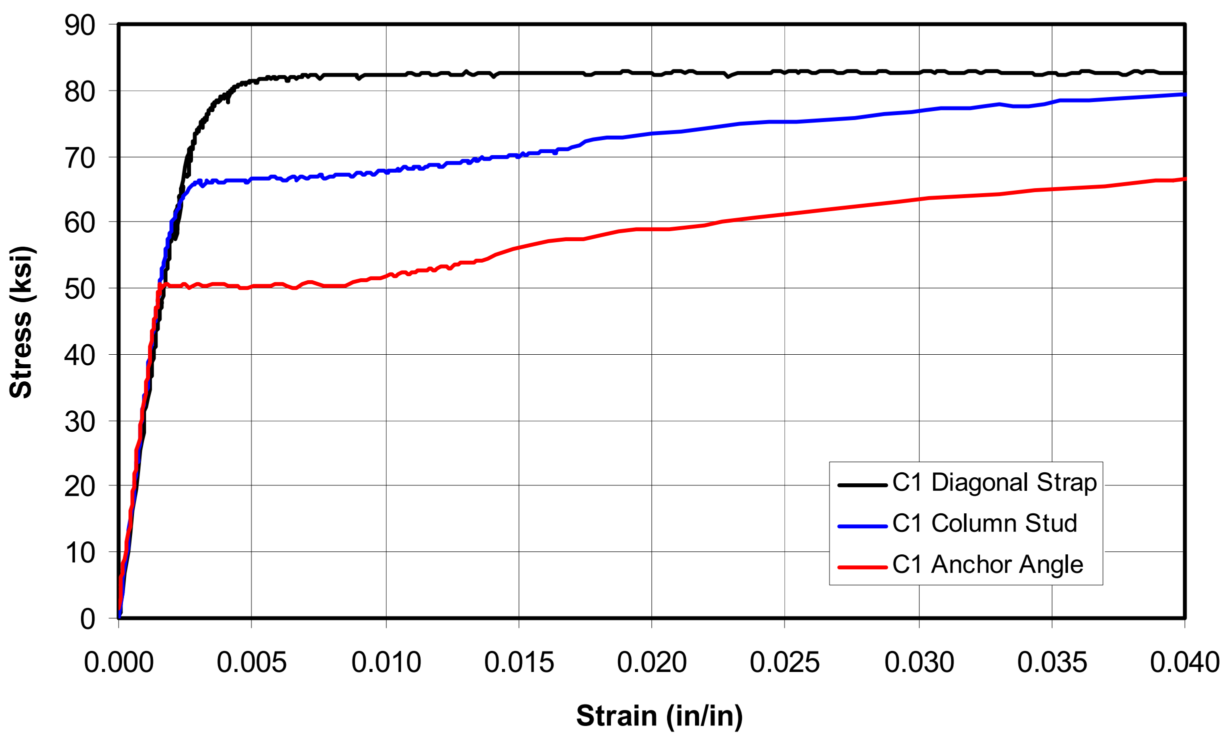

Figure 4-5. Coupon test results for the D1 and D2 panels.

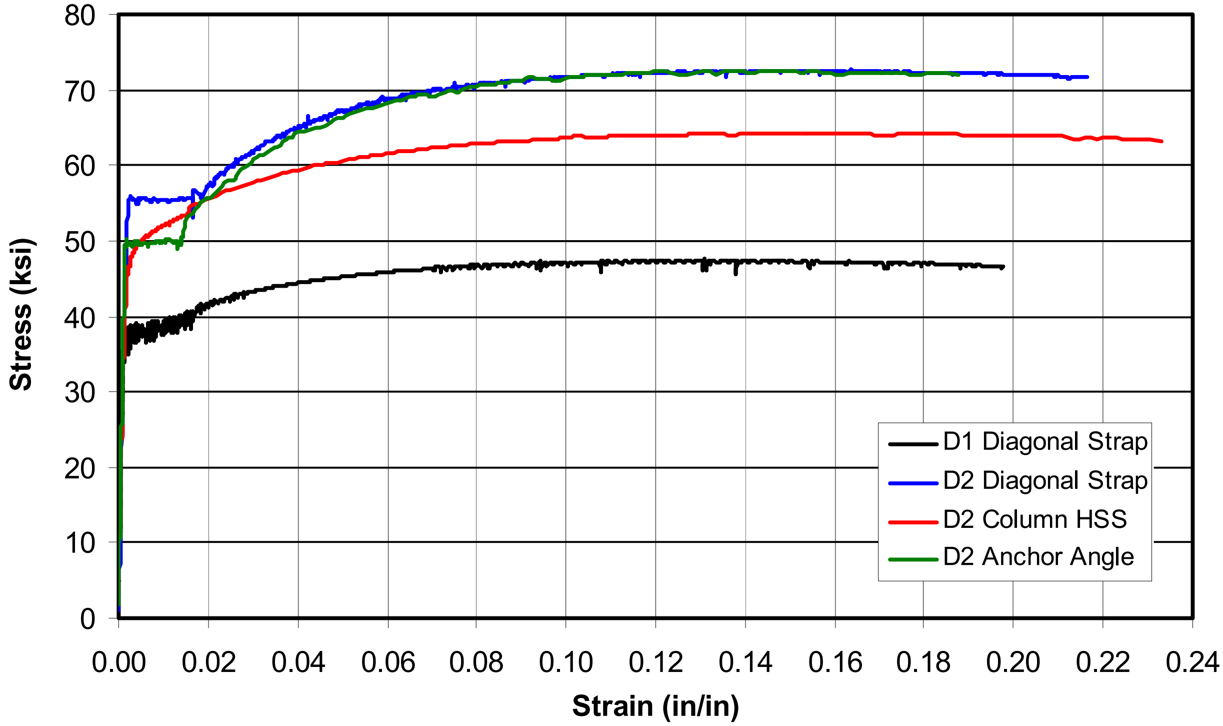

Figure 4-6. Coupon test results at small strains for the D1 and D2 panels.

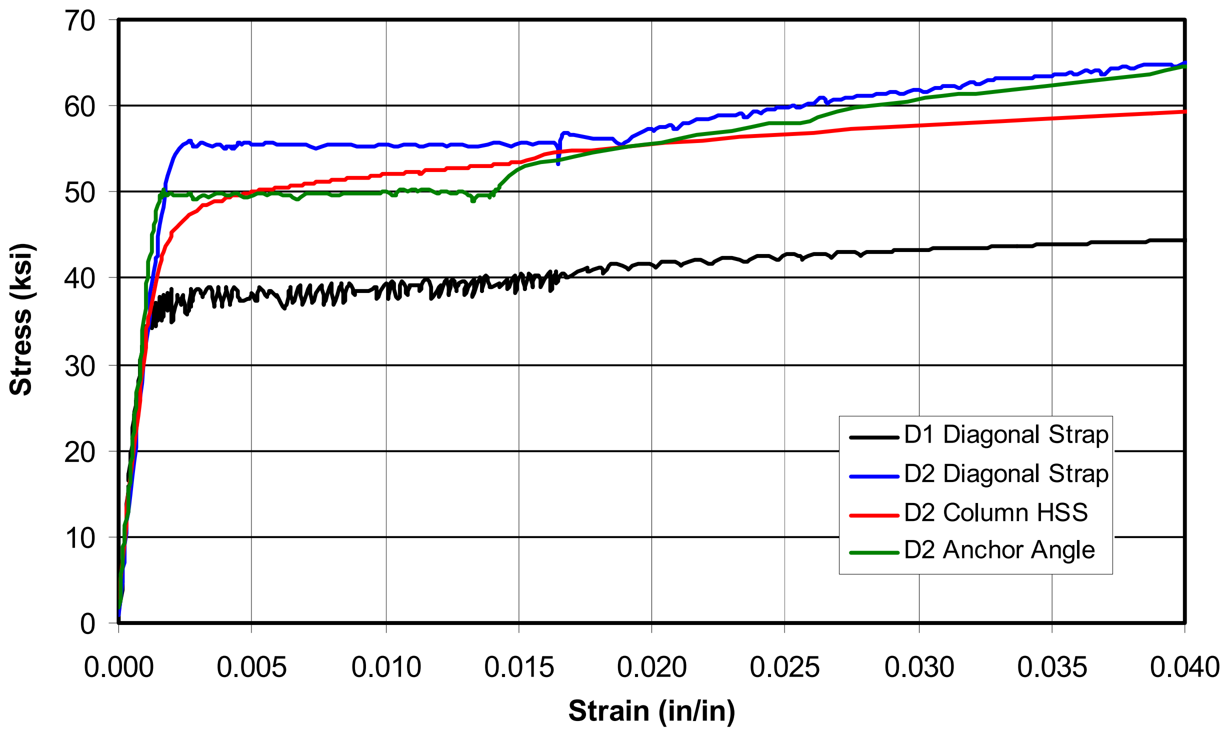

5 Predicted Panel Response Based on Analytical Model and Coupon Test Results

The model developed in Chapter 3 can be modified for predicting shear panel lateral-load-versus-deformation behavior. This model can be expanded to develop predicted envelopes of lateral load capacity versus deformation, which include data points at strap yielding and column yielding. The measured diagonal strap and column material properties presented in Chapter 4 are used in this model to predict panel behavior. These predictions can be compared with test data to evaluate the model.

When the shear panels are loaded laterally, they should behave linearly until the diagonal straps begin to yield. The first point on a plot of the predicted lateral load-versus-deformation plot is the lateral capacity of the diagonal strap alone at lateral yield deformation of the strap. The lateral capacity of a shear panel, based on the strap strength alone, Q_{sy}, when the strap begins to yield, was defined in Equation 3-1. The panel lateral deformation when the strap yields, δ_{sy}, was given in Equation 3-2. The diagonal strap properties and calculation of the strength and deformation values are shown in Table 5-1, and they are plotted in Figure 5-1 for each cyclically tested shear panel. Table 5-2 and Table 5-3 provide additional properties of the test panel straps and columns.

The second point on the plot is the total panel lateral force at strap yielding, Q_{Tsy}, defined in Equation 3-7. This adds the lateral resistance from the two panel columns assuming they are fully fixed at both their tops and bottoms, Q_{csy}, defined in Equation 3-6. The columns can act as a moment frame assuming they are anchored to the floor diaphragms above and below. The degree of fixity of the moment connections is unknown, so Q_{sy} becomes a lower estimate of panel capacity assuming the columns have pinned connections and Q_{Tsy} is an upper estimate of capacity assuming full column fixity. Values for Q_{Tsy} are shown in the third column of Table 5-4 for each test panel.

Table 5-1. Test panel diagonal strap properties and predicted lateral capacity.

Column Type	Panel Width W (in)	Panel Height H (in)	Strap Faces n_s (#)	Strap Width b_s (in)	Strap Thickness (ga)	Strap Thickness t_s (in)	Strap Initial Lat Stiffness k_s (k/in)	Yield Stress of Strap F_{sy} (ksi)	Capacity at Strap Lat Yield Q_{sy} (k)	Design Shear Strength $\phi_t Q_{sy}$ (k)	Lat Defl at Strap Yielding δ_{sy} (in)
A1	121	120	1	4	18	0.0481	17	45.3	6.2	5.9	0.375
A2	121	120	2	8	14	0.0715	98	32.2	26.2	24.8	0.267
A3	123	120	1	4	18	0.0432	15	60.2	7.5	7.1	0.498
C1	121	120	2	8	14	0.0679	93	81.3	62.7	59.5	0.673
D1	121	120	2	8	12	0.1080	148	37.6	46.1	43.8	0.311
D2	119	120	2	8	12	0.0998	136	55.6	62.5	59.4	0.460

Figure 5-1. Predicted lateral load-versus-deflection for all test panels.

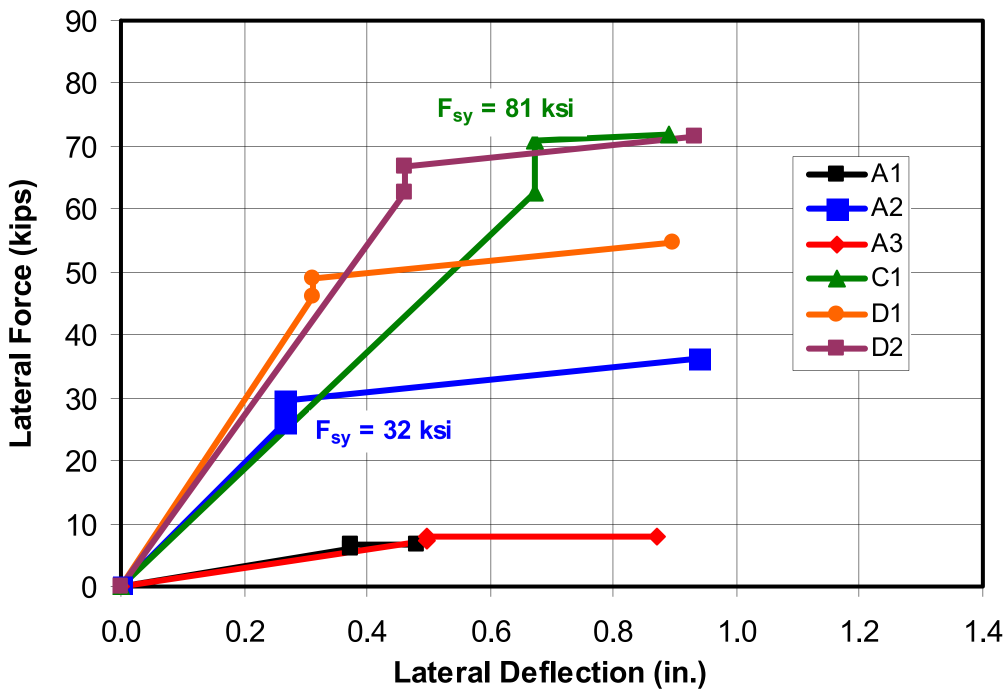

Table 5-2. Additional properties of test panel straps, gravity loads, and columns.

Column Type	Diagonal Strap Ult Stress F_{su} (ksi)	Max Ult Strap Stress F_{sumax} (ksi)	Max Gravity Load/ Panel GL_{max} = (kips)	Column Axial load at Strap Ult P_{vumax} (k)	Column Yield Stress F_{cy} (ksi)	Column Ultimate Stress F_{cu} (ksi)	Column Thickness (ga)	Column Thickness t_c (in)	Number of Studs /Column n	Panel Thickness /Column b_c (in)	Col Stud Flange Width b_f (in)	Column Depth h_c (in)
A1	53.9	53.9	27	20.8	41.4	49.9	18	0.0485	2	6.0	2.0	4.0
A2	50.1	50.1	27	53.8	60.3	72.9	12	0.1004	4	6.0	2.0	8.0
A3	62.5	62.5	10	12.5	41.8	49.9	16	0.0552	2	3.625	2.0	4.0
C1	82.5	82.5	30	78.4	66.3	82.0	12	0.0979	4	6.0	2.0	8.0
D1	47.6	47.6	27	71.4	45.1	53.7		0.1875	1	6.0	6.0	6.0
D2	72.6	72.6	30	97.4	50.0	64.0		0.1724	1	6.0	6.0	6.0

Table 5-3. Area and section modulus of test panels.

Column Type	Nominal Column Area A_c (in^2)	Distance to Extreme Fiber c (in)	In-Plane Mom of Inertia I_x (in^4)	In-Plane Radius of Gyration r_y (in)
A1	0.97	2.00	2.75	1.68
A2	4.02	4.00	31.16	2.79
A3	0.84	2.00	2.10	1.58
C1	3.91	4.00	30.42	2.79
D1	4.27	3.00	23.8	2.36
D2	4.27	3.00	23.8	2.36

Table 5-4. Test panel predicted lateral capacities.

Column Type	Lat Defl at Strap Yielding δ_{sy} (in)	Capacity at Strap Lat Yield Q_{Tsy} (k)	Lat Defl at Col Yielding δ_{cy} (in)	Column Lat Cap @Yield Q_{cy} (k)	Total Lat Cap @CYield Q_{Tcy} (k)	Col Axial Stress @ Strap Yield f_{ca} (ksi)	Col Bend Stress @ Col Yield f_{cb} (ksi)	Col Comb Stress @ Col Yield f_{cr} (ksi)
A1	0.358	6.3	0.677	0.8	6.7	16.9	24.4	41.4
A2	0.268	29.7	1.038	13.0	39.3	6.6	53.7	60.3
A3	0.497	7.8	0.974	0.8	8.3	10.2	31.5	41.8
C1	0.670	71.0	1.001	12.3	75.1	11.8	54.5	66.3
D1	0.309	48.8	0.898	8.6	54.5	8.5	36.6	45.1
D2	0.463	67.5	0.927	8.9	71.9	11.0	39.0	50.0

The third point on Figure 5-1 is where the columns themselves yield. The columns have axial stresses coming from the gravity load and from the vertical component of the diagonal straps in tension that are connected to the top of the columns. The laterally deformed columns also have bending stresses from the P-delta effect of the vertical load and from the applied lateral load. The total lateral capacity at column yielding, Q_{Tcy}, includes braced frame and moment frame components, and are shown Equation 5-1. Values for Q_{Tcy} are shown in the second or center section of Table 5-4.

$$Q_{Tcy} = Q_{sy} + Q_{cy} \qquad \text{(Eq 5-1)}$$

where

Q_{cy} = the lateral force carried by the columns at column yielding.

Q_{cy} is unknown in the above equation. To calculate Q_{cy}, the lateral displacement that would cause the column to yield is calculated. Yielding will occur when the combination of axial and bending stresses exceed the yield strength. The column total stress, f_{cr} at the extreme fiber is given by:

$$f_{cr} = f_{ca} + f_{cb} \qquad \text{(Eq 5-2)}$$

where

f_{ca} = the column axial stress
f_{cb} = the column bending stress.

The column axial stress due to the gravity load and vertical component of the diagonal strap is determined by the following relationship:

$$f_{ca} = \frac{GL_{max} + F_{sy} n_s b_s t_s \left(\frac{H}{\sqrt{H^2+W^2}}\right)}{2A_c} \qquad \text{(Eq 5-3)}$$

where

GL_{max} = the maximum gravity load per shear panel
A_c = the cross-sectional area of a single column.

The bending stress is due to the moment from both the P-delta effect of the vertical forces and lateral force carried by the columns, which is calculated as follows:

$$f_{cb} = \frac{Mc}{I} = \left[\left(GL_{max} + F_{sy} n_s b_s t_s \left(\frac{H}{\sqrt{H^2+W^2}}\right)\right)\delta_{cy} + \frac{Q_{cy}H}{2}\right]\frac{c}{2I_x} \qquad \text{(Eq 5-4)}$$

where

δ_{cy} = the lateral deflection of the panel that causes the column to yield
c = the distance from the neutral axis of the column to the extreme fiber
I_x = the x-axis (in-plane) moment of inertia of a single column.

Equation 5-4 shows the bending stress in the columns is dependent on both δ_{cy} and Q_{cy}, and Equation 5-5 (below) shows the column lateral yield capacity, Q_{cy}, depends on δ_{cy}. Therefore, these values are determined iteratively, by selecting values of δ_{cy} until the total column stress, f_{cr} equals the column yield strength. In Equation 5-4 the GL_{max} value should be the total maximum gravity load supported by all of the columns whose lateral loads are resisted by the shear panel.

$$Q_{cy} = 2\frac{12EI_x\delta_{cy}}{H^3} \qquad \text{(Eq 5-5)}$$

The columns yield before the straps begin to strain harden, so the strength of the straps used in these calculations should be their yield strength.

5.1 Panel A1

Table 5-1 and Figure 5-1 show that panels A1 and A3 have the smallest predicted capacity and stiffness of all the test panels. Table 5-4 indicates the A1 panel has only a 6% greater lateral capacity at column yield than at strap yield. This increase would be even smaller if the full moment capacity of the columns was not developed by the column-to-track connection. The panel lateral deflection at which the columns yield, δ_{cy}, is the smallest of all panels with a value of 0.68 in. The small increase in strength from the columns and the small ductility at column yielding indicate that the hysteretic envelope was expected to be badly pinched. These predictions assume full column fixity, and the columns are anchored with only screwed connections to the track above and below as shown in Appendix A, Figure A-3. These anchors were expected to be much closer to pinned than fixed, so the panel lateral capacity was expected be closer to the first point in Figure 3-1, and was not expected to increase as the panel deformed. The ultimate panel deformation however, should be much greater than the predicted deflection at column yielding at 0.68 in., because the pinned connections will reduce bending stresses on the columns.

5.2 Panel A2

Panel A2 is the same basic configuration as the A1 panel, but it uses much heavier materials. It has much greater predicted capacity and stiffness than the A1 panel. Table 5-4 shows this panel has 33% greater lateral capacity at column yield than at strap yield. This indicates that the column moment frame contribution to panel capacity is much greater than with the A1 panel. This is an upper estimate of column contribution, assuming full fixity of the column to nested stud-and-track connection. The heavy track and nested stud that is welded to the columns, as shown in Figure A-5, would greatly increase the moment resistance compared to the A1 panel. However, this connection detail was intended to provide shear resistance and only a limited moment connection, so the peak lateral capacity was expected to be closer to lateral capacity from the strap only, Q_{sy} (26.2 kips as shown in Table 5-1), than the capacity at column yield, Q_{Tcy} (39.3 kips in Table 5-4). This increase in strength from the columns and the larger panel deformation at column yielding (1.038 in. in Table 5-4) indicate that the hysteretic envelope should not be as badly pinched as for Panel A1.

5.3 Panel A3

Figures A-6 and A-7 show the A3 panel configuration is almost identical to A1. The A3 panel is slightly wider (W = 123 in.), the strap actual thickness is slightly less (Table 5-1), and the strap strength is greater. The A3 column thickness is slightly greater, the yield strength is slightly greater and the ultimate strength is the same. The depth of the panels, which is the width of the columns were much less (b_c in Table 5-2 is only 3.625 in.) than for the A1 panel. The predicted lateral capacity from the strap only is greater for this panel because of the much greater strap strength. The gravity load applied to the panel (GL_{max} = 10 kips) is much less than for A1 (GL_{max} = 27 kips). Table 5-4 indicates the A3 panel has only a 12% greater lateral capacity at column yield than at strap yield. This greater contribution relative to the 6% for the A1 panels is because of the much smaller gravity load. The off-the-shelf anchors used in the A3 panels (Figure A-7), should provide slightly more moment resistance than the A1 panel had. However, fixity of the anchors was expected to be very small, so the peak lateral capacity of this panel was expected to be closer to yield capacity of the straps alone, Q_{sy} (7.5 kips in Table 5-1), than the capacity at column yield, Q_{Tcy} (8.3 kips in Table 5-4). This panel is much different from the A1 panel in that the columns and hold-down anchor uplift resistance are designed assuming the maximum yield (F_{symax}) and ultimate strength (F_{sumax}) of the diagonal straps equals the actual measured strength of the strap material. For the A3 panel the measured yield strength was 60.2 ksi, but the design yield strength was taken as 30 ksi to simulate the worst case loading condition when the diagonal strap yield strength equals twice the specified value for Grade 33 material (see beginning of Chapter 4). The purpose of this test was to evaluate the performance of the columns, connections, and anchors under the worst-case material strength variability of the strap. The panel should deform enough to develop the full yield strength of the straps, but it may not deform much beyond this because the strain-hardened straps that are not permitted in actual design may fracture at relatively small elongations.

5.4 Panel C1

Figures A-8 and A-9 show that the C1 panel is similar to the A2 panel, in that the diagonal straps and columns are the same size. The primary differences are (1) the straps are welded rather than screwed to the columns; (2) the columns anchors are angle sections with stiffeners rather than heavy nested studs and tracks; and (3) that panel columns, connections, and anchors were designed assuming the strap coupon strength equaled the F_{symax}. This anchor detail should provide greater fixity for the columns to act as moment frames. The strap specification in Figure A-9 shows the C1 straps had a measured yield strength of 81 ksi, but the design yield strength was taken as 41 ksi to simulate the worst-case loading condition when the diagonal strap yield strength equals twice the specified value for Grade 33 material (see beginning of Chapter 4). This panel should deform enough to develop the full yield strength of the straps, but it may not deform much beyond this because of the strain-hardened straps. Figure 5-1 shows that the predicted capacity of this panel was much greater than the A2 panel even though the strap and column sizes are the same. This difference is because the strength of the C1 straps is much greater.

Table 5-4 indicates the C1 panel has 20% greater lateral capacity at column yield than at strap yield. Since the column fixity should be greater than for the A2 panel, the actual ultimate capacity should be much greater than when the straps yield, that is if the panel is able to deform significantly before fracturing the strain-hardened straps. The predicted yield capacity from the straps alone, Q_{sy}, is 62.7 kips (see Table 5-1), and the total capacity of the panel from straps and columns at column yield, Q_{Tcy}, is 75.1 kips (see Table 5-4).

5.5 Panel D1

The panel D configuration generally will have the highest capacity and stiffness because the panel columns are hollow structural sections of HSS, so that their thickness can be much greater than for columns built up from standard cold-formed steel studs. The panel D1 test panel uses HSS 6 x 6 x 3/16 in. columns, which is more than 80% thicker than the A2 or C1 column material. The D1 columns have a slightly greater section modulus ($S_x = I_x/c$ in Table 5-3), so they are generally stronger, but their moment of inertia, I_x, is lower, so they are less stiff than the A2 and C1 columns. This panel has the diagonal straps welded to the HSS columns and the anchors consist of heavy studs nested inside heavy tracks, as shown in Figures A-10 and A-11. The D1 panel has welded nested stud anchors, so the peak lateral capacity was expected to be closer to the lateral capacity from the strap only, Q_{sy} (46.1 kips in Table 5-1), than the capacity at column yield, Q_{Tcy} (54.5 kips in Table 5-4). These values indicate the D1 panel has 19% greater predicted capacity at column yield than from strap yield alone. However, the relatively small column fixity of the nested stud anchor connection should result in a relatively modest increase in capacity beyond yield and a fairly pinched hysteretic envelope.

5.6 Panel D2

Figures A-12 and A-13 show that the D2 panel is very similar to the D1 panel. The primary differences are (1) the columns anchors are angle sections with stiffeners rather than heavy nested studs and tracks; and (2) that panel columns, connections and anchors were designed assuming the strap coupon strength equaled the F_{symax}. This anchor detail should provide greater fixity for the columns to act as moment frames. The strap specification in Figure A-13 shows the D2 straps had a measured yield strength of 56 ksi, but the design yield strength was taken as 28 ksi to simulate the worst case loading condition when the diagonal strap yield strength equals twice the specified value. This panel should deform enough to develop the full yield strength of the straps. Figure 4-5 and Figure 4-6 show the D2 diagonal straps were not strain hardened. However, the worst-case loading condition may result in other panel failures not too long after diagonal strap yielding. But because the diagonal straps are not hardened, the panel should reach greater deformations than the C1 panel.

Table 5-1 and Table 5-4 indicate the D2 panel has 15% greater predicted lateral capacity at column yield (Q_{Tcy} = 71.9 kips) than at strap yield (Q_{sy} = 62.5 kips). The strength of the D2 column material is lower than for C1, so the yield capacity, Q_{cy}, of the D2 column is less. Since the column fixity should be good and the straps are not strain hardened, the actual ultimate panel capacity should be much greater than when the straps yield. The hysteretic envelope should be relatively wide.

6 Test Configuration, Procedures, and Instrumentation

Figure 6-1 shows the test frame and configuration used to test all monotonically and cyclically loaded cold-formed steel shear panels. This configuration includes the strong floor that supports the reaction wall and panel base beam. A large, 40 in. stroke horizontal actuator is mounted to the face of the reaction wall on one end and the load beam on the other end.

Figure 6-1. Test frame used for monotonic and cyclic shear panel testing.

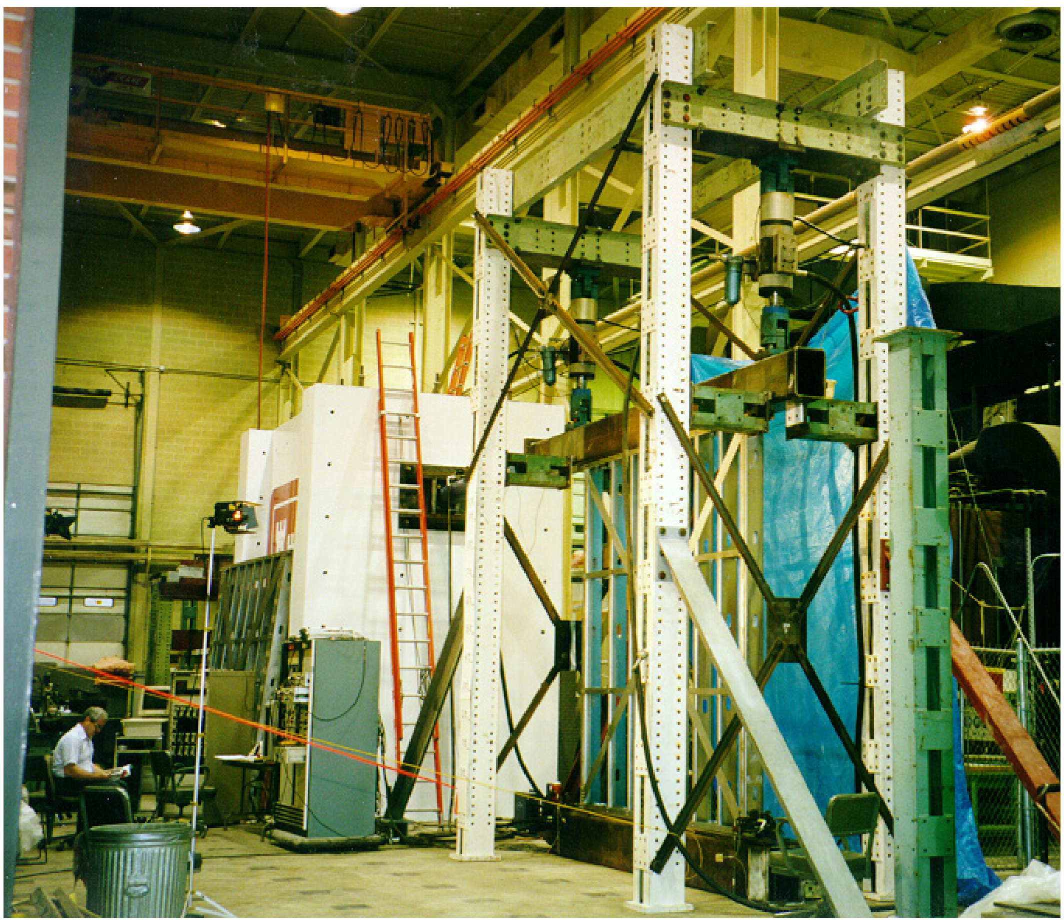

The figure also shows an A2 test panel installed in the frame. The bottom of the test panel is bolted to the top of the base beam, and the top of the panel is bolted to the bottom of the load beam. An additional steel frame was constructed around the test panel to support two vertical actuators which, in turn, provide vertical support for the load beam. The load beam is restrained against out-of-plane motions with Teflon® plates that bear against the polished surfaces of the load beam. These plates are attached to the steel frame with short, horizontally oriented columns. The steel frame is braced to make it very rigid in order to prevent either in-plane or out-of-plane deformation. Figure 6-2 shows schematic drawings of in-plane and out-of-plane views of the test frame.

Figure 6-2. In-plane and out-of-plane views of the test frame.

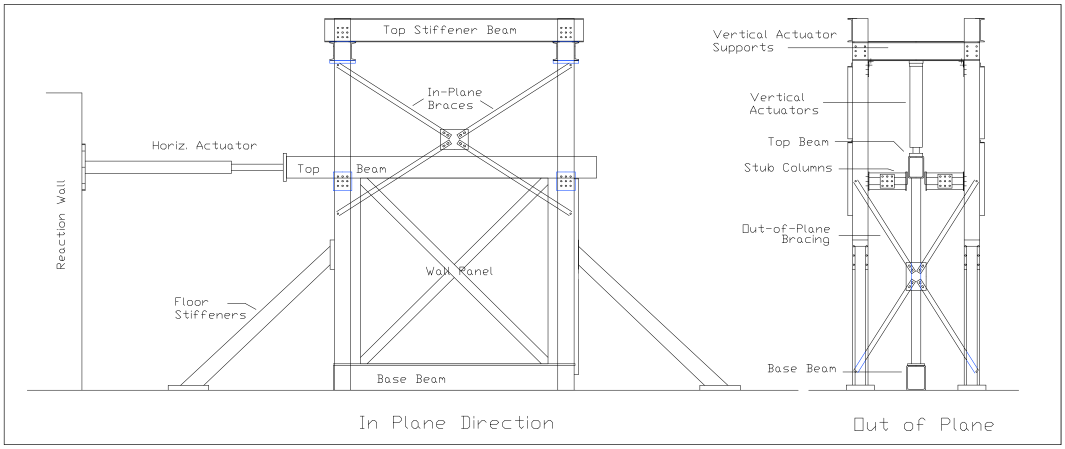

Partly because of the test configurations reported in Caccese et al. (1993) and Driver et al. (1998a), the test configuration used at ERDC-CERL was designed to prevent rotation of the top beam, allowing only pure shear and overall axial deformation of the panel. A constant axial load (2.5 kips/ft width, or 25 kips for a 10 ft wide panel) was applied to the top beam using two vertical actuators, and the top beam was not allowed to rotate. The top beam was allowed to deflect vertically at large horizontal deflection as the columns began to shorten or buckle. This vertical load was maintained so that when one column shortened, a portion of the vertical load was redistributed to the other shear panel column. This redistribution is similar to what will occur in a real building that has multiple shear panels in the same plane, connected on top by the floor diaphragm/floor beam. It is particularly important that the top beam be held horizontal after the columns begin to buckle and deform significantly vertically. The ability of the panels to sustain load even after severe damage is critical to determining panel ductility and seismic design recommendations. Also, the top beam and track/top beam connection must be very stiff to adequately anchor the tension field for sheet steel panels.

Vertical loads equal to the GL_{max} values in Table 5-2 (including the weight of the top beam) were applied to the panels using the vertical actuators. The total load of both vertical actuators was held constant in load control, while the top beam was held horizontal with one actuator slaved to the other in stroke control. Stroke control was used to keep the deflection of the north actuator equal to that of the south actuator. This allowed the load to redistribute between the vertical actuators as needed to maintain the total load and horizontal orientation of the load beam. In a real earthquake the diaphragm on at the top of the wall would remain horizontal if it is rigid and two or more similar panels are installed in the same framing line.

For each panel configuration three specimens were tested, one was tested monotonically, and two were tested cyclically. The monotonic tests were conducted first to define the monotonic load-versus-deflection behavior through ultimate failure of each panel configuration. Monotonic tests also confirmed the calculated yield deflection, δ_y. The calculated yield deflection was the lateral deflection at which the diagonal strap would yield, defined in Equation 3-2. The calculated yield deflection based on the design yield strength was 0.273 in. for all panels. The calculated yield deflections based on the measured diagonal strap coupon yield strength were 0.375 in., 0.267 in., 0.498 in., 0673 in., 0.311 in., and 0.460 in. for test panels A1, A2, A3, C1, D1, and D2, respectively, as shown in the right column of Table 5-1. Recognizing that actual deflections would generally be greater, because of other sources of deformation in the panels, the yield deflection, δ_y, was set to 0.4 in. for all panels. This value agreed well with the observed yield deflection of the monotonically and cyclically loaded panels.

6.1 Monotonic test protocol

Lateral loads were applied using stroke control for both monotonic and cyclic tests. Monotonic tests were push-over tests in which the load was applied laterally at a constant stroke rate. A stroke rate of 0.5 in. per minute was used for the A1, A2, D1, and D2 monotonic tests, while a rate of 1.0 in. per minute was used for A3 and C1. The panels were loaded until ultimate failure or up to a maximum stroke of 15 in. The stroke rate is not critical, but should be slow enough to allow adequate time for making observations. The monotonic tests confirmed that panel yield consistently took place near 0.4 in.

6.2 Cyclic test protocol

The test protocol used should follow a standard method, so that test results can be compared with cyclic test results of other programs. Two similar cyclic test protocols were considered. Both use stroke control for cyclic testing to define hysteretic performance of building components. The first is the Applied Technical Council (ATC) 24, *Guidelines for Cyclic Seismic Testing of Components of Steel Structures* (ATC 1992). The second is the unpublished guidance, *SAC Testing Programs and Load Histories* (SAC n.d.). The ATC-24 guidance calls for a set number of cycles at deformations that are scaled to the measured or estimated panel yield deflections. The second and third columns in Table 6-1 show the deformations and number of cycles at those deformations scaled to a yield deflection of 0.4 in. and gives deformation values up to the 23rd load step, or deformation of 8.4 in. (for ATC-24 guidance).

Table 6-1. ATC-24 and modified SAC cyclic test steps based on 0.4 in. yield deformation.

Load Step #	ATC-24		SAC-2		Modified SAC (inches)
	Peak Deformation (inches)	Number of Cycles	Peak Deformation, ϑ (radians)	Number of Cycles, n	
1	0.2	3	0.00375	6	0.3
2	0.3	3	0.005	6	0.4
3	0.4	3	0.0075	6	0.6
4	0.8	3	0.01	4	0.8
5	1.2	3	0.015	2	1.2
6	1.6	2	0.02	2	1.6
7	2.0	2	0.03	2	2.4
8	2.4	2	0.04	2	3.2
9	2.8	2	0.05	2	4.0
10	3.2	2	0.06	2	4.8
11	3.6	2	0.07	2	5.6
12	4.0	2	0.08	2	6.4
13	4.4	2	0.09	2	7.2
14	4.8	2	0.10	2	8.0
15	5.2	2	0.11	2	8.8
16	5.6	2	0.12	2	9.6
17	6.0	2	0.13	2	10.4
18	6.4	2	0.14	2	11.2
19	6.8	2	0.15	2	12.0
20	7.2	2	0.16	2	12.8
21	7.6	2	0.17	2	13.6
22	8.0	2	0.18	2	14.4
23	8.4	2	0.19	2	15.0*

* Shear test panels at ERDC-CERL were tested monotonically and cyclically up to deformations as high as 15.0 in. (30 in. peak to peak). This deflection reached the rotation limit of the vertical actuators. Modification to the vertical actuator clevis would permit testing up to deformations of 40 in. peak-to-peak.

The SAC testing protocol is a modification of the earlier ATC-24 protocol. The SAC-recommended loading histories call for loading with a deformation parameter based on interstory drift angle, ϑ, defined as interstory height over interstory displacement. The commentary to the SAC document explains that the interstory drift angle of 0.005 radians corresponds to a conservative estimate of the value that would cause yield deformation. The interstory drift deformation that corresponds to an interstory drift of 0.005 radians is 0.63 in. (126 in. x 0.005). Because the SAC protocol was primarily developed for a different, more flexible structural system than the shear panels in this study (welded beam-to-column subassemblies), the interstory drift is modified (scaled) slightly so that the deformation at yield equals 0.4 in. Table 6-1 shows the SAC drift angles and corresponding modified SAC deformation values up through the maximum stroke limitation of the ERDC-CERL shear panel test facility (15 in.).

Most of the cyclic tests were conducted at a stroke rate of 6 in. per minute (Panels A2, D1, and D2). This rate was slow enough to allow adequate time to observe deterioration development while providing reasonable test duration for cyclic tests up to deformations of 15 in. Figure D-2 of Appendix D plots the modified SAC deformation time history up to the first cycle at 14.4 in., at a stroke rate of 6 in. per minute. A stroke rate of 3 in. per minute was used for Panel A1 cyclic tests, where the peak achieved deflections were lower and a slower rate was needed to observe the panel deterioration. A stroke rate of 12 in. per minute was used for both panel A3 cyclic tests and one panel C1 cyclic test.

6.3 Instrumentation

Table D-2 of Appendix D summarizes the purpose, type and location of all sensors used in the shear panel tests. This includes the force measured in the load cells and deflection measured in the LVDTs of the actuators. Figure D-1 of Appendix D shows the locations of all sensors on a schematic drawing.

Measurements taken by channels 7 through 9, as described in Table D-2 and Figure D-1, demonstrate that no significant slippage or uplift took place during any test. These values remained lower than 0.04 in. and 0.14 in., respectively, which are insignificant relative to the very large horizontal deflection. Therefore the horizontal deflection (DH) represents the shear panel deformation with no correction needed for slippage or rotation.

At very large horizontal deflections, the vertical actuators applied load to the top beam at a large angle. Both actuators always had the same angle and applied a net axial load to the top beam of GL_{max} minus the weight of the load beam and half the horizontal actuator (2.45 kips). At large angles, these actuators applied a horizontal component to the top beam that must be combined with the load in the horizontal actuator to calculate the total shear force, TSF. This total shear force can be expressed as

$$TSF = FH \pm FS(sin\theta) + FN(sin\theta) = FH \pm TVF(sin\theta) \qquad \text{(Eq 6-1)}$$

where

FH = the horizontal actuator force
FS = the South actuator force
θ = the Vertical actuator angle (in radians) with respect to vertical
FN = the North actuator force
TVF = the total vertical actuator force
θ = arctan $(\frac{DH}{53"})$ (Eq 6-2)
DH = the horizontal deflection

Lengths of the vertical actuators are 53 in.

Then the total shear force, TSF (when positive horizontal deflection is to the south), becomes:

$$TSF = FH - TVF\left(\sin\left(\arctan\left(\frac{DH}{53"}\right)\right)\right) \qquad \text{(Eq 6-3)}$$

All panel test results plot this total shear force versus shear deflection.

7 Performance of Test Panels

Each of the shear panels shown in Table 7-1 were tested either monotonically or cyclically in the ERDC-CERL test frame shown in Figure 6-1. Drawings of each shear panel are shown in Figures A-2 through A-13 of Appendix A. Three specimens of each panel type were tested, with the first tested monotonically (e.g., panel A1a) and the other two tested cyclically (e.g., panels A1b and A1c). The test frame and test control procedure were evaluated by cyclically testing an extra A2 panel specimen (A2 Trial). Table 7-1 summarizes the results of all monotonically and cyclically tested shear panels. Tables in Appendix B provide details on damage progression with respect to lateral deformation for all these test panels. The following sections summarize the performance of each shear panel with plots of their total shear force, TSF (see Equation 6-1) versus horizontal deflection, DH (defined in Chapter 6).

Table 7-1. Summary of test panel performance.

Test Panel	Load Type	Load Rate (in./min)	Linear Shear Stiffness (kips/in.)	Shear Load at 0.4 in. Deflection (kips)	Lateral Deflection at Ultimate Shear Load (in.)	Ultimate Shear Load (kips)
A1a	Monotonic	0.5	13	4.0	1.1	5.2
A1b	Cyclic	3.0	13	4.0	1.2	5.9
A1c	Cyclic	3.0	13	4.3	1.2	6.5
A2a	Monotonic	0.5	49	18.7	7.8	36.4
A2 Trial	Cyclic	1.5	63	20.6	6.3	33.9
A2b	Cyclic	6.0	58	20.9	5.6	34.5
A2c	Cyclic	6.0	63	21.7	3.9	34.4
A3a	Monotonic	1.0	9	3.5	5.0	9.1
A3b	Cyclic	12	10	3.9	5.9	9.2
A3c	Cyclic	12	13	4.4	3.1	9.2
C1a	Monotonic	1.0	76	25.4	1.7	67.1
C1b	Cyclic	12	92	31.0	2.0	65.3
C1c	Cyclic	6	96	27.3	2.1	69.8
D1a	Monotonic	0.5	108	36.3	8.7	59.1
D1b	Cyclic	6.0	98	36.3	3.9	58.0
D1c	Cyclic	6.0	95	33.9	4.0	57.8
D2a (North)	Monotonic	0.5	69	24.4	1.7	64.2
D2a (South)	Monotonic	0.5	69	24.4	1.8	59.1
D2b	Cyclic	6.0	72	28.7	2.3	71.6
D2c	Cyclic	6.0	64	23.9	2.2	66.7

The A3, C1, and D2 test panels were all detail-validation test panels. A major concern about cold-formed steel construction is the impact of the large material strength variability. Therefore the A3, C1, and D2 test panels were all configured to evaluate the effectiveness of design recommendations in accounting for this variability. The most critical condition is when the diagonal straps have their maximum strength, and other panel components have their minimum design strength. In large seismic motions, the stronger diagonal straps would behave elastically until larger response motions of the building occur. The building response acceleration and resulting inertia forces would be greater with the stronger straps, loading the panel connections, columns, and anchors at higher levels. These components each have potentially brittle modes of failure that must be prevented. Chapter 11 accounts for this strap strength variability and provides recommendations that prevent brittle modes of failure, based partly on the results of these panel tests.

7.1 A1 test panel results

Figure 7-1 plots the measured lateral load versus deflection of the A1a, monotonically loaded shear panel. This figure also plots the predicted lateral load versus deflection for this panel, shown earlier in Figure 5-1. The top of this panel was pulled to the south (left in Figure A-2 of Appendix A). The A1 test panels performed poorly because the columns were not well anchored and did not have adequate shear capacity to resist the lateral forces applied by the diagonal straps. The A1 panel diagonal straps were connected to the columns at their ends with thirteen #10-16 screws as shown in Figure A-3. The columns were screwed to the track at both their top and bottoms using eight #10-16 screws as shown in the same figure. Table B-1 of Appendix B describes how this panel failed by the shear failure of the screws that connect the top of the south (left) column to the panel track on the same face as the diagonal strap.

Figure 7-1. A1a monotonic test panel measured and predicted lateral load versus deflection.

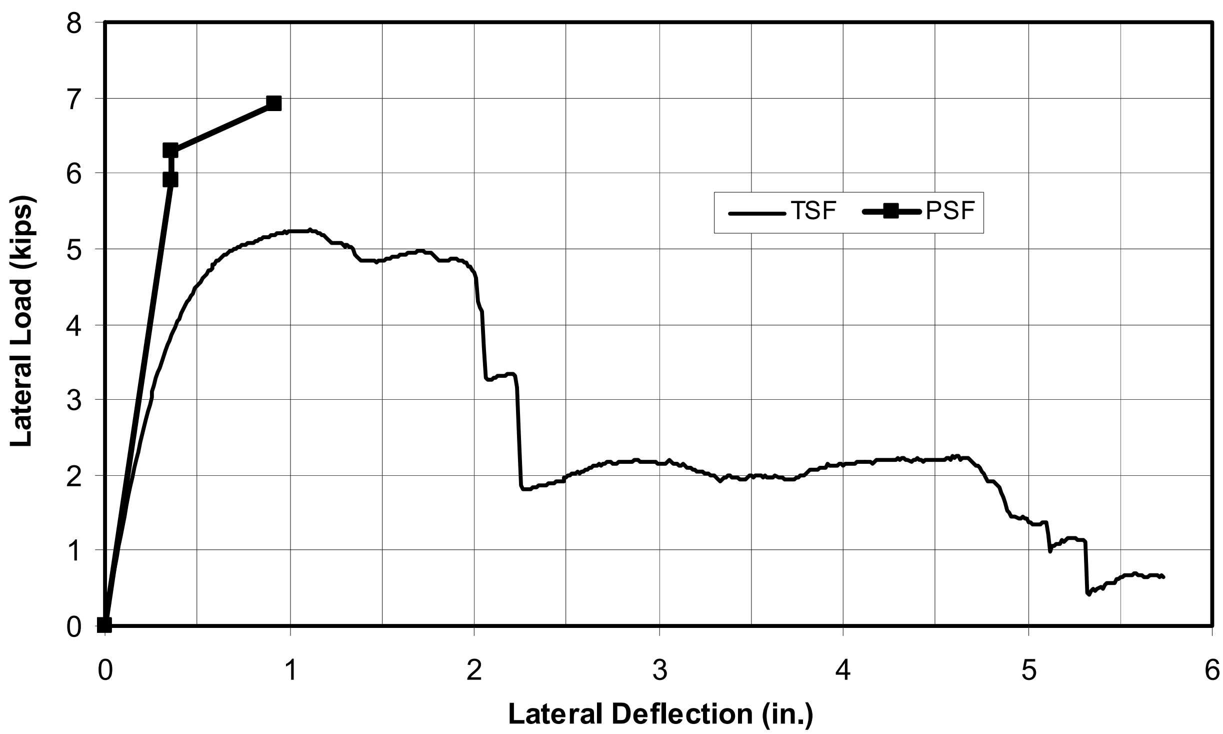

Figure 7-2 shows an overall view of the failed A1a test panel, where the panel failure was at the top of the left (south) column, which is the top left corner of the picture. The left side of the picture shows the scale of the panel. The screw connection failure was a combination of the shear failure of the screws themselves and tearing of the column at the screw connections (see Figure 7-3). The diagonal strap and column were both 43 mil (18 ga) in thickness, while the heavier track was 68 mil (14 ga), explaining why the tearing took place in the column where it was attached to the track with only eight screws. After the complete failure of this joint, at 2.1 in., the panel lateral resistance dropped dramatically, as shown in Figure 7-1. The diagonal straps were only installed on the front face of the panel. Figure 7-3 shows that after the screwed connection failure the column twisted so that a secondary load path developed from the front face diagonal strap through the twisting column and into the back-face column connection to the track. This column also continued to resist the vertical load applied to it without buckling. However, the screwed connection at the column-to-track joint is considered a brittle failure and is unacceptable performance. This panel configuration violates the recommendations presented in Chapter 11 on column and anchor shear capacity; following those recommendations would prevent the failure seen in this test panel.

Figure 7-2. Overall view of failed A1a monotonically tested shear panel.

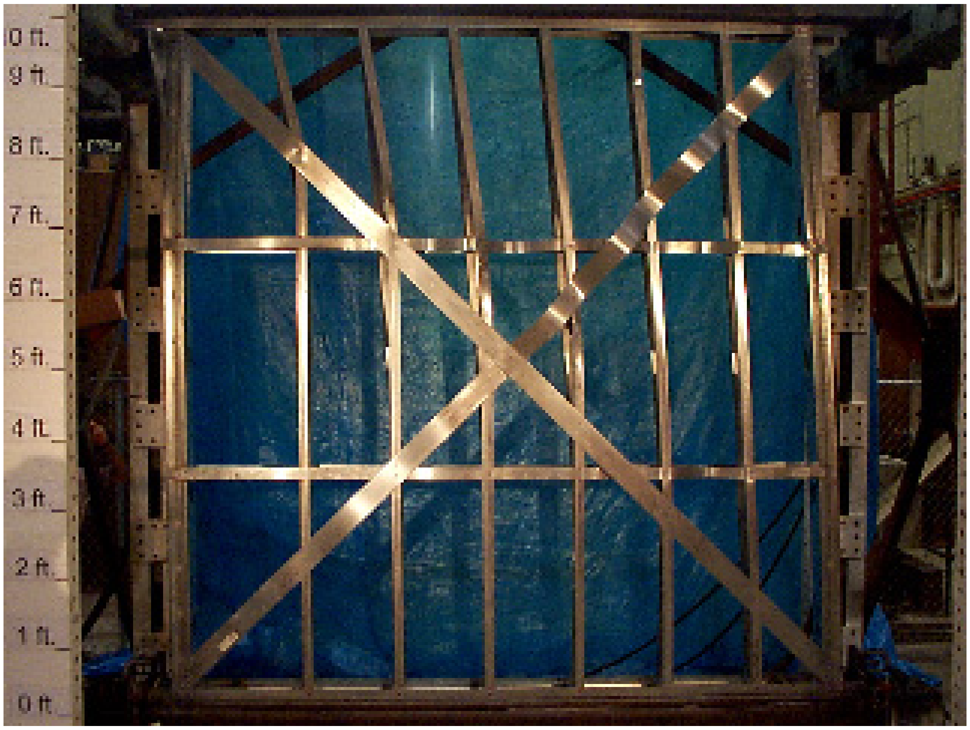

Two secondary load paths developed after 2 in. of lateral deformation. The first was the diagonal strap to the twisted column to the back face track described earlier. The second was from the same strap to the intermediate studs, which carried a small amount of lateral load in weak-axis bending, to screwed connections to the track. The intermediate stud closest to the failed column connection was most efficient in resisting lateral load because the distance it spanned from the connection to the strap to its connection to the track was the least of the intermediate studs. Figure 7-1 shows that these secondary load paths develop only 42% of their ultimate capacity. Table B-1 indicates that shear failure of the screws at the back face of the top of the south column takes place at 5.0 in., explaining the large drop in resistance seen near 5 in. in Figure 7-1. The plot of the predicted lateral capacity is at strap yielding is greater than the ultimate measured capacity, indicating that the diagonal strap likely did not yield before the screwed connection began to fail.

Figure 7-3. Close-up view of column-to-track screw connection failure and column twisting in panel A1-a monotonic test.

Figure 7-4 plots the lateral load versus deflection of the A1b cyclically loaded shear panel. Comparison between the measured and predicted capacity in this figure indicates that the diagonal straps likely began to yield. Table B-2 indicates the straps began to yield at 0.4 in. Table B-2 shows that at 1.2 in. deflection the south column began to twist at the top track, indicating that the screwed connection between the column and track was beginning to fail similar to the A1a panel. Failure of the top south connection would have been due to lateral deflection to the south, which is positive deflection in Figure 7-4. The figure shows that lateral resistance began to drop dramatically due to this failure, decreasing from a peak of 5.9 kips to 3.4 kips at 1.5 in. When the panel was loaded in the other direction, just one screw sheared at the bottom south connection of the diagonal strap to the column at 1.2 in. lateral deflection. However, larger deformation cycles of 1.6 in. produced tearing in the south column at the screwed connection to the bottom track on the front face, which had the diagonal strap attach just inches above. Table B-2 indicates the top of the north column, buckled at 1.6 in. deflection in the same negative direction. At 3.2 in. positive deflection the south column screwed connection to the top track failed completely. Figure 7-4 shows almost complete loss of lateral capacity at 4.0 in of positive deflection, when the south column had twisted and torn to such an extent that little lateral load was carried through the column to the back face of the top track. Finally, at 5.6 in. of lateral capacity the entire panel collapsed under gravity load.

Figure 7-5 shows the measured lateral load versus deflection of the cyclically loaded A1c panel, plus the predicted capacity. The failure of this panel began in an identical manner as the A1b cyclically loaded panel, where the screwed connections between the columns and tracks began. Since the failure occurred at the same lateral deflection and mode of failure was identical, it was decided to stop the test at 1.6 in. lateral deflection and take apart these joints so the development of damage in the column could be more closely inspected. Figure 7-5 shows that the measured capacity of this panel was almost identical to the A1b panel up to the point where the test was stopped.

Figure 7-4. A1b cyclic test panel measured and predicted lateral load versus deflection.

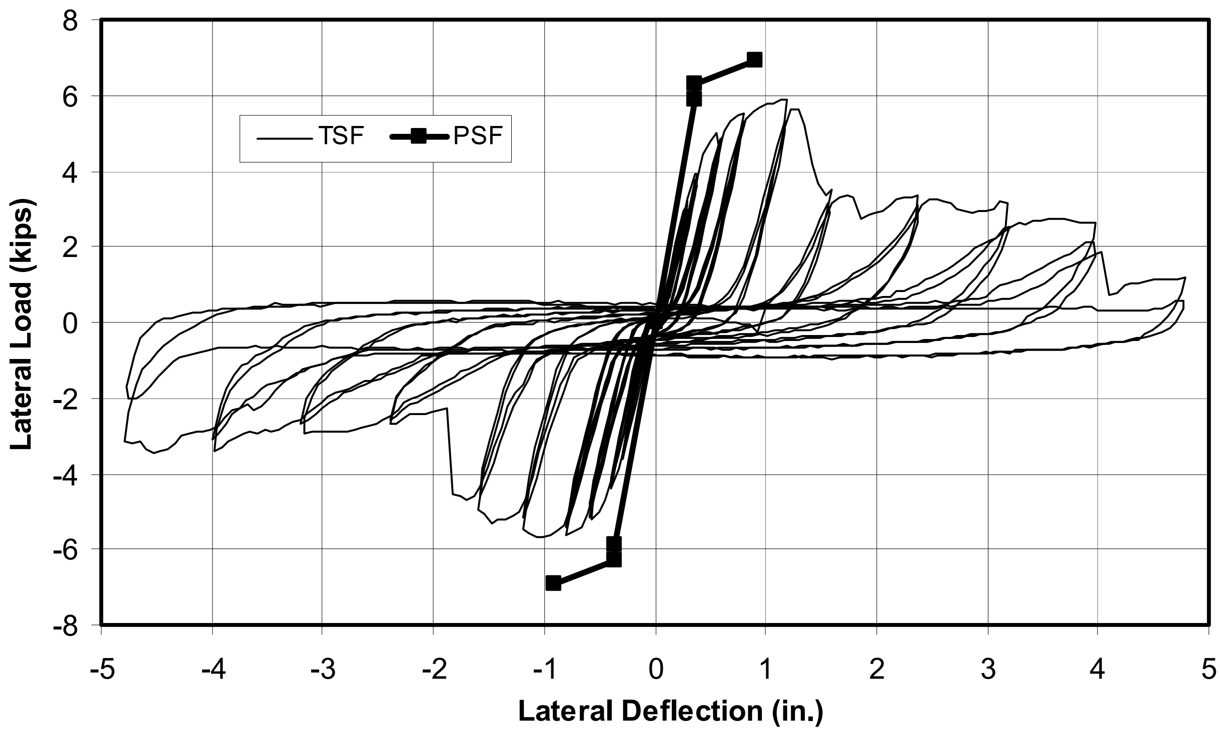

Figure 7-5. A1c cyclic test panel measured and predicted lateral load versus deflection.

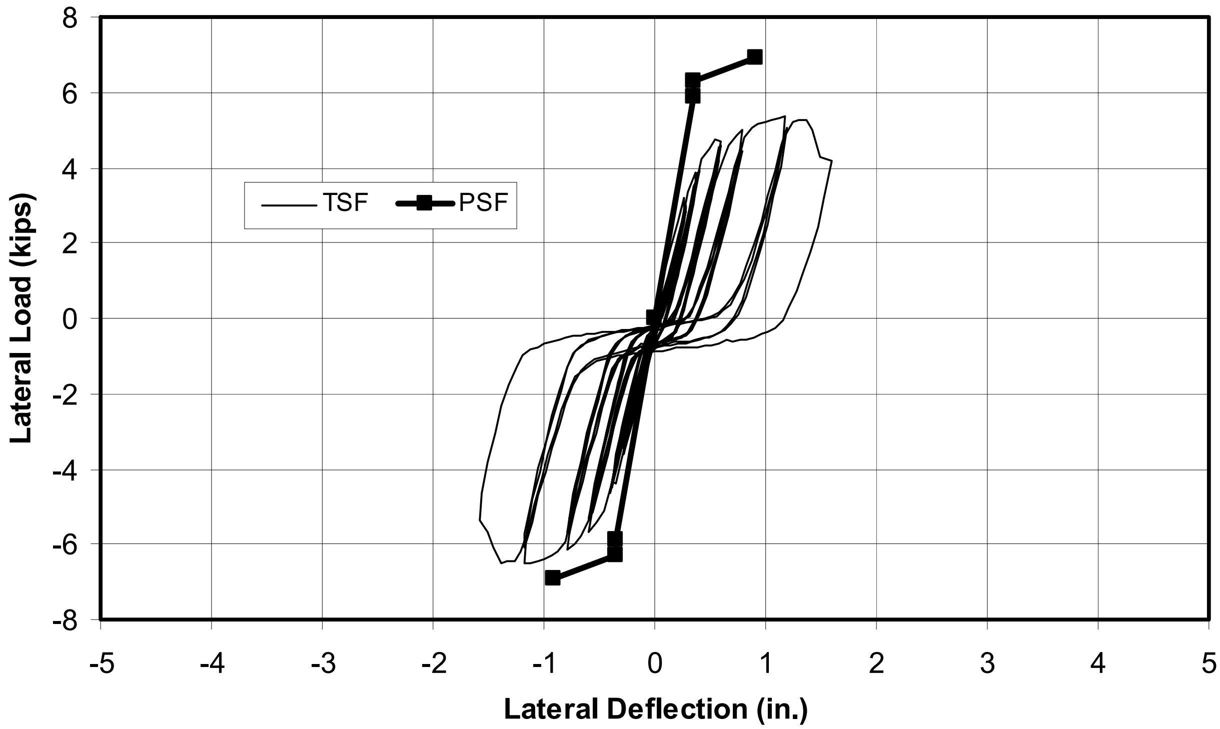

Figure 7-6 through Figure 7-9 show close-up pictures of the top or bottom of both columns at their connection to the top or bottom track. The diagonal straps were attached to only the front of the A1 panel, and these straps were removed from the column so the area of the column below the strap could be inspected. The screws between the tracks and columns were also removed and the tracks were pried back, exposing the condition of the columns behind the track. The joints shown in Figure 7-6 through Figure 7-9 are shown in ascending order of column damage. Figure 7-6 shows the top of the right (north) column. Just below the pried-up track shown at the top of this figure is the second row of screw holes that were screwed to the track. The next row of holes in the column were where the first row of screws were attached to the diagonal strap. The strap pulled in tension to the left and down at this joint, causing the lateral deformation in the column between these two rows of screw holes. Note that the column base metal is essentially undamaged at the screw holes and the only distress to this joint is the shear deformation. Figure 7-7 shows the bottom of the right column, where the column is deformed much more in shear between the row of screws that were attached to the top of the track and the row above that were attached to the bottom of the strap. The column here has buckled locally in a failure mode called *shear buckling*. At this point, the screw holes have begun to elongate, but the column has not torn at the screw holes. Figure 7-8 shows the top of the left (south) column, where the opposite end of the diagonal strap that was attached to the joint in Figure 7-7 is anchored. Here the column has shear buckled even more than in Figure 7-7, and the column material has torn significantly starting at the screw holes. Note that elongation of the strap, and deformation of the joints in both Figure 7-7 and Figure 7-8 would have needed to deform laterally a total of 1.6 in. The amount of deformation in these joints suggests the straps may not have yielded. Figure 7-9 shows a view of the bottom of the left column where the damage was the greatest of all four. Here the shear buckling of the columns is the greatest, with much of the deformation due to the significant tearing through much of the front face of the column. The deformation in this joint was greater than the others, while the deformation in the joint connected to the opposite end of the same strap is the least (Figure 7-6), because the total of these joint deformations and strap elongation also needed to equal 1.6 in. in the lateral direction. Figure 7-9 shows the strap that was removed from the front face, and laid against the back face. This figure also shows the panel anchors, simply consisting of loose steel plates laid inside the heavy track and bolted down to the test frame. The figure shows that these plates were spaced about 0.5 in. from the exterior and 1 in. from the interior face of the column so they would not unintentionally brace the columns. This panel violates recommendations provided in Chapter 11 on the shear capacity of the columns and anchors. It also highlights the potential vulnerability of light-gage cold-formed steel materials to buckling or tearing, failures modes that must be prevented for ductile seismic design.

Figure 7-6. Top of right (north) column after A1c panel test.

Figure 7-7. Bottom of right (north) column after A1c panel test.

Figure 7-8. Top of left (south) column after A1c panel test.

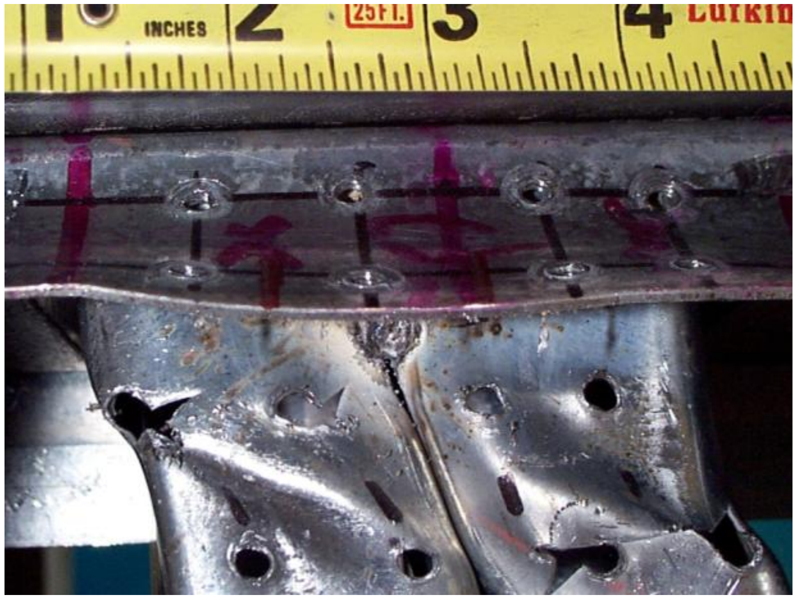

Figure 7-9. Bottom of left (south) column after A1c panel test.

7.2 A2 test panel results

Figure 7-10 plots the measured lateral load versus deflection of the A2a, monotonically loaded shear panel. This figure also plots the predicted behavior shown in Figure 5-1. The top of this panel was pulled to the south (left in Figure A-4 of Appendix A). Figure 7-10 shows that the A2 shear panel deformed significantly without loss of lateral capacity, demonstrating excellent ductility. The panel lateral resistance was still 33.6 kips (92%

of the ultimate capacity) when the test was stopped at 15 in. of lateral deformation. Figure 7-10 shows this panel had significant over-strength, developing much greater resistance beyond yield capacity. Comparison between the measured and predicted capacity in Figure 7-10 suggests that much of this was due to the columns acting as a moment frame. However, the A2 diagonal strap coupon plots shown in Figure 4-1 and Figure 4-2 reveal that much of the increase in panel capacity was due to development of greater strap strength with increasing strain.

Figure 7-10. A2a monotonic test panel measured and predicted lateral load versus deflection.

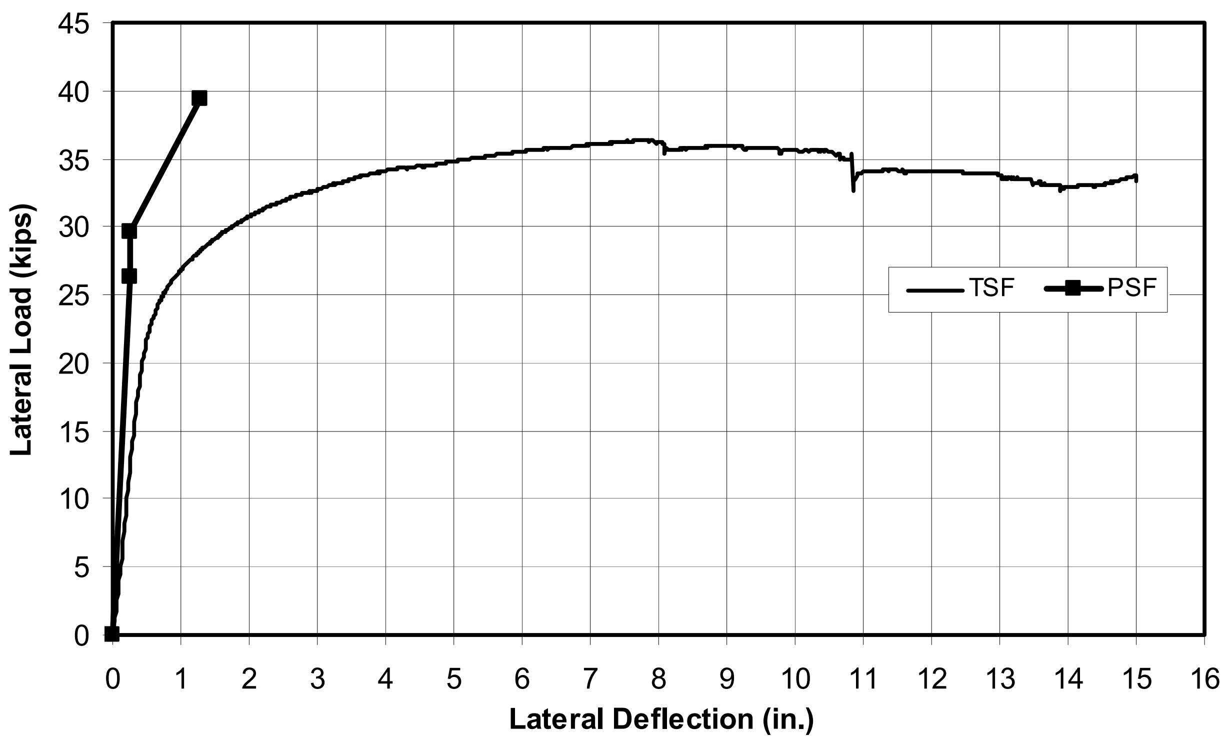

Using the coupon data in Figure 4-2, the strap stress is 32.2 ksi at a strain of 0.003 in./in., which equates to 26.1 kips panel capacity (Equation 3-1) at 0.72 in. lateral panel displacement (Equation 3-2). At larger strap strains, such as 0.03 in./in., the stress would be 40.7 ksi, which equates to 33.0 kips panel capacity at 7.2 in. panel displacement. These displacements are due to strap elongation only, but actual panel displacements would be greater due to rotation of the columns at their anchors. This demonstrates that most of the increase in panel capacity after yielding is due to increase strap stress, and a smaller portion is due to the columns acting as a moment frame. The predicted behavior shown in Figure 7-10 assumes no rotation in the column anchors. In fact, the A2 anchor detail permits large rotations, so that the measured deformations are much greater than predicted.

Figure 7-10 shows that the strap begins to yield at about 0.5 in. lateral deformation and the panel is less stiff than predicted. This lack of stiffness is due to the joint rotation permitted at the column anchors. Table B-4 indicates that the panel anchors begin to fail with cracking at the column to nested stud welds, at the lips of the nested studs, at 2.1 in. deflection. These cracks progress to weld fracture at 2.9 in. deflection. The track and nested studs failed in shear with vertical base metal cracks along the columns. At 5.3 in. deflection, the welds at the back of the columns crack, and they completely fail at the bottom of the north column at 5.9 in. deflection. These failures at the column anchors do reduce the fixity of the columns, and do reduce the moment frame capacity of the column, but the overall panel capacity does not begin to drop until slight loss in capacity at 7.9 in. Screws between the straps and columns began to fail at 6.2 in, but this did not reduce panel capacity. The lips of the nested studs drove into the column material, causing local buckling and eventually puncturing the columns, but this did not reduce capacity.

An additional A2 panel (A2 Trial) was constructed and tested cyclically before any other shear panel in order to test the test frame, test procedure and control, and means for documenting the tests. This test revealed that the test control method was effective, loading cyclically as planned, while holding the load beam horizontal with the appropriate vertical load. The test also demonstrated that the data channels shown in Table D-2 and Figure D-1 were recording properly and that visual observations could be made while testing at a faster load rate than used in the A2 Trial panel test. Table 7-1 shows that the A2 Trial panel test used a load rate of 1.5 in/min, while the other A2 cyclically load panels used a rate of 6 in./min. This panel and the A2a monotonic panel were painted with a whitewash material (lime and water), so that yielding or other deformations of the panel could be clearly seen on the galvanized cold-formed steel material surfaces. The whitewash was applied after the panels were installed in the test frame because it is a brittle coating and would otherwise flake off during panel installation. These early tests revealed that panel deformation and failure modes were clearly visible, and these observations were not enhanced with the white-wash. Therefore, the whitewash material was not applied to other test panels.

Figure 7-11 plots the load-versus-deformation performance of the A2 Trial shear panel, along with the same predicted capacity shown in Figure 7-10. Table B-5 documents the panel observations, but the amplitude of panel deformation at which these observations were made were often not recorded in this trial test. In this panel greater damage occurred in the diagonal strap-to-column screwed connections than in the monotonically loaded panel. The damage to the screw connection (screw rotation and shear) also took place at smaller deformations than in the monotonic test. This difference may be due to the multiple cycles of load reversals on these fasteners, often referred to as *low-cycle fatigue*. This panel was tested to 15 in. in the positive direction without significant loss of capacity (see observations in Table B-5), but only to 9.6 in. in the negative direction. Figure 7-11 plots the measured capacity in both directions through the 9.6 in. cycles. The measured capacity shown in Figure 7-11 was slightly greater in this cyclic test than in the monotonic test (Figure 7-10) up to deflections of 2.0 in. Beyond 2.0 in. lateral deflection, the lateral capacity increased much less than it did in the monotonic test. It appears that the increase in capacity in the cyclic test was due to the increase in stress of the strap material as indicated in the coupon tests (Figure 4-2), while the additional contribution from the columns acting as a moment frame was much less than it was in the monotonic test. The nested stud and track anchors for the columns failed at lower deformations in this cyclic test than under the monotonic loading.

Figure 7-12 plots the load-versus-deformation performance of the cyclically loaded A2b test panel, along with the predicted capacity. Table B-6 documents the panel observations including detailed records of the lateral deformation at which various failures modes took place. Figure 7-12 shows that the panel capacity in the positive direction was slightly greater than in the negative direction, but the average of the two agrees with the A2 Trial panel values. Figure 7-12 shows that the A2b panel was tested cyclically to 15 in. in both directions, with no loss of lateral capacity.

Figure 7-11. A2 Trial cyclic test panel measured and predicted lateral load versus deflection.

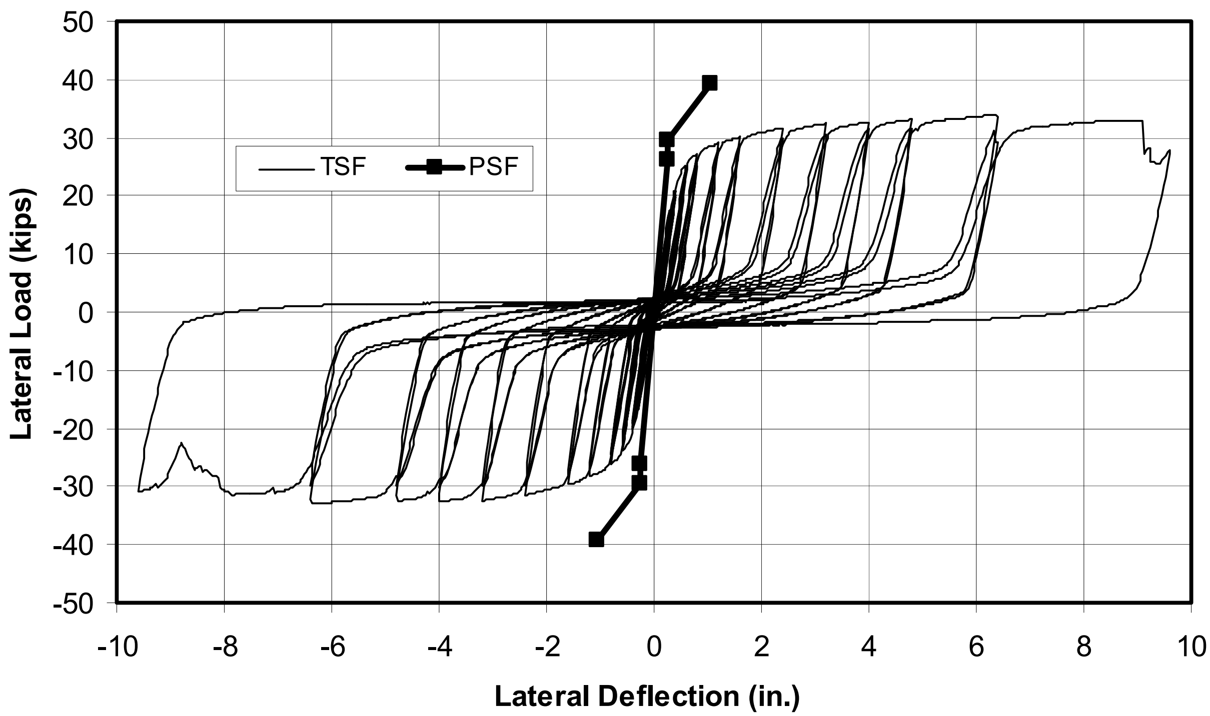

Figure 7-12. A2b cyclic test panel measured and predicted lateral load versus deflection.

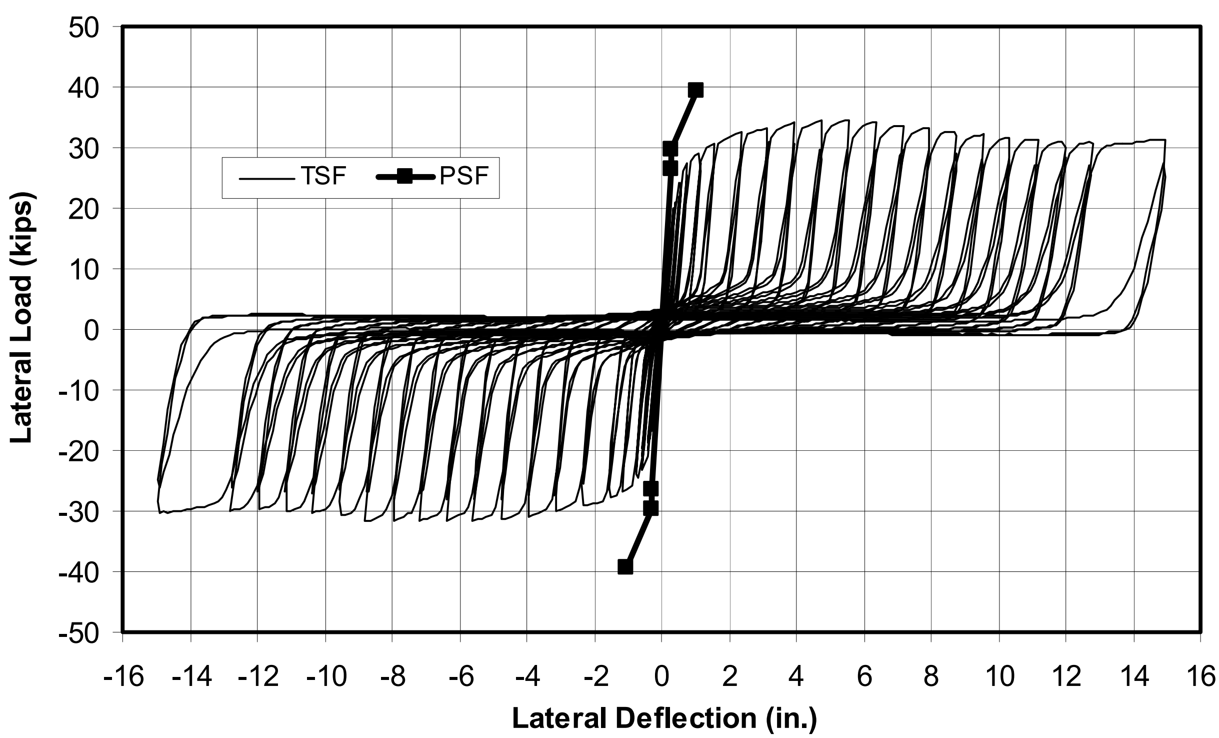

The diagonal straps of this panel began yielding at 0.4 in. lateral deflection; the welds joining the nested stud lips to the columns began to crack at 1.2 in.; these welds fractured at 2.4 in.; some tracks in the column anchors began to buckle at 3.2 in. while others failed in shear; the weld at the web of the track to the column fractured at 6.4 in.; and the tracks at these anchors fractured in shear at 6.4 in. Figure 7-13 shows a buckled track at the top of the north column after the end of the A2b test. A few diagonal strap-to-columns screws failed in shear early in the test, but these caused no reduction in capacity because the straps continued to yield and elongate throughout the length of the straps. A number of screws at the track-to-column connections failed, which led to a small reduction in the moment resistance of the column anchors.

Figure 7-13. Top of north column showing buckled track after the A2b cyclic test.

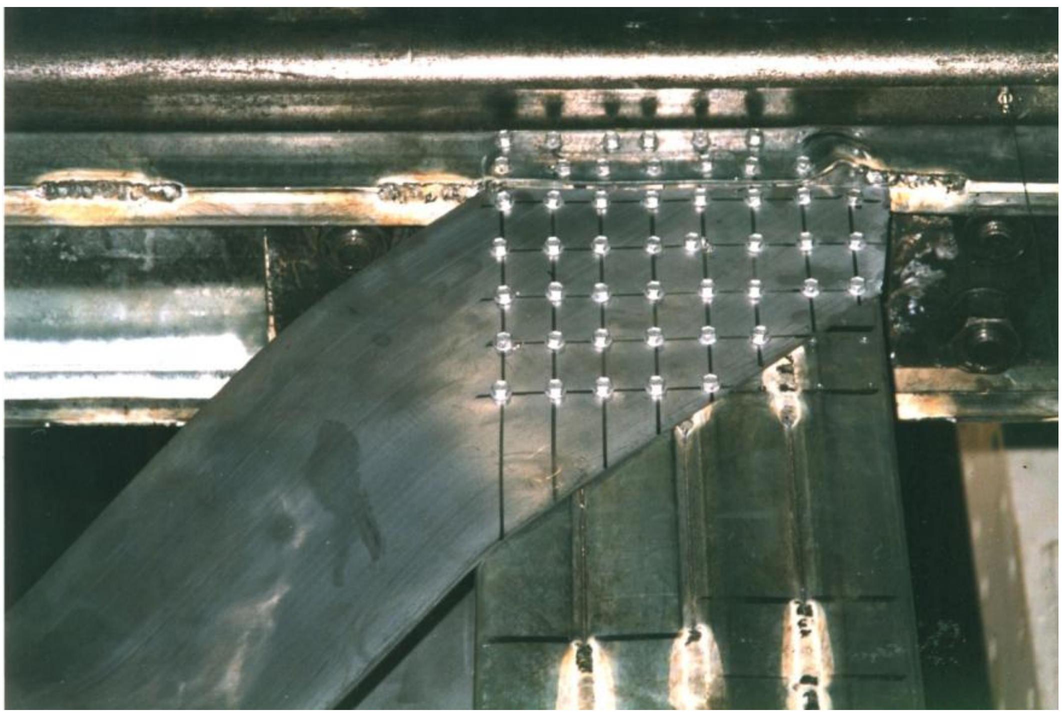

This panel reached its greatest average (of positive and negative) ultimate capacity of 33 kips at a lateral deformation of 5.6 in. This capacity included the effects of the increased strap stress at greater strains, plus a contribution of the columns acting as moment frames. After 5.6 in. deflection, the small decrease in capacity was due to the damage to the column anchors, which reduced the moment frame capacity, plus the increasing moment loading of these anchors due to the P-delta effects of the large deflection. Table 5-2 shows that the total vertical load, GL_{max}, was held at 27 kips, making the moment due to P-delta effects significant at large deflections.

Figure 7-14 plots the load-versus-deformation performance of the A2c test panel, along with predicted capacity. Table B-7 documents the panel observations and failure modes. Figure 7-14 shows that the panel capacity was slightly greater in the positive direction than the negative, and the average agreed well with the other two cyclically tested A2 panels. Figure 7-14 shows this panel was tested to 12.8 in. in both directions, with the only loss in capacity taking place at 11.8 in. in the negative direction. Table B-7 indicates this panel failed in a very similar manner as A2b, but with the degree of failure appearing to take place at smaller deformations. Table B-7 shows that the north column began to tear at the bottom anchor at 5.6 in. and on top at 6.4 in. At very large panel deformations, the nested stud lip punched through the interior face of the 12 gage columns. Figure 7-15 shows an overall view of the A2c panel deformed 12.8 in. in the negative direction at the end of this test. This panel provided excellent ductile behavior, resisting the full lateral load of the diagonal straps. However, the welding of a nested stud inside the track was considered an expensive way to provide column anchorage. The diagonal strap had a yield strength, F_{sy}, of only 32 ksi. Had this strength been much greater (see Chapter 4 on strength variability) it is likely that brittle modes of failure in the strap connections and anchor would have prevented the good ductility seen in these panels. Finally, the load-versus-deflection plots for this panel show very pinched hysteresis envelopes, indicating that the columns contribute very little lateral resistance when deforming in the opposite direction of a peak excursion in one direction. These panels would provide limited energy dissipation compared to panels with less-pinched hysterics from improved panel moment fame capacity.

Figure 7-14. A2c cyclic test panel measured and predicted lateral load versus deflection.

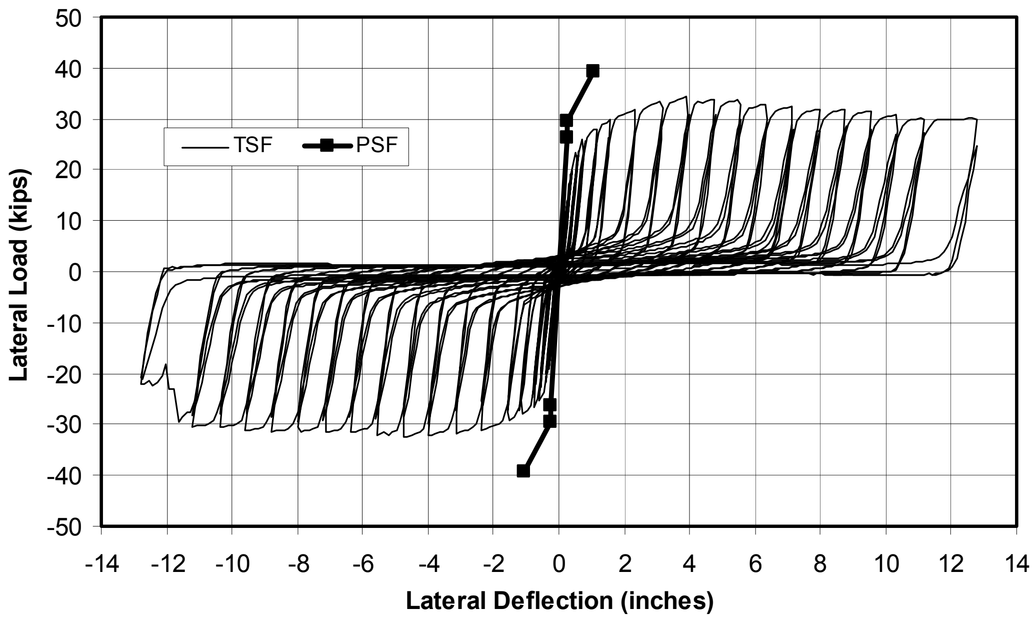

Figure 7-15. Overall view of the A2c panel, deformed 12.8 in. in the negative direction.

7.3 A3 test panel results

The A3 test panels used off-the-shelf hardware (Simpson Strong-Tie S/HD8) to anchor both the top and bottom of the panel columns. These anchors were installed on both faces of each column as shown in Figures A-6 and A-7. Figure A-7 shows that each anchor was screwed to the columns with 18 #10-16 self-tapping screws, using the holes closest to the ends of the columns. Several additional screw holes were available, but only 18 were used because 18 were needed to resist the design uplift force assuming a design yield strength of the diagonal straps of 30 ksi. The actual strap yield strength was 60 ksi (see Table 4-1), but designing several components of this panel for a strap strength of only 30 ksi tested this panel for the maximum strength variability of the straps, providing the detail validation needed for this panel configuration. This panel used the same basic configuration as the A1 panel and had similar capacity. In addition to the off-the shelf anchors and strap strength variability design, this panel differed from A1 in that the total vertical load, GL_{max}, was much less at 10 kips (Table 5-2 shows a 27 kip load was applied to the A1 panel).

Figure 7-16 plots the measured lateral load versus deflection of the A3a monotonically loaded shear panel. This panel was first tested in the positive direction (left in Figure A-6). Detail A and Note 2 in Figure A-7 show that two screws (#10-16 Teks) were used on each side of the columns to lightly attach the track to the columns (one on either side of the individual studs). These screws were not intended as part of the panel design, but were added simply to fix the top and bottom tracks to the panel so it could be moved. The first half of Table B-8 shows that these nonstructural screws that connected the top of the south (left) column to the track began to fail at 1.3 in. lateral deflection, and these failures resulted in the spiked loss of capacity on the positive side of the plot in Figure 7-16. The measured data in Figure 7-16 shows that this panel did not reach its predicted yield capacity until a deflection of 1.9 in. and the shape of this plot at 1.9 in. also indicates yielding of the diagonal strap. Therefore, the screw connection failure began before strap yielding. Table B-8 shows major distortion of the top of this column above where the strap was screwed to the column at 2.8 in. deflection. The two screws between the front face of the track and the column provided the initial shear support for the column, but the intended design was for the anchors to provide this support. The thin material of the columns prevented the anchors from serving this purpose because the column buckled in shear once the screws to the tracks failed. The thin column material could only provide insignificant shear capacity in tension. The anchors at the in-plane interior side of the columns were intended to support the columns by the columns bearing up against them when the straps were loaded in tension. However, the columns buckled in shear, preventing the development of bearing resistance. The anchors on the in-plane exterior face were intended to provide hold-down resistance for both uplift and bending of the column. The screws connecting the anchors to the columns on the exterior face should not be relied upon to resist tensile force. However, these screws did not fail, but rather the thin column failed locally in bending between the screws and the column face. These off-the-shelf anchors may have worked had they been welded to the columns along their exterior vertical edge, where they meet the exterior side; and exterior face of the column, where the straps are attached. This would have resulted in the load applied to the columns by the diagonal straps being carried directly in tension through the columns to this anchor. However, such an anchor would provide little moment resistance, so if a welded anchor were used it would be even more effective to use a smaller version of the anchors used in the C1 shear panels (see Figure A-9). The screwed connection between the loaded diagonal strap and the top of the left column failed at 5.0 in. of lateral deflection. Figure 7-16 shows the test was stopped shortly after the failure of this connection.

Figure 7-16. A3a north and south monotonic test panel measured and predicted lateral load versus deflection.

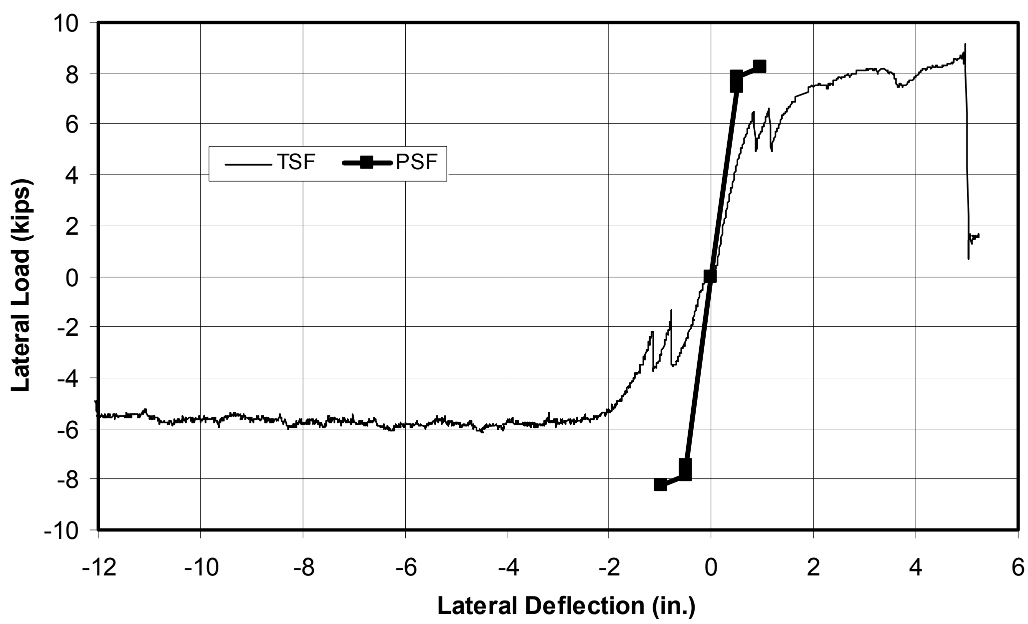

Figure 7-17 is a photograph of this test panel after the diagonal strap connection to the column had failed. Figure 7-18 zooms in on the details of this failed connection, showing the failure was a net area failure of the strap material between the screws. This figure also, shows the final condition of the column and anchor after the failures described above. These include the two screws between the track and column; the shear buckling of the columns. After the column was buckled to the extent shown in this photograph, the screws between the exterior anchor and column pulled out, and some load was resisted in bearing when the column collapsed against the interior anchor. The anchors have not deformed on either side of the columns, so that the columns could still act as a moment frame with one anchor being in axial compression, while the other is in tension.

Figure 7-17. Overall view of A3a monotonically tested panel after it failed in the positive direction.

This panel was tested in the negative direction also by pulling the top of the panel to the north (right in Figure A-6). This provided a potentially useful second monotonic test since the diagonal strap, column connections, and anchors were essentially undamaged in this direction. The bottom half of Table B-8 documents the failure progression in this test, showing similar failure of the screwed connections between the tracks, followed by the columns and the shear buckling of the columns. However, the screws connecting the track to the column failed in shear, and shear buckling of the column took place at smaller lateral loads so that the diagonal strap never did yield in this second monotonic test. Figure 7-16 appears to show good ductile behavior when the panel is loaded in the negative direction, but in fact the performance in this direction is very poor because the modes of failure are highly variable in their capacity.

Figure 7-18. Close-up view of the A3a panel showing failed strap connection and column anchor.

Figure 7-19 shows the performance of the cyclically loaded A3b test panel, along with the predicted capacity. Table B-9 documents the failure progression, showing that the screws between the track and column failed at 0.45 in. when loading in the negative direction, and at 0.9 in. in the positive direction. These failures explain why the development of panel capacity was limited to about 6 kips at these deflections. The columns failed in shear buckling at 1.2 in. in the positive direction and at 1.8 in. in the negative direction. The measured capacity of this panel reaches the predicted yield strength of the straps alone (7.43 kips) at lateral deflections of 1.7 in. in the positive direction and 1.5 in. in the negative. The moment frame capacity of the slender, poorly anchored columns is very small, so it is clear that the diagonal straps yielded in both directions before 2.0 in. deflection.

The A3 strap coupon data in Figure 4-2 show that the strap stress increases only slightly above its yield value of 60.1 ksi, reaching an ultimate value of only 62.6 ksi. This ultimate stress value is reached at small strains of only 0.0285 in./in., which would equate to a lateral deformation due to strap yielding of only 6.84 in. The straps would not have elongated to this extent especially since much of the panel deformation is due to deformation of the columns at their anchors. Still, the increase in panel capacity based on the ultimate strap stress is a reasonable upper bound, having a value of only 0.32 kips, which is an increase to 7.75 kips. The average of the maximum positive and negative panel capacity shown in Figure 7-19 is 8.82 kips, so the increase in strap strength accounts for only a small portion of the measured maximum capacity. The remaining increase in capacity must be from a combination of the columns acting as moment frames and both the deformed columns and interior studs acting as diagonal tensile trusses at large lateral deformations.

Figure 7-19. A3b cyclic test panel measured and predicted lateral load versus deflection.

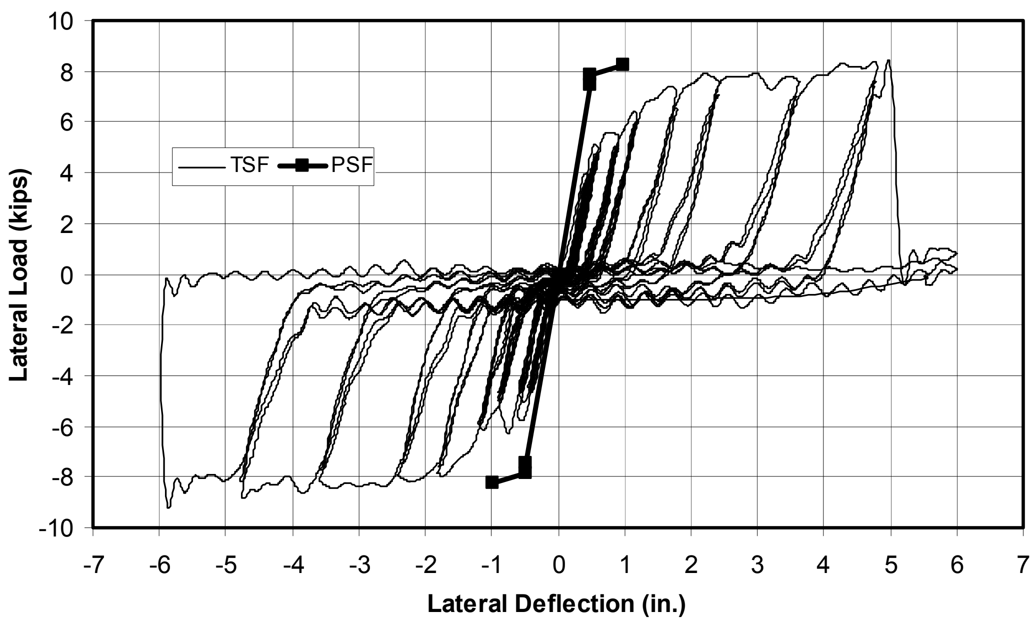

Figure 7-19 shows a sudden loss of capacity at 5.0 in. in the positive direction. This was caused by a net area failure across the screws that fastened the diagonal strap to the bottom of the north column. Figure 7-18 showed the same type of failure at the top of the south column of the A1a monotonically tested panel. The picture shows that the failure occurred between the screws, where the strap material between the screws ruptures. The load applied to this rupture surface is equal to yield stress of the strap times the gross area of the strap. The screw pattern used in this joint detail creates a critical rupture planes that are both vertical and horizontal along the screws so that the total failure plane is much larger than the width of the straps. The load applied to this rupture surface is resisted by all the screws in the connection to the column. The strap stress is greatest at the rupture surface because the load on the strap decreases by the load picked-up by individual screws as the strap progresses into the joint. The strap yields locally near the screws along this rupture surface and the material elongates as the strains increase. As load increases on the strap, the stresses along this surface reach their ultimate value (62.6 ksi, shown in Table 4-1 for the A3 strap). The strap continues to elongate further locally, but the strength increases no further, until the local strap strains reach their ultimate values and the material fractures. The coupon data in Table 4-1 shows that the A3 coupons had an average strain at fracture of only 0.075 in./in. (elongation of 7.5%). The particular coupon specimen plotted in Figure 4-1 for the A3 straps shows an even smaller maximum strain of only 0.054 in./in. Even more important than the small maximum strain, Table 4-1 shows that this strain-hardened strap material had an ultimate-to-yield stress ratio of only 1.04, far below the required minimum of 1.08 for ASTM A1003/A 1003M, Type H material (ASTM 2013b). When the design recommendations presented in Chapter 11 are used on this test panel, it indicates that a net area failure should take place at this rupture surface, even when resistance factors are increased to 1.0, before the gross section of the strap yields. In actual panel construction, strain-hardened material would not be permitted in the straps, reducing the vulnerability to net area failures. This test demonstrates that if the recommendations presented on the design rupture strength in these connections in Chapter 11 are followed, net area failures can be prevented.

Figure 7-20 shows the performance of the cyclically loaded A3c test panel along with predicted capacity. Table B-10 documents the failure progression, showing that the bottom of the north column began to deform before complete failure of the screws between the track and column. At the other corners the screws between the track and column failed before significant column deformation.

Figure 7-20. A3c cyclic test panel measured and predicted lateral load versus deflection.

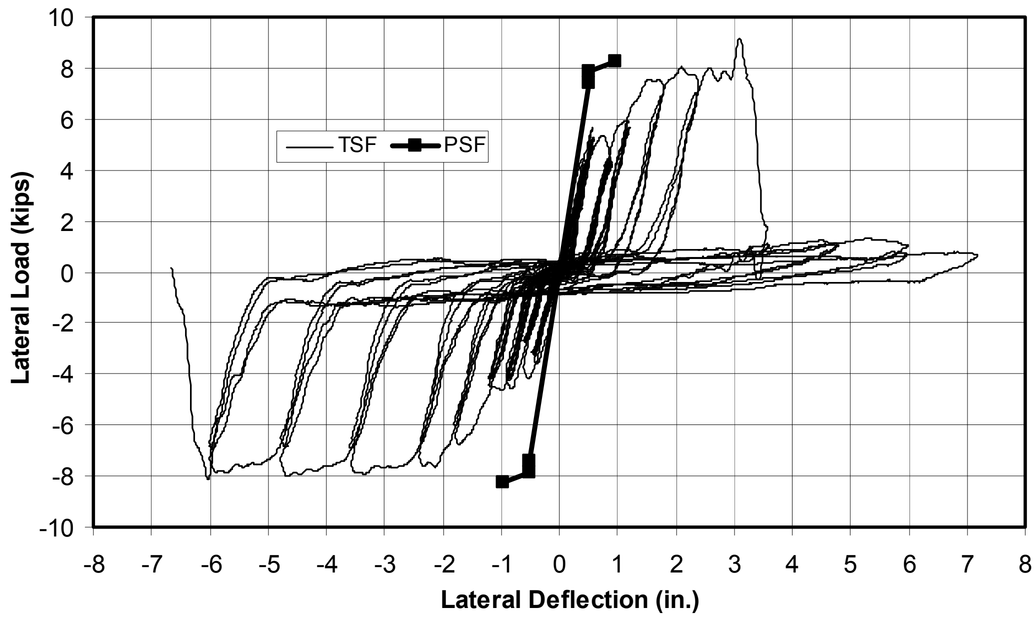

Figure 7-21 shows the bottom of the left column where column deformation permitted screw rotation so that they began to pull out from the strap. The column deformation also causes the strap to deform, creating additional stress concentrations at the critical rupture surface. The screw deformation at the strap column connection shown in Figure 7-21 is more typical than the lack of rotation seen in Figure 7-18.

Table B-10 shows that the strap at the bottom of the north (right) column had a net area failure at this joint, causing the loss of resistance seen in the positive direction in Figure 7-20 at 3.3 in. The strap at the top of the north column had a net area failure, causing the loss of capacity at 6.2 in. in the negative direction. The strap yield capacity is developed at similar deformations of 1.5 in. in the positive direction and 2.1 in the negative direction, as was seen in the A3b test. The measured capacity suggested the straps did yield, but much of the deformation of the panel was due to deformation of the columns where the straps were connected. Figure 7-20 shows that this panel reached an average peak capacity of 8.64 kips, well above the predicted capacity based on the strap yield strength (7.43 kips). This panel lost capacity in the positive direction at a smaller deformation of only 3.3 in., demonstrating the variability in this type of brittle failure. This panel provided fairly good ductile behavior, especially if the diagonal straps were constructed with the ASTM A1003/A 1003M, Type H material

(ASTM 2013b). The off-the-shelf anchors, which were screwed to the columns, were failures because they did not prevent shear buckling of the columns.

Figure 7-21. Bottom of left column of the A3c panel, showing column deformation and screw rotation.

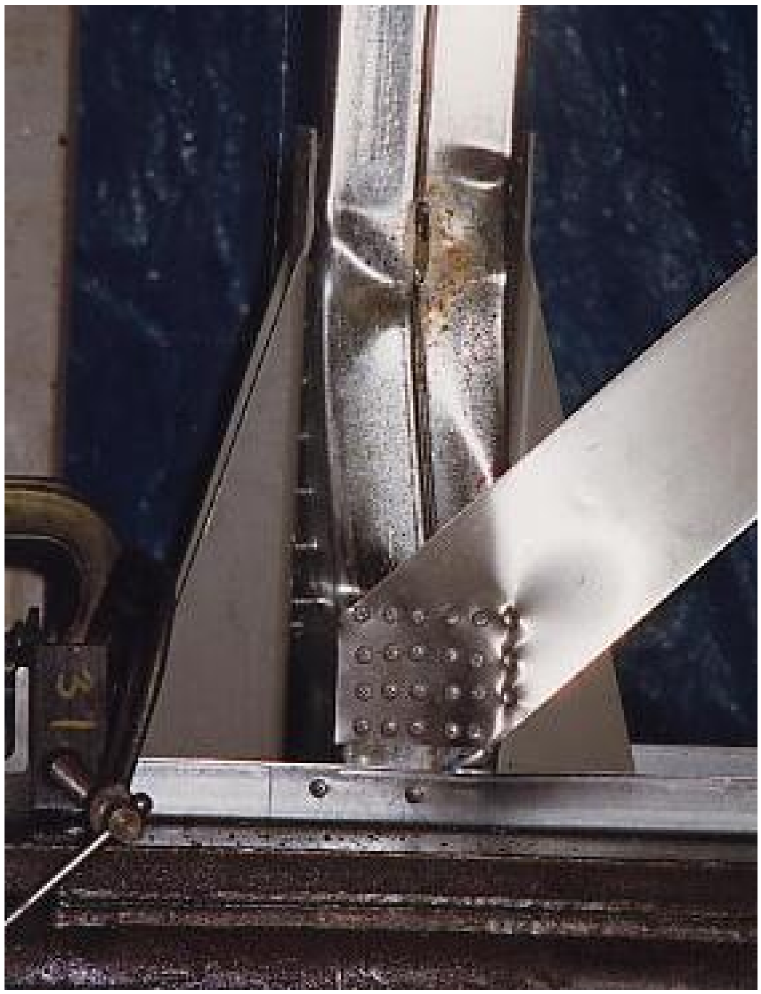

7.4 C1 test panel results

The C1 test panels are another detail validation panel configuration. It is a heavier version of the A3 panel, but with the straps welded rather than screwed to the columns; and the anchors built up from L6 x 6 x 0.5 in. angle sections and a 0.75 in. triangular stiffener plate (see Figures A-8 and A-9 for details). The actual yield strength of the diagonal straps was 81 ksi, but several components of the panels were designed assuming a yield strength of 41 ksi in order to validate adequate ductile behavior for the maximum strap overstrength. Table 5-2 shows that the vertical load, GL_{max}, was held at 30 kips for all the C1 test panels. Figure 7-22 plots the measured lateral load versus deflection for the C1a monotonically loaded shear panel. The predicted behavior, shown earlier in Figure 5-1, is also plotted.

Figure 7-22. C1a monotonic test panel measured and predicted lateral load versus deflection.

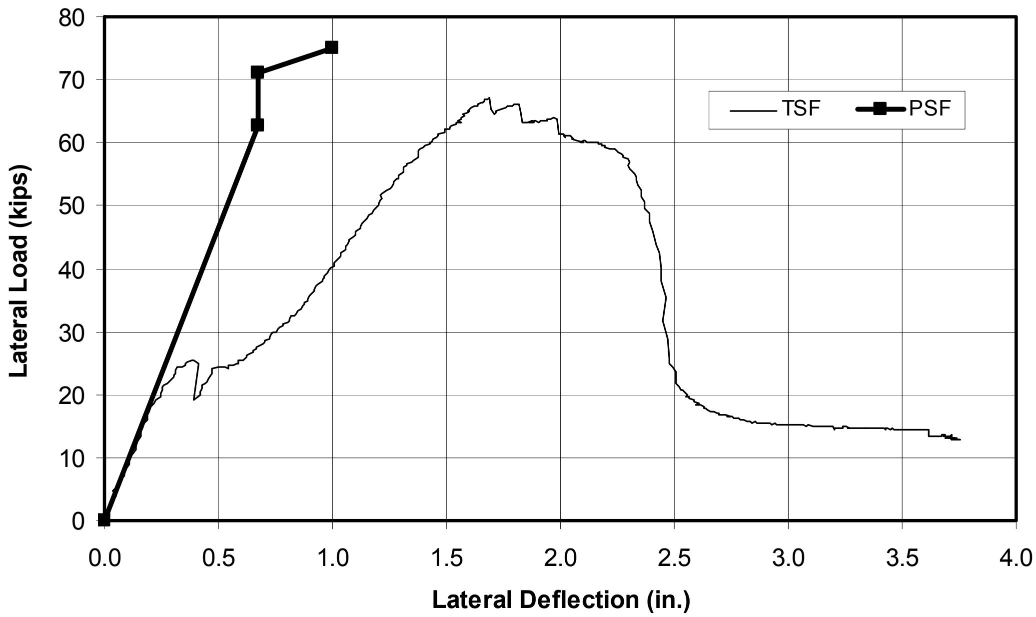

Detail A and Note 2 in Figure A-9 show that a 0.5 in. long tack weld was used to lightly attach the track to each side of the outer studs in the columns. These welds were not intended as part of the panel design, but were added simply to fix the top and bottom tracks to the panel so it could be moved, similar to the two screws in the A3 panels.

Table B-11 documents a few observations on the behavior of this panel. When the vertical load was being applied, one of the nonstructural welds failed and another failed at the top of the north column at 0.5 in. of lateral deflection, resulting in the drop in capacity seen in Figure 7-22. The plot shown in Figure 7-22 shows that the predicted yield strength of the strap alone was reached at 1.5 in. deflection. Figure 7-22 indicates that if the columns were fully fixed, the full lateral yield capacity of the columns would have been reached at only 1.0 in. of lateral deformation. Clearly the columns are not fully fixed, but this does indicate that the column moment frame contribution at the 1.5 in. lateral deflection should have been significant, indicating the straps very likely did not yield. If the straps had yielded, the shape of the plot of lateral load versus deflection would show a gradual rolling over of the panel capacity. The sharp drop seen at 1.7 in. deflection indicates that minor brittle failures such as another nonstructural track weld failure may have occurred before strap yield was reached. These nonstructural weld failures, unfortunately shock loaded the panel, and may have led to earlier rupture of the diagonal straps.

The C1 panels had one strap in both diagonal directions on both the front and back face of the panel. Table B-11 shows that the diagonal strap on the front face began tearing near the bottom of the south column first, followed by the back face strap at the same location. Both straps tore gradually as the panel deformed laterally. Figure 7-22 shows a sudden loss of capacity at 2.3 in., when both straps would have been tearing. Figure 7-23 shows the front face of this connection after significant tearing of the strap. The lower tear in the strap began first, where the strap was welded to the left edge of this column, and the tear progressed along the weld and across the strap. As the strap crack pried open and rotated, the tear above it began from the top side of the strap. Figure 7-22 shows a complete loss of capacity at 3.7 in. deflection, when both straps failed completely.

Figure 7-23. Front face of the bottom of the south (left) column, showing strap tearing in the C1a panel.

Figure 4-3 shows that the C1 strap was severely strain hardened, so that the ultimate stress was almost no greater than yield. The elongation was reasonably good, but because the ultimate stress was not much greater than yield, there was little opportunity for the strap to deform and redistribute forces throughout the straps. The strap stress concentrations at the heat-affected zones of the welds provided an ideal location for a brittle fracture to begin and propagate through the strap. The recommendations developed in Chapter 11 would not permit the use of strain-hardened straps, because this material must be the ASTM A1003/A 1003M, Type H. This test was not a complete failure because it demonstrated that lateral load close to the yield strength of the panel could be resisted without brittle failures of the columns, connections, or anchors.

Figure 7-24 plots the performance of the C1b cyclically loaded panel. Table B-12 indicates that the track-to-column weld failures at 0.6 and 0.8 in. deflection caused the early loss of capacity seen in Figure 7-24. Table B-12 indicates that a small fracture began to form in the column material next to the vertical weld between the northeast edge of the bottom of the north column and the vertical edge of the anchor angle. The center-right side of Figure 7-25 shows this base metal fracture after the crack had opened.

Figure 7-24. C1b cyclic test panel measured and predicted lateral load versus deflection.

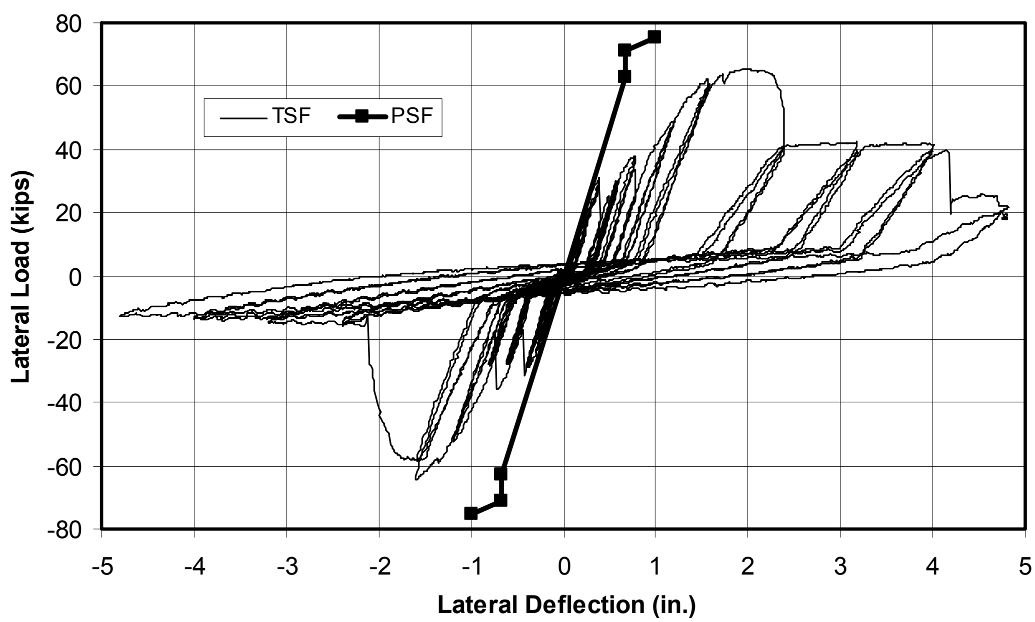

Figure 7-25. Base metal fracture of the bottom of the north column along the welded connection to the anchor.

This column tearing was clearly in the heat-affected zone of the weld to the anchor. Soon the diagonal straps began to fracture in the heat-affected zones of the welds to the columns. The strap failures near their connections led to the almost complete loss of capacity at 2.0 in. deflection in the negative direction, seen in Figure 7-24. The strap on the back face failed in the other direction in a similar manner, causing the large loss of capacity at 2.3 in. in the positive direction.

The sudden loss of capacity seen at 4.2 in. deflection in the positive direction is due to the development of a vertical tear in the column, along the top of the anchor angle shown in Figure 7-25. The column subsequently tore even further, leading to the loss in capacity seen at 4.8 in. Figure 7-26 shows that one end of three diagonal straps tore in the manner defined above, and the column tore near the anchor beginning at the front face of the bottom of the north (right) column.

Figure 7-26. Overall view of the C1b panel after failure of three straps and column.

This picture was taken a few seconds after the final failure of the strap at the bottom of the south (left) column, when the panel was displaced about 2.2 in. in the negative direction, where the top of the panel was displaced to the right. The peak measured capacity was only 65.3 kips at 2.0 in. deflection in the positive direction and 64.3 kips at 1.6 in. deflection in the negative direction. These ultimate capacities are only slightly greater than the predicted capacity of the strap alone at strap yield (62.8 kips), suggesting that the straps of this panel most likely did not yield in either direction.

Figure 7-27 plots the performance of the C1c cyclically loaded shear panel. Table B-13 indicates that the nonstructural track-to-column welds failed at 0.3 in. through 1.6 in., explaining the early loss of capacity seen at these deflections in Figure 7-27.

Figure 7-27. C1c cyclic test panel measured and predicted lateral load versus deflection.

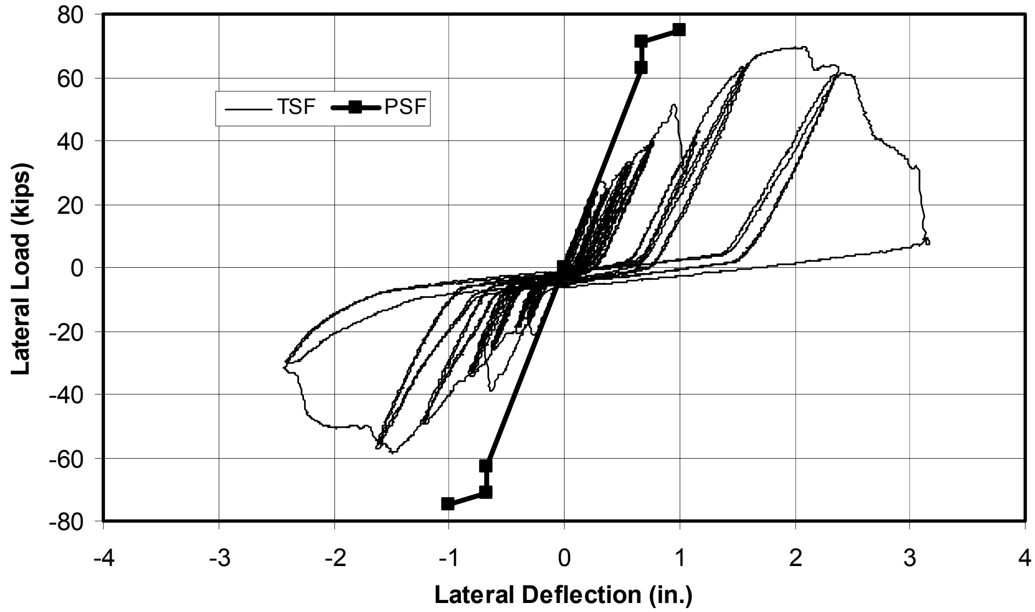

The peak measured capacity for this panel in the positive direction was 69.8 kips at 2.1 in. deflection, while the capacity in the negative direction was much less at 58.4 kips. This capacity in the positive direction is significantly greater than the predicted capacity of the strap alone at strap yield (62.8 kips), suggesting that the straps of this panel likely did yield when the panel deformed in this direction. The gentle rolling over of the plot (at 1.7 in.) without loss of capacity also suggests the diagonal straps yielded. The straps did begin to fracture at 1.5 in. deflection in the negative direction, and they also began to fracture in the positive direction at 2.2 in., so the strap yielding was relatively minor. Poor ductility was seen in the C1 panels because strain-hardened material was used in the straps. However, these panel tests demonstrate that panels designed in the C configuration (built-up columns, with welded strap connections and the type of anchors used in the C1 test panel) should perform in a ductile manner without brittle failures even at the maximum estimated strength in the diagonal straps.

7.5 D1 test panel results

The D configuration panels use hollow structural section (HSS) columns instead of the columns built up from studs used in the C1 test panels. The column material used in the D1 test panels is much thicker, 3/16 in., than the stud material that tore in the C1b test panel column (0.098 in). The diagonal straps are welded to the columns like the C1 panel. The D1 test panels used a heavy track (97 mil or 12 gage) and nested studs (97 mil or 12 gage) welded inside the track and to the columns to provide column anchorage. These anchors were intended to resist shear loads on the columns, and provide only minimal resistance to rotation. Figures A-10 and A-11 provide the details on the design of this test panel. The D1 panel uses heavy 97 mil (12 gage) intermediate studs, as did the A2 panel. These are much heavier than the 33 mil (20 gage) intermediate studs used in the C1 test panels. The diagonal straps used in the D1 panel are 97 mil (12 gage) thick, which are heavier than those used in the A2 and C1 panels, though the strength of the strap material was only 37.6 ksi (see Table 5-1), much less than the 81.3 ksi strain-hardened material used in the C1 panel straps. Table 5-2 shows that the vertical load, GL_{max}, applied to the D1 test panels was 27 kips.

Figure 7-28 plots the measured lateral load versus deflection for the D1a monotonically loaded test panel. The predicted behavior plotted earlier in Figure 5-1 is also plotted for comparison. Table B-14 documents the progression of failure of this panel, showing that the straps began to visibly yield beginning at 0.95 in., while Figure 7-28 suggests they began to yield at 0.8 in. The coupon data in Figure 4-5 and Figure 4-6 show the D1 strap material had a fairly low yield strength (37.6 ksi in Table 4-2); the stress/strain plot plateaued until 0.008 in./in. strain, equivalent to 1.92 in. panel lateral deflection; and then increased fairly linearly until 0.035 in./in. strain, equivalent to 8.4 in. lateral deflection. Using the coupon data in Figure 4-6, the lateral capacity of the straps alone would have been 46.1 kips at strap yield, as plotted in Figure 7-28. At the strain of 0.035 in./in., the coupon stress was 43.9 ksi, which would have given a lateral capacity from the straps alone of 53.9 kips at a lateral deflection of 8.4 in., assuming no flexibility in the column anchors. However, Figure 7-28 shows that the D1a shear panel reached a peak capacity of 59.1 kips near the 8.4 in. deflection. Therefore, the columns acting as moment frames or the interior studs must have contributed at least 5.2 kips of lateral resistance (59.1 kips minus 53.9 kips). The nested stud and track column anchors would not have been very effective moment connections, so it is doubtful that even half the yield capacity of the columns could have been reached. Table 5-4 shows that the predicted yield capacity of both columns was 8.6 kips.

Figure 7-28. D1a monotonic test panel measured and predicted lateral load versus deflection.

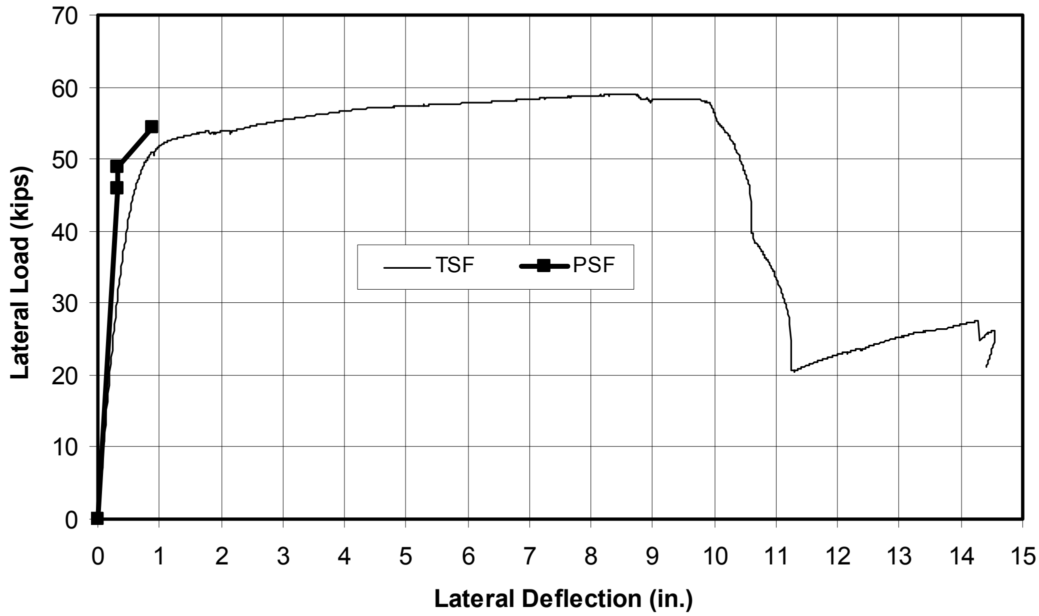

Figure A-10 shows that all 97 mil interior studs were connected to both the top and bottom tracks with 1 in. long weld along the lip of the track. Anchor bolts were installed close to each interior stud. The diagonal straps were also connected to the intermediate studs with 1 in. weld at both edges of the straps. The interior stud-to-track welds and stud-to-strap welds would have acted as pinned connections. These interior studs would have had some weak-axis bending capacity to resist lateral load applied by the straps in tension, especially for those studs closest to the columns, because of their short span. At very large lateral deflections, the interior studs would also resist lateral load in tension. Therefore, it is likely that the interior studs contributed a few kips to ultimate capacity of the D1a panel at the large deflection where the ultimate capacity was reached.

Table B-14 shows that cracks formed in the lips of the nested stud where it was welded to the columns at both the top of the south column and bottom of the north column, beginning at 1.0 in. deflection. The track below the outside edge of the bottom of the north column began prying up with the column at 1.4 in. deflection; this track tore vertically along this edge of the column at its back face at 2.1 in.; and tore through both faces at 4.0 in. Figure 7-29 is the back face of the bottom of the north column showing the pried-up and torn track. The failure in the lip of the nested stud where it is welded to the column is seen just above the track tear.

Figure 7-29. Back face of the bottom of the north column showing the pried-up and torn track at the center of the picture.

This tear is on the left side of the column. Just 0.5 in. to the left of the column, sitting inside the nested stud, is a 1 in. thick steel uplift plate that was bolted to the base beam restraining the nested stud and track anchor from rotation. These plates began to deform slightly in bending. The nested stud lips and flanges began buckling against the columns at the interior sides of the columns at 9.3 in. deflection. Table B-14 shows that all the damage up until 10 in. was to the anchors in nested studs or tracks. The moment capacity of these anchors decreased as the damage progressed, so the lateral loads would have gradually redistributed from the columns acting as a moment frame to the interior studs.

Table B-14 shows that the sudden loss of capacity near 10 in. deflection, seen in Figure 7-28, was due to diagonal strap tearing on the back face near the column, and by 11.2 in. the strap had torn through on the front face near the column. Significant loads were redistributed to the interior studs after the strap failures at the columns, so the panel still carried over 20 kips by the interior studs and columns. The stud weld connections to the track began to fail, and finally the welded strap connections to the interior studs failed at 14.5 in. After this failure the test was halted, although the panel resistance remained at 20 kips.

Figure 7-30 plots the lateral load-versus-deflection performance of the cyclically loaded D1b panel. Table B-15 indicates this panel fails in the same order as the D1a monotonically loaded panel. Figure 7-31 provides an overall view of the D1b panel at several inches of lateral deflection.

Figure 7-30. D1b cyclic test panel measured and predicted lateral load versus deflection.

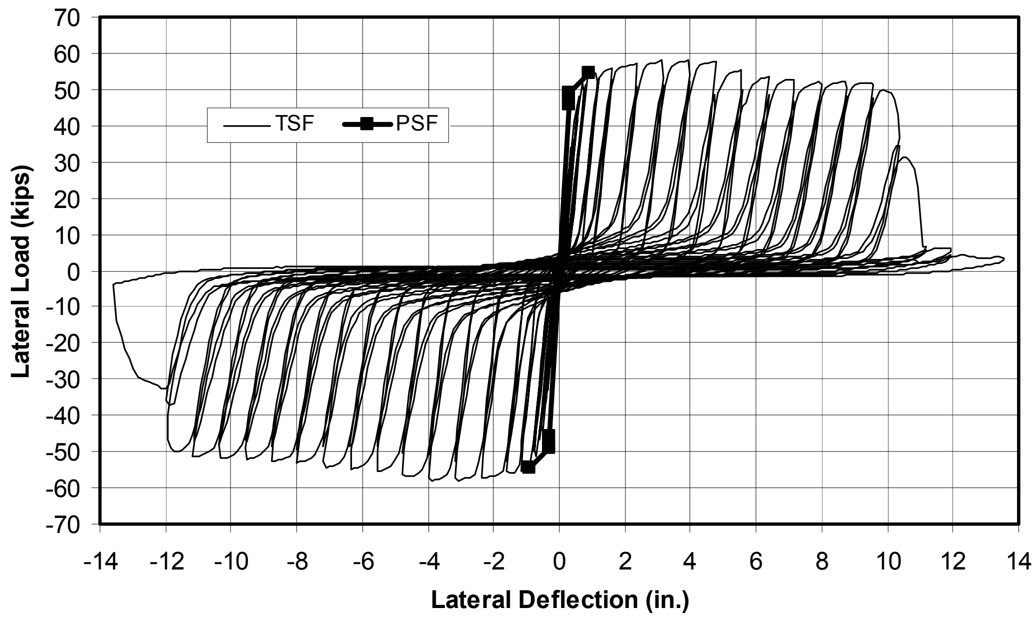

The progression of failure of all D1 test panel is summarized as follows:

- nested stud base metal failure near the welded connection between the nested stud lip and column
- bending of the track and nested stud anchor and bending of the 1 in. thick anchor plate
- shear tearing of the track and nested stud at the column
- track base metal failure near the welded connection between the track web and column
- fracture of the diagonal straps near the welds to the columns
- nested stud lip was driven into and buckled at the 3/16 in. thick column face.

Table B-15 indicates the strap weld connections to several interior studs began to fail at only 3.2 in. lateral deflection. This does not significantly reduce capacity immediately, but it does reduce the ability to redistribute forces from the straps to interior studs, particularly later in the test. This loss of ability can be seen in the gradual reduction in capacity beginning at 4 in. in Figure 7-30.

Figure 7-31. Overall view of the D1b test panel at several inches of lateral deflection.

The failure of the strap welded connections to the interior stud would shock load the strap-to-column connections, possibly causing earlier failures of the primary connections to the columns. Though strap connections to the interior studs provide a secondary load path, design recommendations in Chapter 11 discourage strap connections to these studs in order to avoid the shock loading. The interior studs can then be constructed with much lighter material, unless greater axial capacity is needed to resist gravity loads.

Table 7-1 and Table B-16 show that the performance and failure progression of the D1c cyclically tested shear panel was very similar to the D1b panel. However, the test data were not available for plotting.

7.6 D2 test panel results

The D2 test panels are another detail validation panel configuration. This panel used the same HSS columns used in the D1 panels, the straps were welded to the columns, and the anchors were L8 x 6 x 0.5 in. angle sections with ¾ in. triangular stiffener plates (see Figures A-12 and A-13 for details). The actual yield strength of the diagonal straps was 56 ksi, but several components of the panels were designed assuming a yield strength of 28 ksi, in order to validate adequate ductile behavior for the maximum strap overstrength. Table 5-2 shows that the vertical load, GL_{max}, was held at 30 kips for all the D2 test panels. Figure 7-32 plots the measured lateral load versus deflection for the D2a monotonically loaded shear panel. This panel was tested monotonically, loading first to the north (positive) until failure and then to the south. The predicted behavior shown earlier in Figure 5-1 is also plotted. Detail A and Note 2 in Figure A-13 show that two 0.5 in. long tack welds were used to lightly attach the track to each face of the columns. These welds were not intended as part of the panel structural design, but were added simply to fix the top and bottom tracks to the panels so they could be moved.

Table B-17 shows that the nonstructural track welds of the D2a monotonically loaded panel failed at very small deflections of 0.7 in. when loaded in the positive (north) direction and 0.5 in. when loaded in the negative (south) direction. Figure 7-32 shows that the weld failures caused the temporary loss of resistance at these deflections. Had these nonstructural welds not existed, Figure 7-32 suggests the lateral resistance would have developed in a similar manner, but with a smaller slope or panel stiffness. Table B-17 shows that the when the panel was loaded to the north (positive in plot), the diagonal strap on the front face failed at 1.7 in., and the strap on the back face failed at 1.9 in., explaining the sudden loss in capacity seen in Figure 7-32. The predicted yield capacity of the straps alone was 63.0 kips, and the maximum capacity reached in the positive direction shown in Figure 7-32 was only 59.1 kips, indicating both diagonal straps most likely fractured before either yielded. The diagonal straps failed at similar amplitudes when the panel was loaded in the negative direction. The plot in the negative direction in Figure 7-32 suggests the strap on one face failed at 1.7 in. lateral deflection at a load of 64.2 kips, and the second failed at 1.8 in. and 36.7 kips.

Figure 7-32. D2a north and south monotonic test panel measured and predicted lateral load versus deflection.

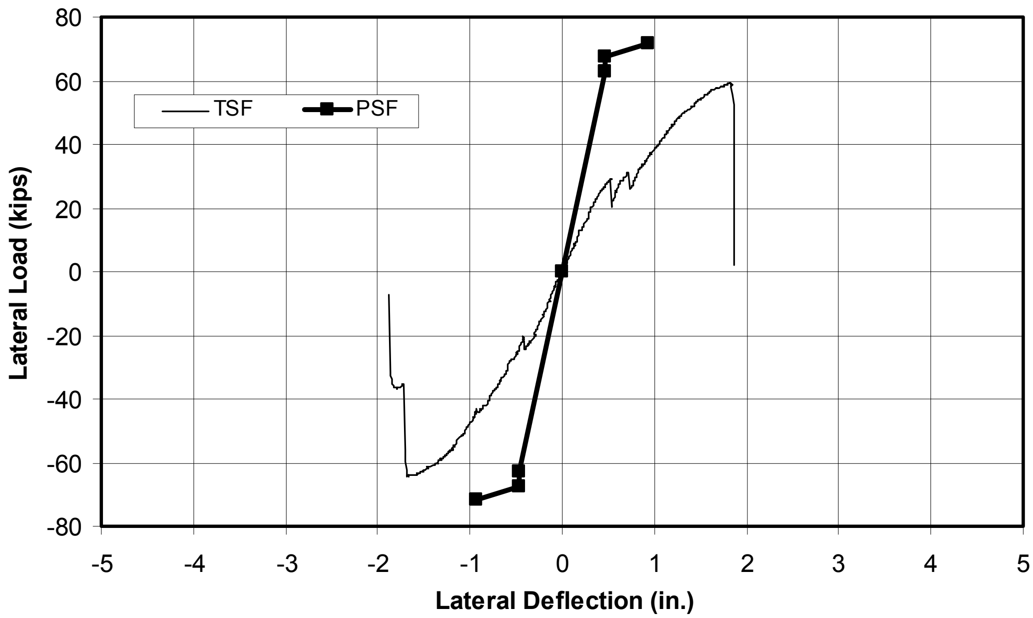

The peak capacity in the negative direction and the gentle decrease in slope just before this peak was reached suggest that both straps may have yielded. The reduced panel resistance that reached 36.7 kips suggested that one strap was still intact at 1.7 in., and that it failed soon after this. All of the diagonal strap failures in this panel began near the welds to the column, and then suddenly fractured through the center of the strap away from the weld. The panel capacity and ductility of this panel is clearly limited by the use of the strain-hardened straps. Had better quality straps been used, the straps would have yielded and elongated significantly, and the columns, connections, and anchors would most likely have continued to resist loads, providing good ductile performance with the columns providing a flexible but fairly strong secondary moment frame. The cyclic tests that follow support this claim.

Table B-18 shows that the cyclically loaded D2b shear panel failed in the same manner as the D2a panel, with the track weld failures followed by the fracture of the diagonal straps. However, the diagonal strap failures took place at larger panel deflections and larger measured capacities. Table B-18 and Figure 7-33 indicate that the back strap failed at 2.1 in. deflection in the positive direction, causing the panel resistance to drop to 40 kips, followed by later cycles where the front strap failed at 2.6 in and the resistance dropped to 11 kips. This table and figure show that the front strap failed at 2.1 in. in the negative direction, causing the panel resistance to drop to 45 kips, followed by later cycles where the back strap failed at 3.5 in. and the resistance dropped to 13 kips.

Figure 7-33. D2b cyclic test panel measured and predicted lateral load versus deflection.

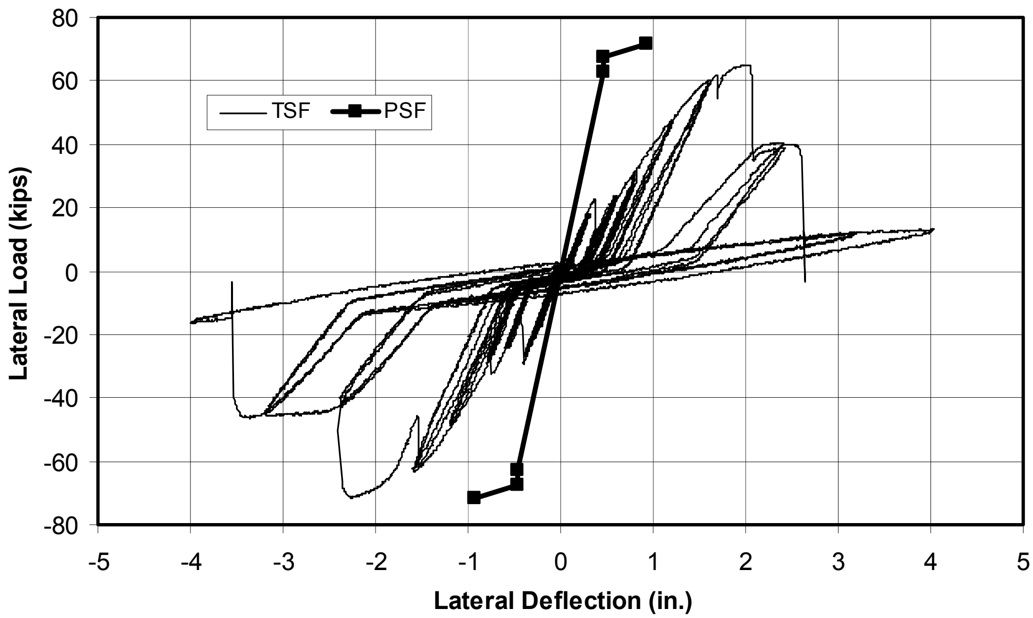

Figure 7-34 shows an overall photograph of this panel shortly after the front face strap failed at the bottom of the north (right) column at 2.6 in. in the positive direction. The straps near the bottoms of both columns show typical strap failure, where a crack in the strap begins near an edge of the strap near the welds to columns and progresses to the interior of the straps.

Figure 7-34. Overall view of the D2b test panel
after the front strap failed at the bottom of the north (right) column at 2.6 in.

In the positive direction, a peak capacity of 65.0 kips was reached at 2.0 in. deflection. This exceeds the predicted yield capacity of straps alone of 63.0 kips and the shape of the measured data in Figure 7-33 suggests that the straps had begun to yield in the positive direction. In the negative direction, a capacity of 71.6 kips was reached at 2.3 in. deflection. This peak capacity far exceeds the predicted yield capacity of the strap and is almost equal to the predicted total capacity of the panel when the straps are at their yield strength and the columns have begun to yield. The contribution of the interior studs is not included in the predicted strength, but that should be relatively small. The greater capacity in the negative direction, plus the gentle reduction in slope around 2 in. deflection indicate the straps have clearly yielded in the negative direction. The performance of the D2b panel shown in Figure 7-33 was not very ductile because of the strain-hardened straps, but this test clearly shows the straps yielded and no other brittle failures occurred in the columns, strap connections, or column anchors, showing that this detail validation test did demonstrate that the recommendations presented in Chapter 11 will produce ductile performance. Figure 7-33 shows that after failure of both straps in both directions, the columns acting as moment frames and the interior studs develop lateral resistance of 13 kips in the positive direction and 16 kips in the negative direction. This demonstrates that columns and interior studs do provide somewhat of a redundant system that widens the hysteretic envelopes and should prevent building collapse even if the straps fail completely.

Table B-19 provides only a few observations on the failure of the D2c cyclically loaded panel. Still, these observations and the panel performance shown in Figure 7-35 indicate this panel behaved similarly to the D2b panel although its capacity and lateral deflection at failure were slightly lower.

Figure 7-35. D2c cyclic test panel measured and predicted lateral load versus deflection.

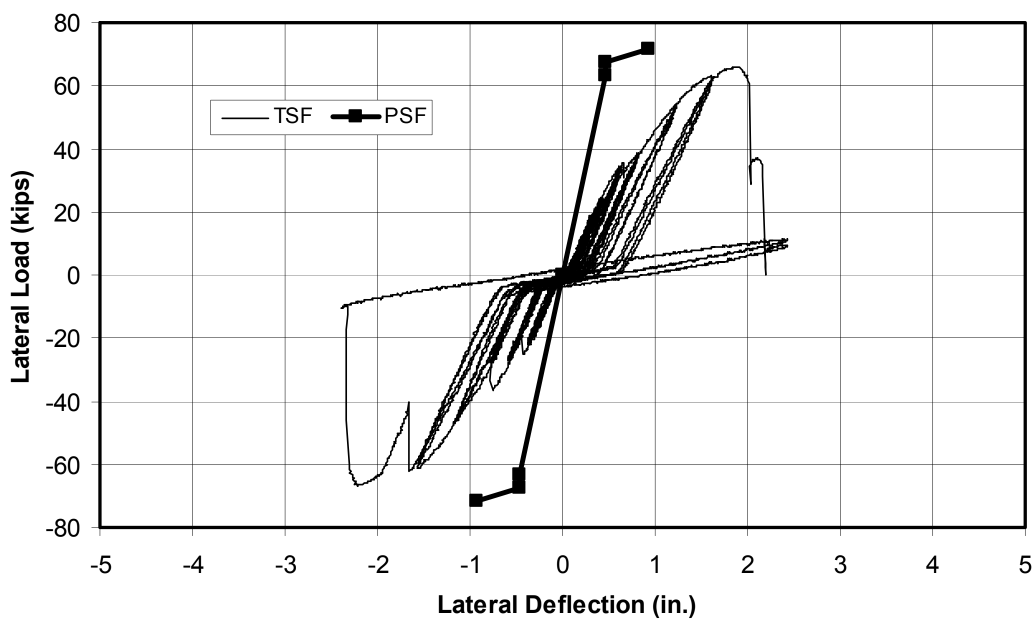

This panel reached a peak capacity of 65.8 kips at 1.9 in. deflection in the positive direction, exceeding the predicted yield capacity of the straps alone. This capacity, plus the plot shape, suggests the straps did yield in this direction. Figure 7-35 shows a strap on one face of the panel failed in this direction at 2.0 in., dropping the panel resistance to 36 kip, followed by failure of the strap on the other face at 2.2 in. The panel reached a peak capacity of 66.7 kips at 2.2 in. in the negative direction. This capacity and the plot shape also indicate the straps yielded in this direction. Both straps failed at 2.3 in. deflection.

These shear panel tests demonstrate that all three shear panel configurations with diagonal straps (A, C, and D) as the primary lateral-load-resisting element can be designed in a way that ensures effective ductile performance needed for resisting seismic loads. The tests of the lightweight A1 and A3 panels showed how critical it is to design the panels so the columns and anchors have adequate shear capacity for the maximum diagonal strap strength. The heavy nested stud and track that made up the anchors for the A2 and D1 shear panels did provide sufficient shear support for the panel columns. However, the extensive welding would be an expensive way to provide panel anchorage, and the anchors must have sufficient capacity for the maximum strength of the straps. The anchors used in the C1 and D2 panel configurations, however, would be relatively inexpensive. They can be designed for the strap overstrength and turn the columns into a true moment frame, making the panels a more redundant, more energy dissipating system. The off-the-shelf anchors used in the A3 panels could provide sufficient shear and hold-down resistance if they were welded to the columns, but a lighter version of the anchors used in the C1 panels would work better because they would make the columns moment frames. The C1 and D2 panel tests demonstrate shear panels designed using ASTM A1003/A 1003M, Type H strap material (ASTM 2013b), and other provisions described in Chapter 11 of this report can provide very ductile performance, even if the diagonal straps are at their maximum levels. The A3 panel tests demonstrate that lightweight panels can be designed that also have good ductile performance using practical anchor details, and this is illustrated in the example problem in Chapter 12.

References

ACI. 2011a. *Building Code Requirements for Structural Concrete and Commentary (ACI 318-11)*. Farmington Hills, MI: American Concrete Institute.

ACI. 2011b. "Guide for Design of Anchorage to Concrete: Examples Using ACI 318 Appendix D." ACI 355.3R-11. Farmington Hills, MI: American Concrete Institute, ACI Committee 355.

AISC. 2010a. "Specification for Structural Steel Buildings." ANSI/AISC 360-10. Chicago, IL: American Institute of Steel Construction.

AISC. 2010b. "Seismic Provision for Structural Steel Buildings." ANSI/AISC 341-10. Chicago, IL: American Institute of Steel Construction

AISC. 2011. *Steel Construction Manual*. 14th Edition. AISC 325-11. Chicago, IL: American Institute of Steel Construction.

AISI. 2007a. "North American Specification for the Design of Cold-Formed Steel Structural Members." AISI Specification S100-07. Washington, DC: American Iron and Steel Institute.

AISI. 2007b. "Commentary on North American Specification for the Design of Cold-Formed Steel Structural Members." AISI S100-2007-C. Washington, DC: American Iron and Steel Institute.

AISI. 2008. *AISI Manual: Cold-Formed Steel Design*. Washington, DC: American Iron and Steel Institute.

ASCE. 2010. *Minimum Design Loads for Buildings and Other Structures*. ASCE/SEI 7-10. Reston VA: American Society of Civil Engineers. doi: http://dx.doi.org/10.1061/9780784412916.

ASTM. 1995. "Standard Practice for Static Load Test for Shear Resistance of Framed Walls for Buildings." E 564-95. West Conshohocken, PA: ASTM International.

ASTM. 2013a. "Standard Specification for Steel Sheet, Zinc-Coated (Galvanized) or Zinc-Iron Alloy-Coated (Galvannealed) by the Hot-Dip Process." ASTM A653. West Conshohocken, PA: ASTM International.

ASTM. 2013b. "Standard Specification for Steel Sheet, Carbon, Metallic- and Nonmetallic –Coated for Cold-Formed Framing Members. Standard ASTM A1003/A1003M-13b. West Conshohocken, PA: ASTM International.

ASTM. 2013c. "Standard Specification for Cold-Formed Welded and Seamless Carbon Steel Structural Tubing in Rounds and Shapes." ASTM A550/A500M. West Conshohocken, PA: ASTM International.

ASTM. 2014a. "Standard Specification for Structural Bolts, Steel, Heat Tread, 120/105 ksi Minimum Tensile Strength. Standard ASTM A325. West Conshohocken, PA: ASTM International.

ASTM. 2014b. "Standard Test Methods and Definitions for Mechanical Testing of Steel Products. ASTM A370. West Conshohocken, PA: ASTM International.

ATC. 1992. "Guidelines for Cyclic Seismic Testing of Components of Steel Structures." ATC-24. Redwood City, CA: Applied Technology Council.

_______. 1995. "Structural Response Modification Factors." ATC-19. Redwood City, CA: Applied Technology Council.

_______. 1997. *A Critical Review of Current Approaches to Earthquake-Resistant Design*. ATC-34. Redwood City, CA: Applied Technology Council.

AWS. 2008. "Structural Welding Code - Sheet Steel." AWS D1.3/D1.3M:2008. Doral, FL: American Welding Society.

_______. 2012. "Recommended Practices for Resistance Welding." AWS C1.1M/C1.1:2012. Doral, FL: American Welding Society.

Caccese, Vincent, Mohamed Elgaaly, and Ruobo Chen. 1993. "Experimental Study of Thin Steel-Plate Shear Walls under Cyclic Load." *Journal of Structural Engineering* 119(2): 573–587. doi: http://dx.doi.org/10.1061/(ASCE)0733-9445(1993)119:2(573).

Driver, Robert G., Geoffrey L. Kulak, Alaa E. Elwi, and D.J. Laurie Kennedy. 1998a. "FE and Simplified Models of Steel Plate Shear Wall." *Journal of Structural Engineering* 124(2): 121–130.

Driver, Robert G., Geoffrey L. Kulak, D.J. Laurie Kennedy, and Alaa E. Elwi. 1998b. "Cyclic Test of Four-Story Steel Plate Shear Wall." *Journal of Structural Engineering* 124(2): 112–120. doi: http://dx.doi.org/10.1061/(ASCE)0733-9445(1998)124:2(112).

Elgaaly, Mohamed, Vincent Caccese, and C. Du. 1993. "Postbuckling Behavior of Steel-Plate Shear Walls under Cyclic Loads." *Journal of Structural Engineering* 119(2): 588–605. doi: http://dx.doi.org/10.1061/(ASCE)0733-9445(1993)119:2(588).

Foutch, Douglas A., and James Wilcoski. 2005. "A Rational Approach for Determining Response Modification Factors for Seismic Design of Buildings Using Current Code Provisions." *Earthquake Spectra* 21(2): 339–352.

ICC. 2011. "Cold-Formed Steel Light-Frame Construction." Section 2211 in *2012 International Building Code*. Washington, DC: International Code Council.

Larson, Jay W. 1998. In-house report. Bethlehem, PA: Bethlehem Steel Corporation.

Matsen Ford Design Associates. 1997. *U.S. Army Corps of Engineers Barracks Prototype, Department of the Army*. Prepared for the National Association of Architectural Metal Manufacturers (NAAMM), Glen Ellyn, IL. Waukesha, WI: Matsen Ford Design Associates.

NEHRP. 2009. *Recommended Seismic Provisions for New Buildings and Other Structures*. FEMA P-750. Gaithersburg, MD: National Earthquake Hazard Reduction Program.

SAC Steel Project. 1997. "SAC Testing Programs and Loading Histories" (unpublished guidance).

Serrette, Reynaud. 1997. *Additional Shear Wall Values for Light Weight Steel Framing*. Final report. Washington, DC: American Iron and Steel Institute.

USACE. 1997. *After-Action Report: Shear Wall Testing and Cold Formed Steel Design, Whole Barracks Renewal*. Fort Lewis, WA: MCA PN 41545 and PN 46748. Seattle, WA: U.S. Army Corps of Engineers, Seattle District.

_______. 1998. *Design of Cold-Formed Load Bearing Steel Systems and Masonry Veneer / Steel Stud Walls*. Technical Instructions TI 809-07. Washington, DC: Headquarters, U.S. Army Corps of Engineers, Engineering and Construction Division, Directorate of Military Programs. https://www.wbdg.org/ccb/ARMYCOE/COETI/ARCHIVES/ti809_07.pdf

Wilcoski, James. 2014. "Excel Cold-Formed Steel Seismic Design Tool." Champaign, IL: Engineer Research and Development Center. Spreadsheet available at http://nees.org/warehouse.

APPENDICES

Appendix A: Prototype Barracks Building and Cold-Formed Steel Test Panel Drawings

This appendix shows a typical three-story barracks framing layout and the six panels tested by ERDC-CERL. The elevation views are a good representation of the typical shear wall panel layout. However, the connection details have been modified since testing the earlier panels and only the details shown in test panels C1 and D2 are recommended. Designers should use the new diagonal strap-to-column connection and column anchorage details shown in the design example in Chapter 12.

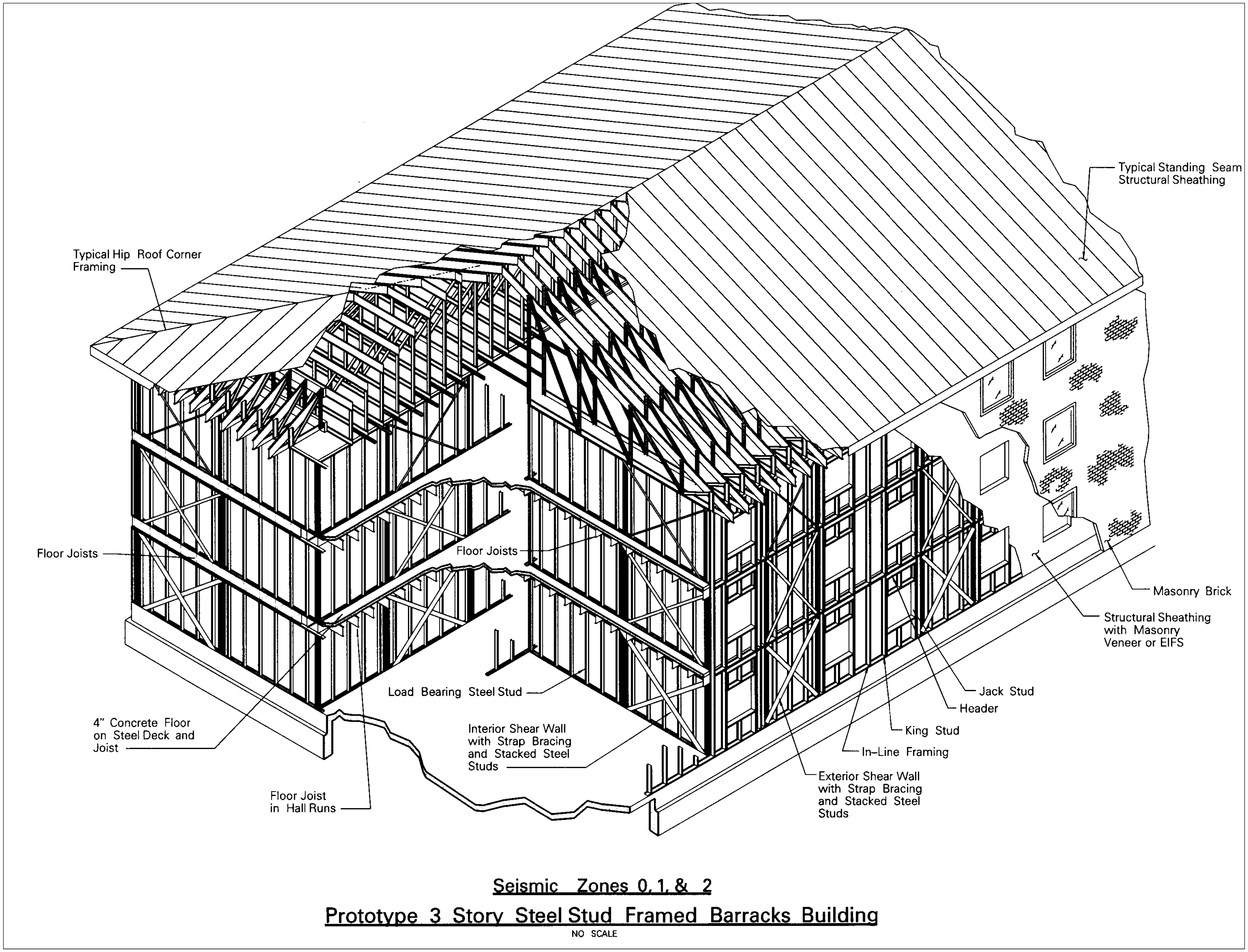

Figure A-1. Prototype 3-story barracks 3-D drawing.

Figure A-2. Test panel A1.

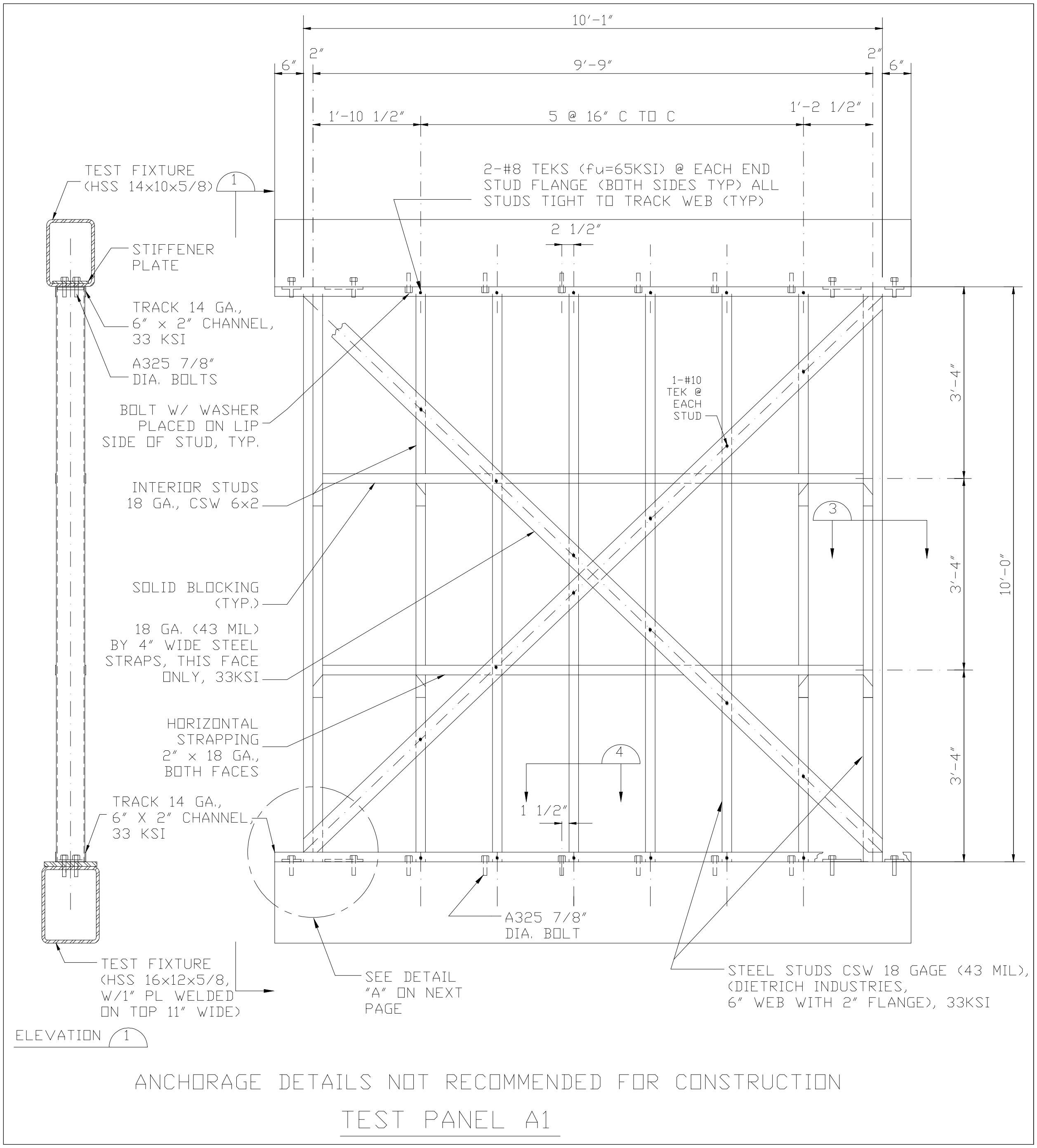

Figure A-3. Test panel A1 details.

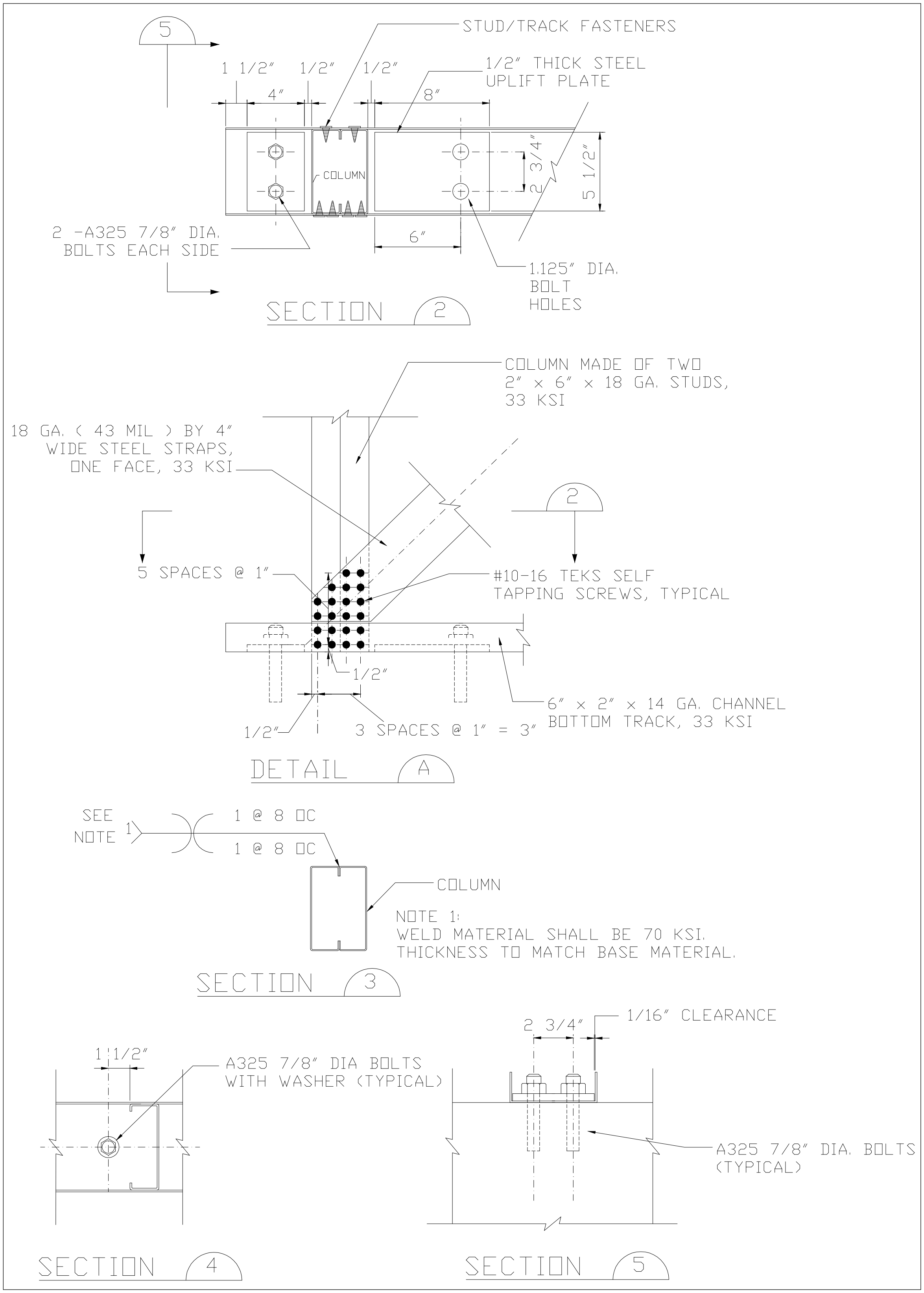

Figure A-4. Test panel A2.

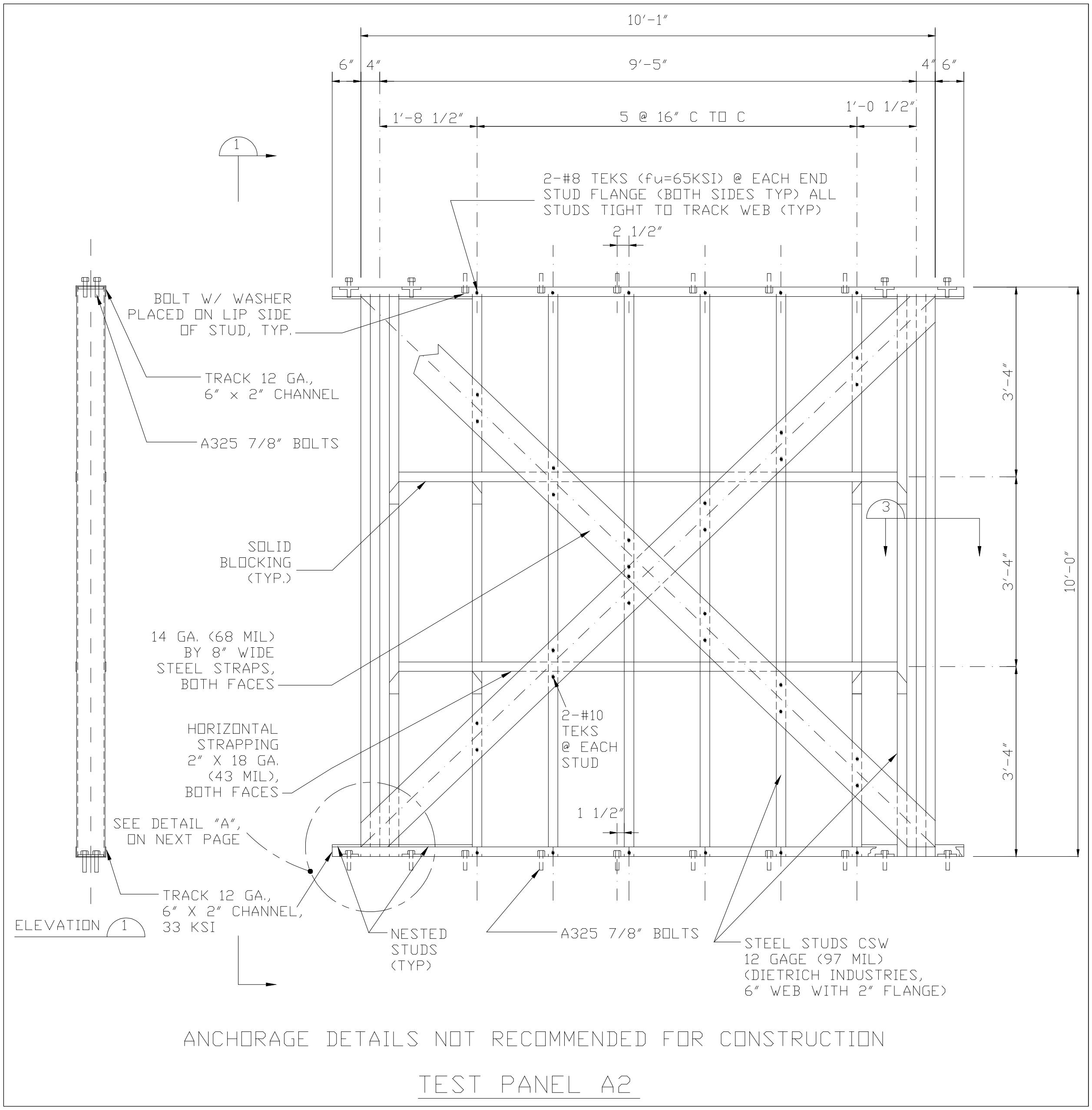

Figure A-5. Test panel A2 details.

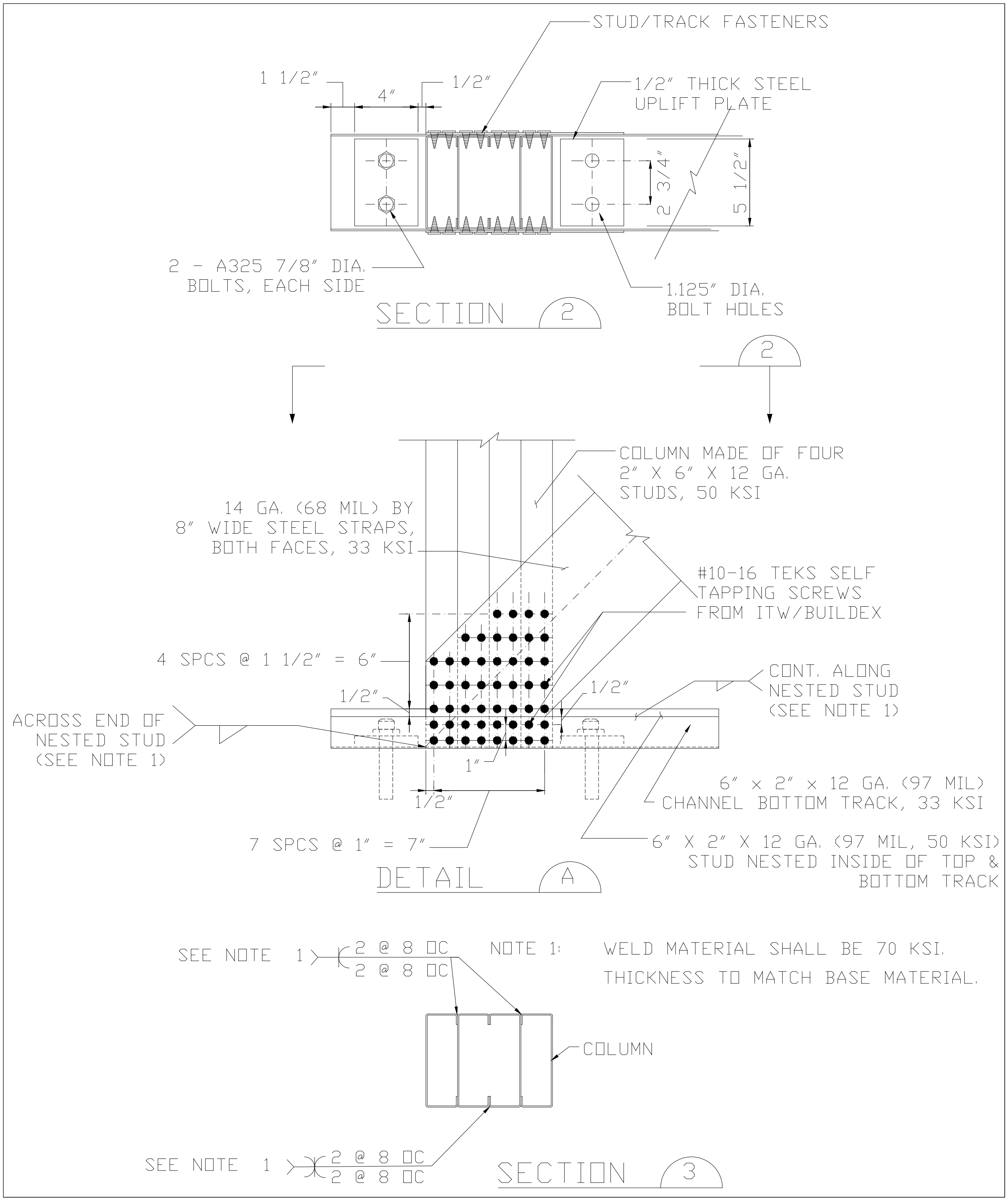

Figure A-6. Test panel A3.

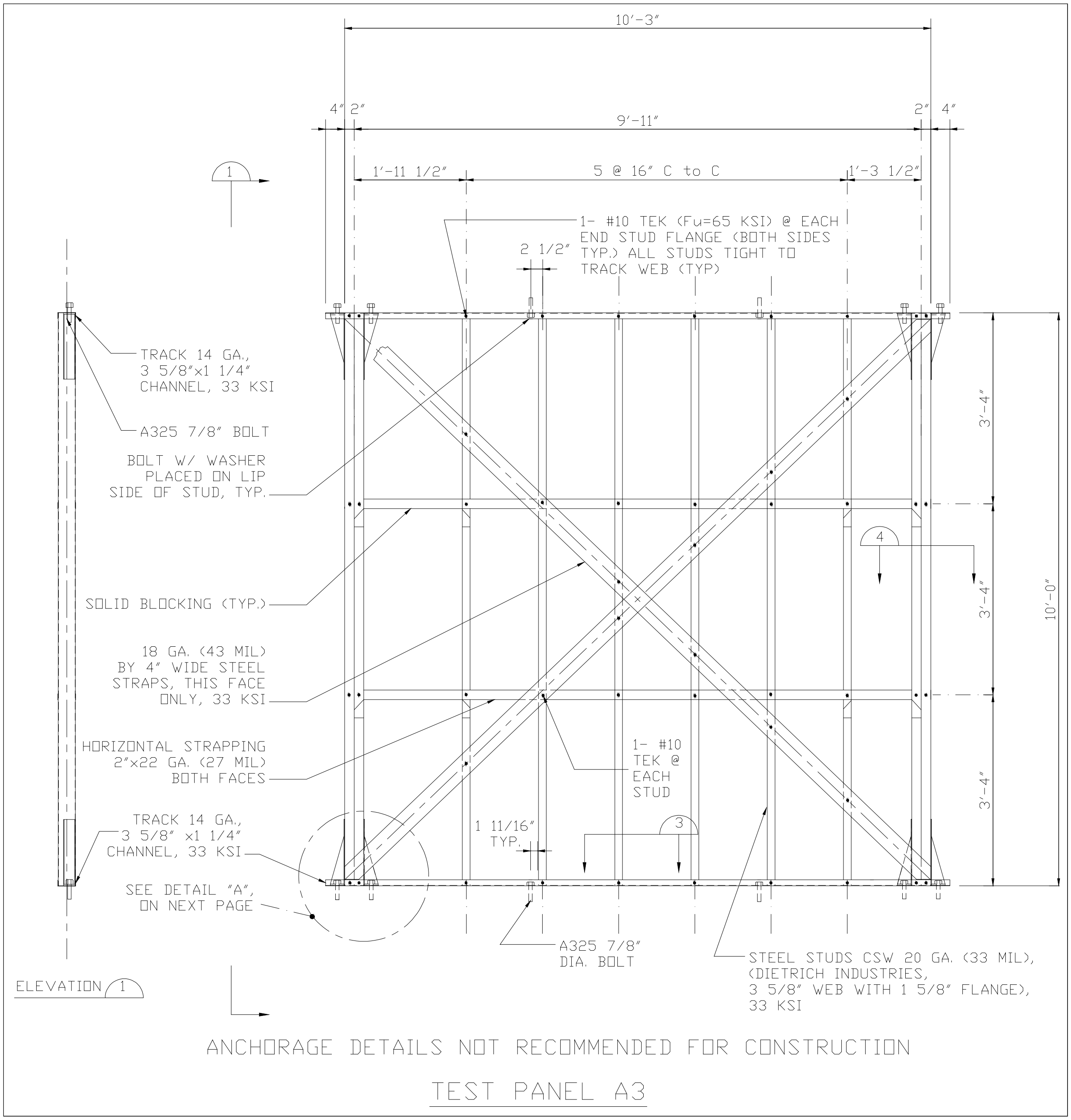

Figure A-7. Test panel A3 details.

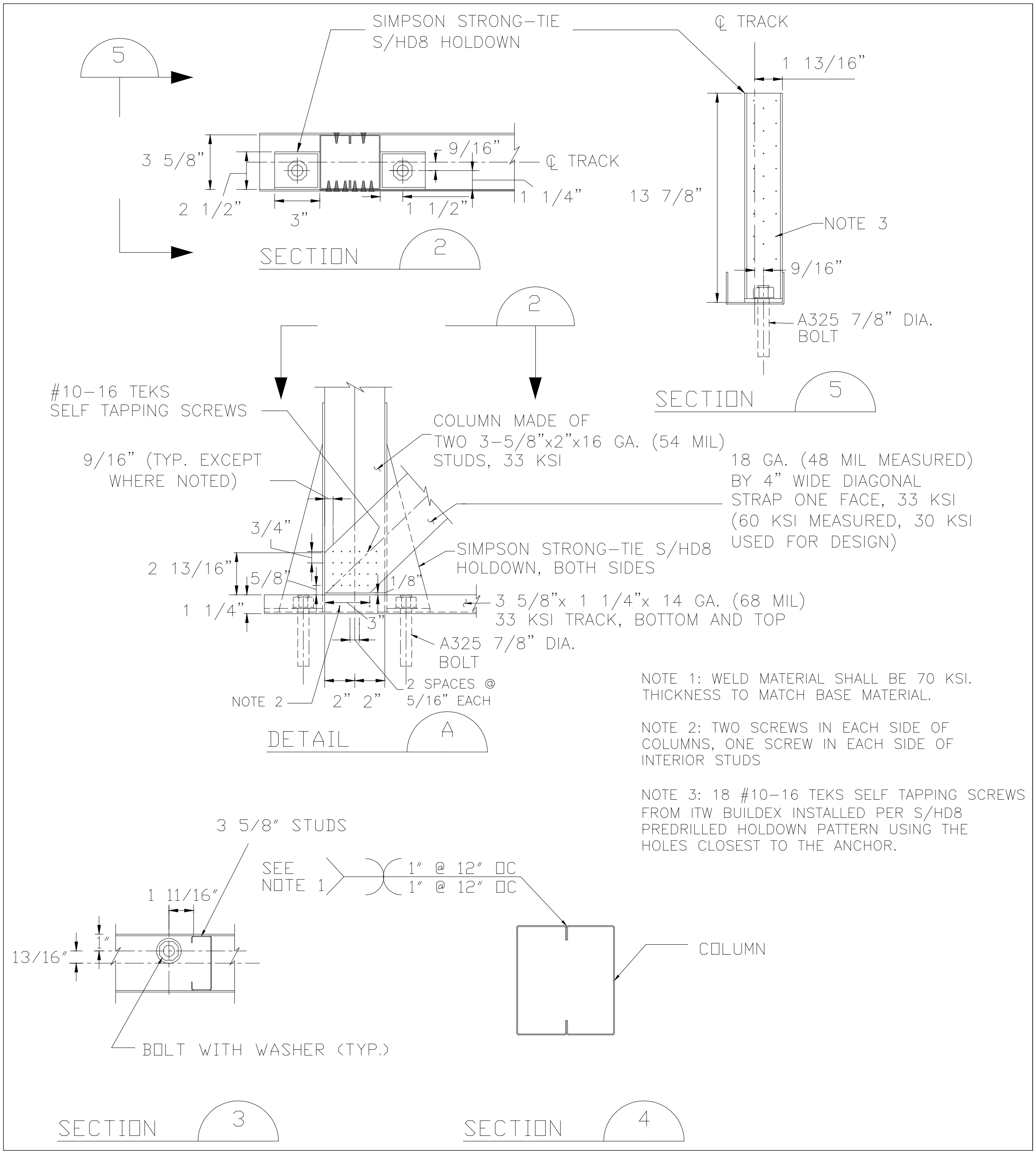

Figure A-8. Test panel C1.

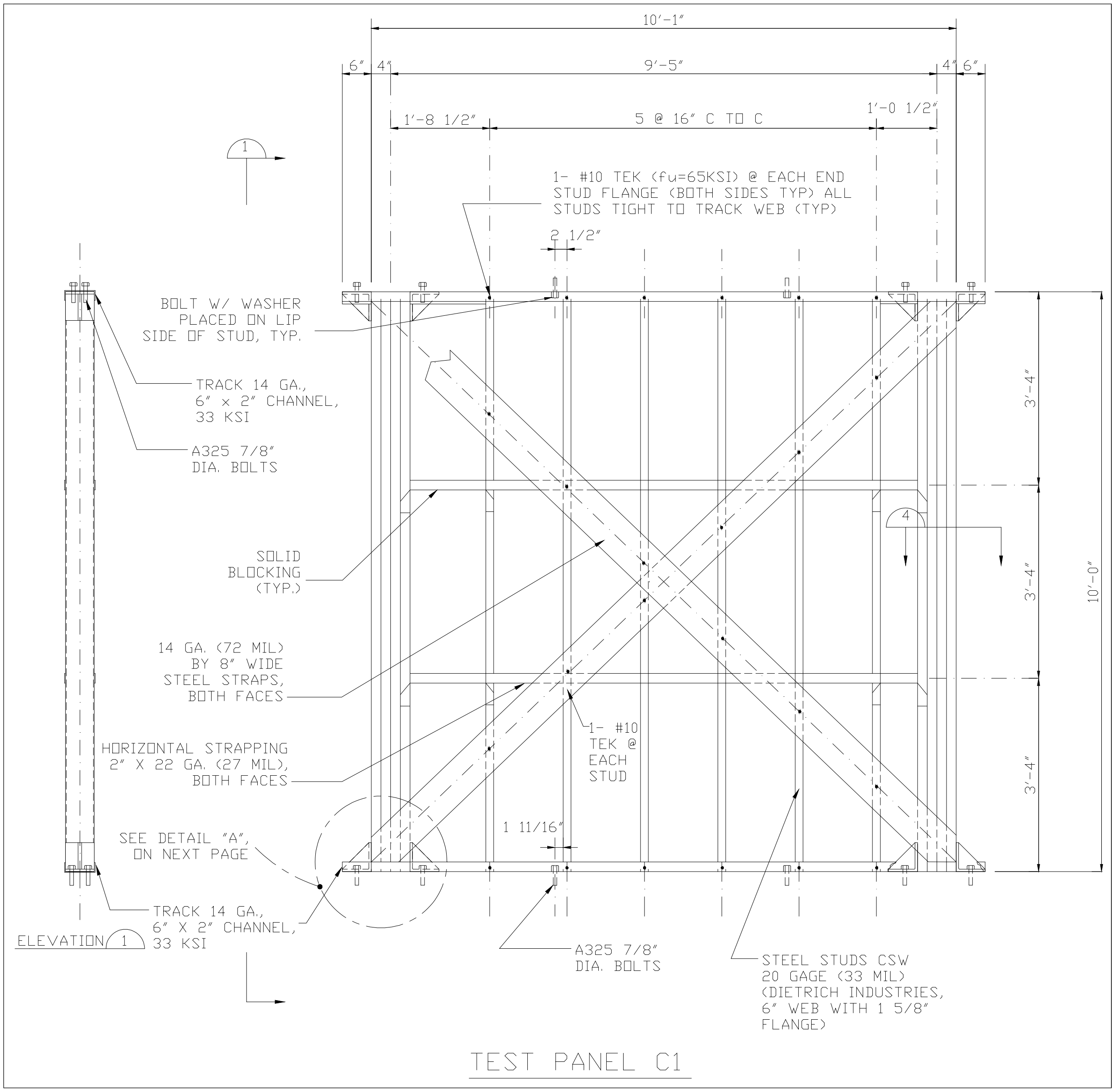

Figure A-9. Test panel C1 details.

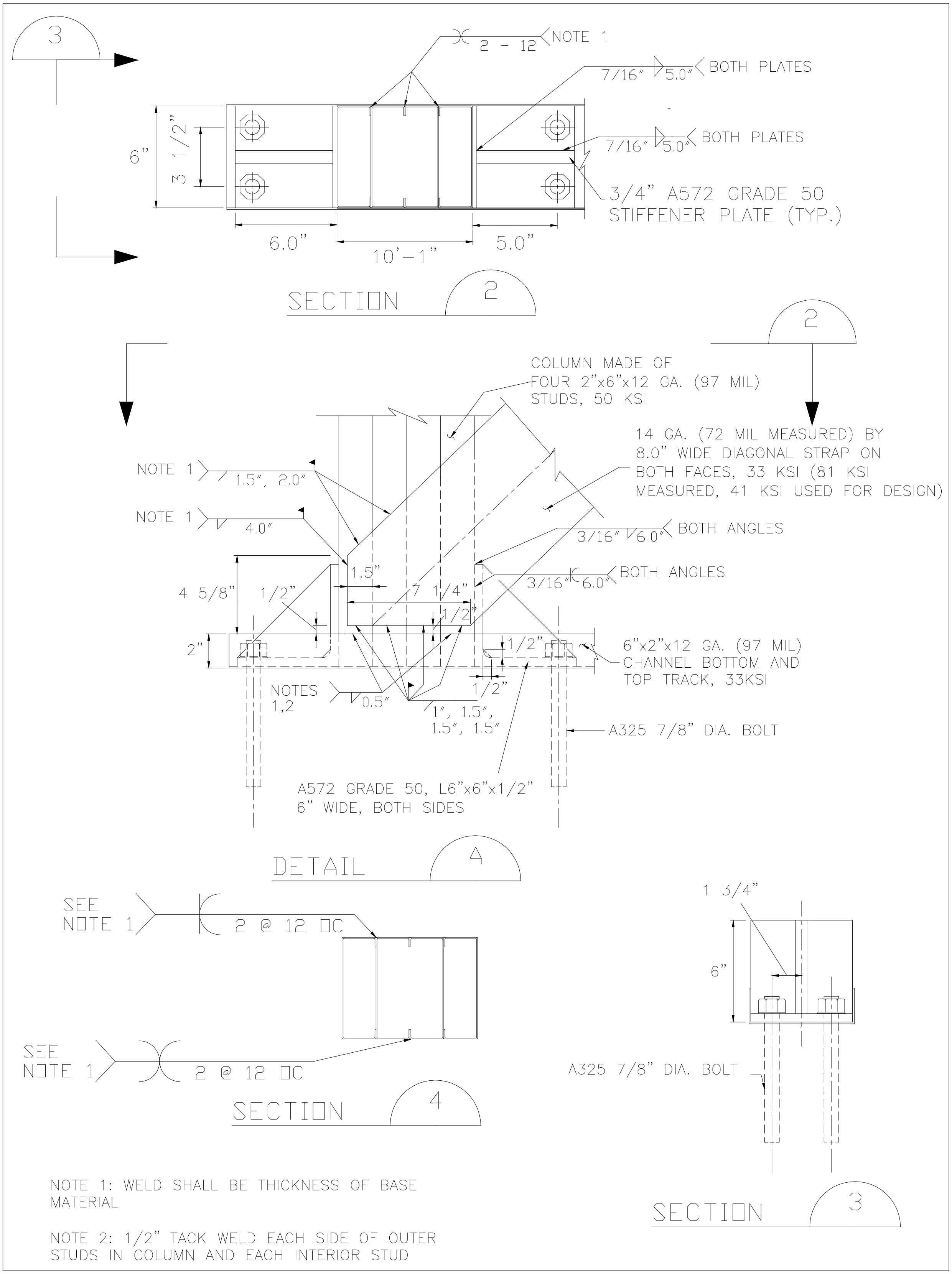

Figure A-10. Test panel D1.

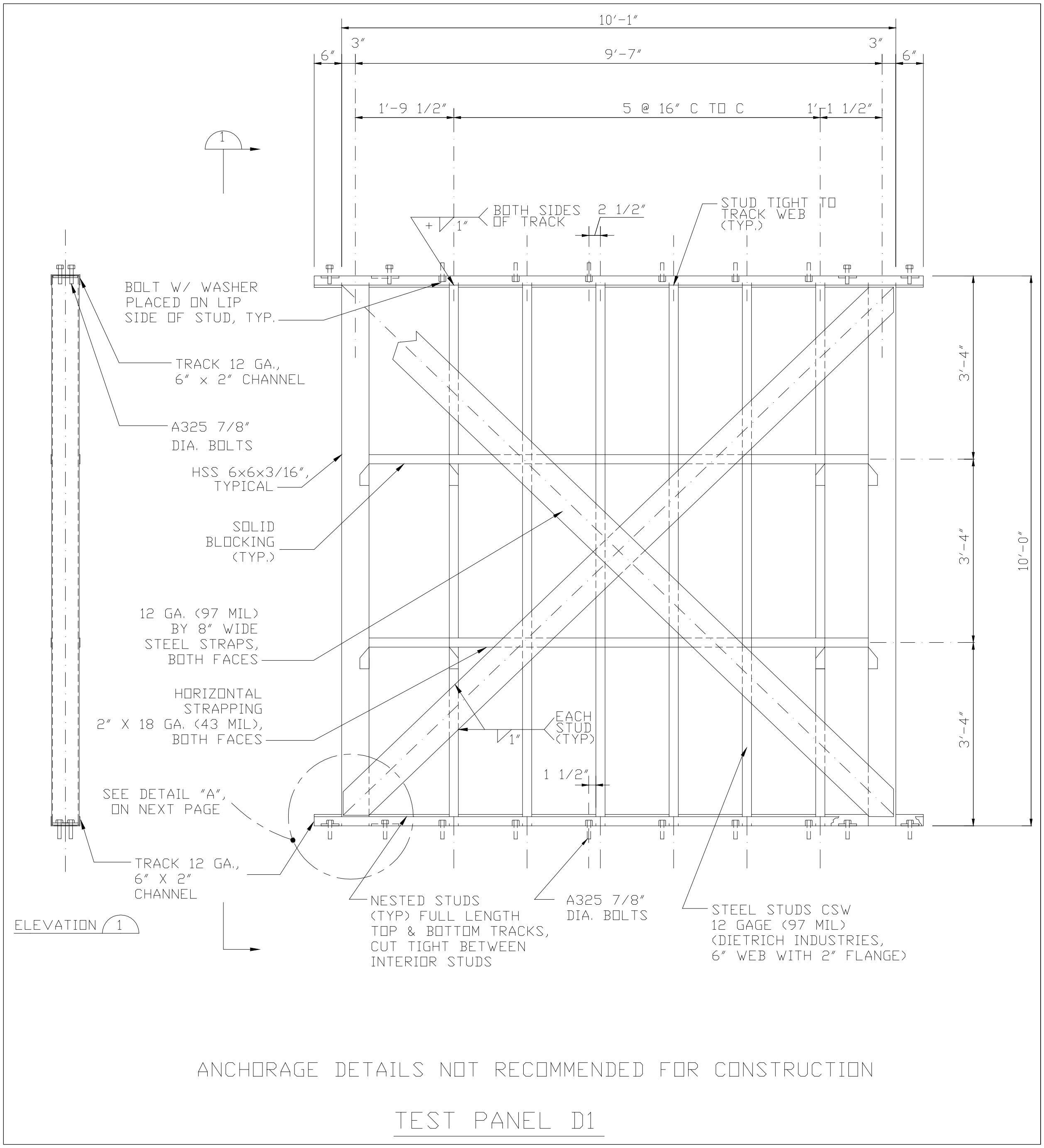

Figure A-11. Test panel D1 details.

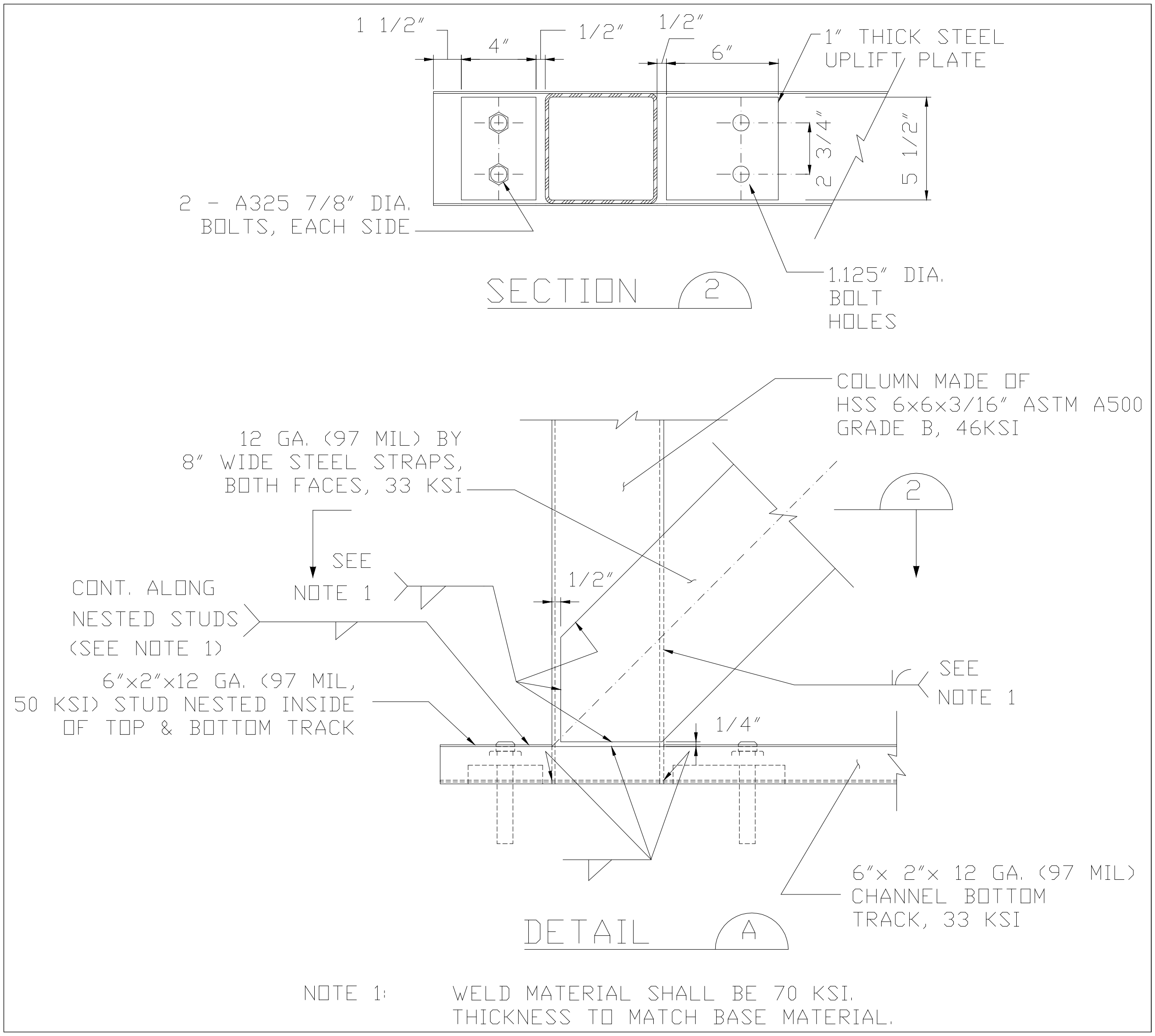

Figure A-12. Test panel D2.

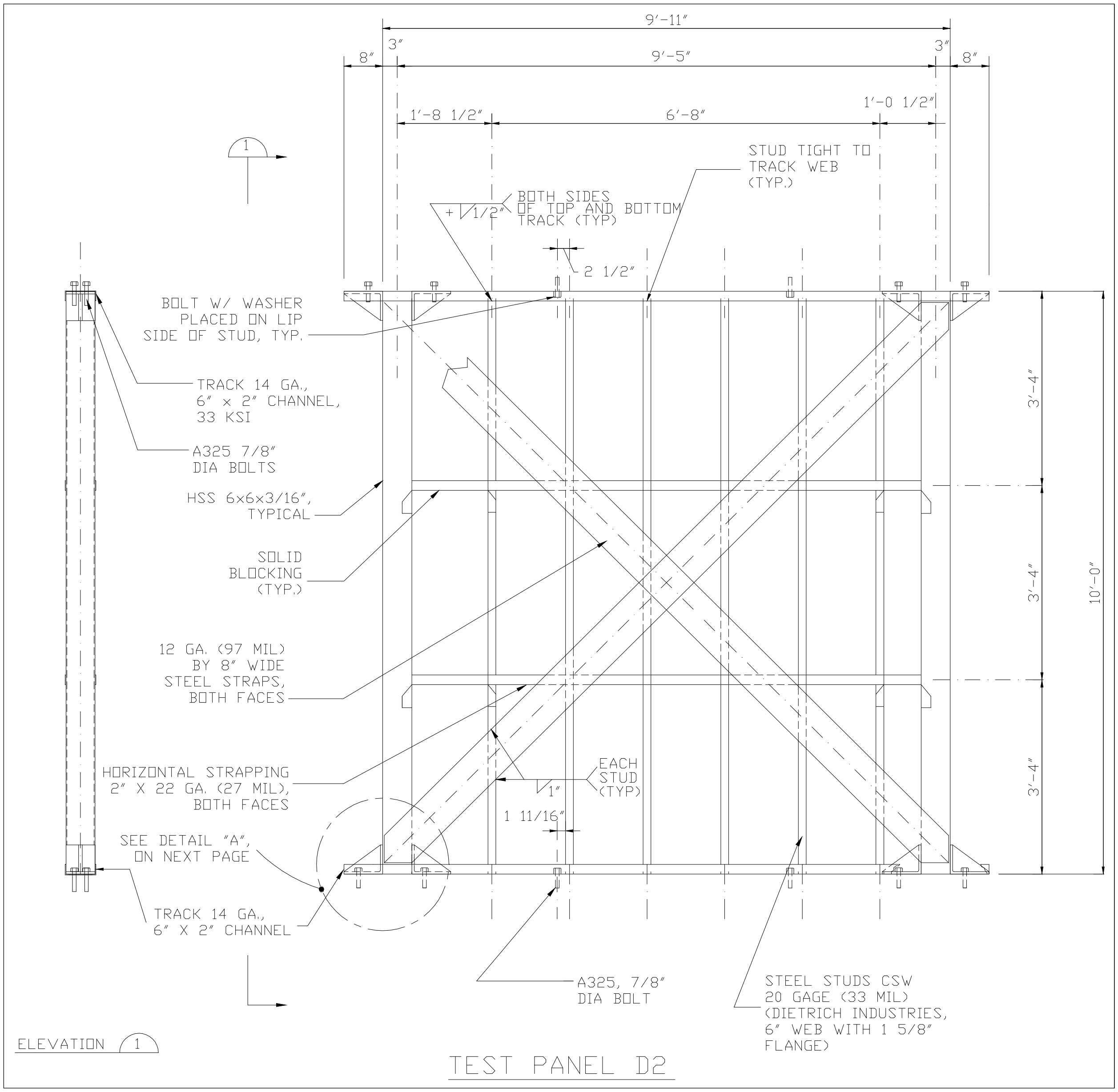

Figure A-13. Test panel D2 details.

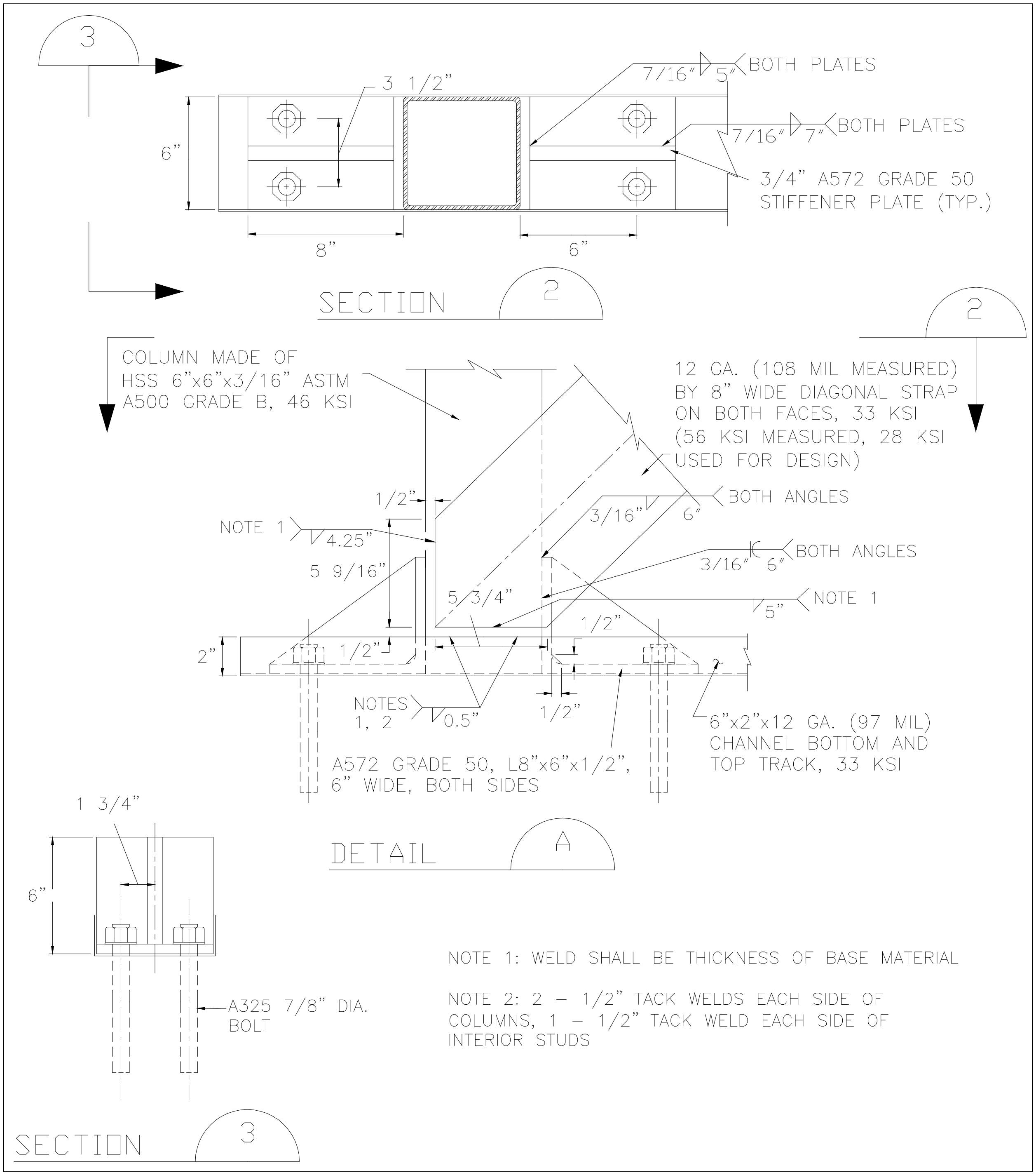

Appendix B: Cold-Formed Steel Test Observations

The following tables provide details on damage progression with respect to lateral deformation for all monotonically and cyclically loaded test panels.

Table B-1. Panel A1a monotonic observations.

Shear Deflection (in.)	Location	Failure or Other Observation
1.0	North (right) column, bottom corner	Local buckling at column knockouts – effectively redistributed loads to other portions of column cross-section.
1.4	South column, top corner	Top of tension strap began detaching, screws failed in shear at column/track connection. Column tearing in shear at column/track connection. Column began to twist at this connection because of column/track failure at the diagonal strap face of column while the other column face continued to carry shear forces to the track.
2.0	Top horizontal strap at south column	Buckling of horizontal strap.
2.1	South column, top corner	All screws at south column – top strap/column connection failed in shear.
3.5	Bottom of third stud in from north	Interior stud twisted and buckled.
3.5	North column	Buckling at two knockouts at the center and near the top of the exterior face of the north column.
3.8	First and third stud in from south column	Buckling of interior studs near their top at the diagonal and horizontal straps.
3.85	Second & third stud in from north column	Buckling of interior studs near their bottom at the diagonal and horizontal straps.
4.5	Second, third & fourth stud in from south column	Buckling of interior studs near their bottom at the horizontal strap.
4.8	North column, top corner	Column bending at the top (local buckling on the north face??).
5.0	South column, top corner	Shear failure of screws at back face of column/track connection.
5.4	North column	Buckling at two knockouts at the center and near the bottom of the interior face of the north column.
6.9	First stud in from south column – top	Screws at stud/track connection failed in shear.
7.8	Second stud in from south column – top	Screws at stud/track connection failed in shear.
8.3	Bottom of north column	Buckling at knockout at the south interior face of the north column.
9.0	Top of south column	Screws (3 or 4) failed in shear at the column/track connection.
9.7	North column, 1 ft down from top	Studs making up the column begin to separate.
10.4	Entire panel	Gross buckling of the columns and interior studs.

Table B-2. Panel A1b cyclic observations.

Shear Deflection (in.)	Location	Failure or Other Observations
0.4	Diagonal straps	Straps yield.
0.6	North and south columns	Buckling at column knockouts.
1.2	Second stud	Buckling of knockout near bottom of stud.
1.2	South column, upper corner	Column is twisting at top track (exterior face).
1.2	South column, lower corner	One screw sheared at lower south corner of column/strap connection
1.6	South column, upper and lower strap connections	Column is tearing between track flange tip and strap connection. There is large twisting at the column's midspan.
1.6	North column, upper corner	Buckling of column at the top track.
2.4	North column, upper corner	Kinking of column at top corner.
2.4	South column, upper and lower corners	Major tearing of column at track flange tip; screws, strap and track connection holding well.
2.4	South column at blocking stiffeners	Large buckling of columns at stiffeners.
2.4	6th stud	Buckling of middle knockout.
3.2	South column, upper corner	Tear halfway across column face between strap and track connections. All screws on strap side of track connection have failed. Screws on opposite side are beginning to fail.
3.2	South column, lower corner	All track screws have failed; only 2 strap screws have failed.
3.2	All studs	Twisting of interior studs near the strap connections (torsional buckling). All stud/bottom track connections have failed.
3.2	Fourth stud	Kinking of the column in the front face of stud near the knockout. Buckling of stud near the bottom track.
4.0	Bottom track	Buckling of stud flanges (front).
4.8	Bottom track	Buckling of stud flanges (back).
4.8	South column, upper corner	All track screws have failed; part of torn column still attached.
4.8	North column, upper corner	Kinking of exterior column flange (back).
5.6	Columns & interior studs	Total collapse of structure.

Table B-3. Panel A1c cyclic observations.

Shear Deflection (in.)	Location	Failure or Other Observations
0.4	Diagonal straps	Yielding of straps.
0.4	Sixth stud – top	Flange buckling in front; possible fabrication error.
0.4	South column, lower corner	Slight elastic shift in alignment of bottom track fasteners from strap connection fasteners. Column is still twisting at the connection.
0.6	North column, lower corner	See 0.4 in., south lower corner.
0.6	Fourth stud – top	Distortion around knockout.
0.6	North column	Column starting to twist at mid-height.
0.8	North column, upper corner	Local buckling of column knockout (interior face).
0.8	South column, lower corner	Permanent offset between strap and track connection.
1.2	North column, upper corner	Buckling of knockout on exterior face of column.
1.2	North column, lower corner	Buckling of column base at bottom track connection.

Shear Deflection (in.)	Location	Failure or Other Observations
1.2	South column, upper corner	Fasteners shearing in strap/column connection. Gaps are forming between the studs in the column. The top edge of the column/strap connection is pulling away from the plane.
1.2	South column, lower corner	Rotation and translation of bottom outer edge of column.
1.2	Strap on back of panel	Strap yielding on back of panel.
1.6	South column	Column has torn at top and bottom track connections.
1.6	North column, lower corner	Local deformation of top row of fasteners at joint. Pictures were taken of interior of column through the knockout.
1.6	South column, upper and lower column connections	Column is torn on face between track and strap connection.

Table B-4. Panel A2a monotonic observations.

Shear Deflection (in.)	Location	Failure or Other Observations
0.8	Diagonal strap	Buckling of strap.
2.1	North column, lower corner	Weld cracking at base (exterior front) of column at column/bottom track connection.
2.6	South column	Weld failure at lower column stiffener.
2.9	South column, upper corner	Weld fracture at column/track connection.
3.0	South column, upper corner	Fasteners breaking.
3.0	South column, lower column	Local buckling of knockout at exterior face.
3.6	North column, lower corner	Holes yielding at base of column.
4.1	Sixth stud – bottom	Stud rotated counterclockwise to the south.
4.4	North column	Local buckling of knockouts in exterior face of column.
5.3	North column, lower corner	Weld cracking at base of column (exterior face -back).
5.9	North column, lower corner	Weld failure along entire base of column/track connection.
6.2	South column, lower corner	Fasteners in column/strap connection failing in shear. Large buckling of column at track flange.
6.2	South column, upper column	Buckling of column flange at track.
7.1	First stud – top	Weld failure at nested stud connection.
7.4	North column, lower corner	Buckling of bottom track (back).
7.9	South column, upper corner	Weld failure at column/track connection.
8.2	North column, lower corner	Horizontal straps buckling.
9.2	South column, upper corner	Column is tearing at top track.
9.4	Interior studs – top	Fasteners failing in shear at top of studs (stud/track connection).
10.3	North column, lower corner	Bottom track yielding (buckling up) between sixth stud and column.
10.5	North column, lower corner	Tearing of web column at the base.
10.7	North column, upper corner	Fasteners connecting strap to studs on back shearing off.
11.2	North column, lower corner	Bottom track beginning to tear at column connection. (Front)
11.7	South column, upper corner	Column is pulling out of the connection.
12.6	Sixth stud – top	Fasteners shearing off at stud/top track connection.
13.2	Second stud	Second stud is twisting and fasteners are failing at both connections.

Shear Deflection (in.)	Location	Failure or Other Observations
14.2	South column	Local buckling of the knockouts.
14.2	South column, upper corner	Top track fractured at first column of fasteners.
Conclusion of test	North column, upper column	Weld at column/upper track connection fractured. Many fasteners at top and bottom of column sheared but the fastener heads remained affixed to the form.

Table B-5. Panel A2b trial cyclic observations (data are incomplete).

Shear Deflection (in.)	Location	Failure or Other Observations
0.5	Diagonal Straps	Buckling in both straps.
0.5	Sixth stud – bottom	Fasteners bending away from column at stud/ track connection.
0.5	Second stud – bracing	Fasteners on strap beginning to pull out.
0.5	First stud – bottom	Fasteners pulling away from base.
0.5	North column, lower corner	Slight bowing of second knockout from the bottom (exterior). Weld cracking at base of column at exterior face. Local buckling of knockouts near the bottom of the column.
0.5	North column, lower corner	Welds fracturing at top and base of column interior face. Buckling of all knockouts along exterior face.
0.5	South column, lower corner	Crack at welds in two directions into the column web (exterior).
0.5	South column, upper corner	Warping of knockouts. Local buckling of track near the back edge.
0.5	North column, upper corner	Large crack width at top of column across top weld. Buckling of top track near the back edge. Strap fasteners pulling out from studs.
6.4	North column, lower corner	Fracture through column at base.
6.4	Second stud – strap	Fasteners pulling out of studs.
6.4	North column, upper corner	Fasteners popping out of column/strap connection.
6.4	Fourth and fifth stud	Noticeable deformation of fastener holes in strap connections.
9.6	South column, upper corner	Bolts popping out of joint. Connection failure (back). Large web fracture at top of column at exterior face.
9.6	South column, lower corner	Buckling of column at base. Fasteners pulling out from column/strap connection.
9.6	Diagonal straps	Excessive buckling of bracing.
9.6	North column, upper corner	Fracture through column web on exterior face.
13.2	South column, upper corner	Column fracture completely through web. Fasteners popping out at joint
13.2	First, second, & third studs	Top fasteners in studs.
13.2	Stud –top	Failed.
15.0	South column, lower corner	Weld failure along bottom of track in nested stud. Column buckling on interior face.
15.0	Fourth & fifth studs - top	Studs twisting.

Table B-6. Panel A2b cyclic observations.

Shear Deflection (in.)	Location	Failure or Other Observations
0.6	Diagonal straps	Straps yielding.
1.2	South column, lower corner	Weld crack at stiffener front and back.
1.6	North column, upper/lower corner	Weld fracture at column.
2.4	South column, lower corner	Weld crack through stiffener.
3.2	North column, lower corner	Screw head sheared off (top row upper). Buckling of bottom track. Failure of 2 track screws at buckle point.
4.0	North column, lower corner	Buckling at column cutout. Buckling at column base.
4.8	North column, lower corner	Screw failure at top track (top row). Screw shearing at bottom track.
5.6	South column, upper corner	Fracture of column weld at top track. Tearing of column.
6.4	South column, lower corner	More weld failures at bottom of column. Column base beginning to bend.
6.4	South column, upper corner	Weld of nested stud failed.
6.4	South column	Weld fracture of column at track connection (interior).
6.4	South column, lower corner	Tearing of lower track near column intersection.
7.2	North column, lower corner	Upward buckling of track web at base of column at outer face. Tearing of track flange near weld at column base.
7.2	South column, lower corner	Fastener failure at column base. Bottom track lifting up off base beam (back).
8.0	South column, lower corner	Fasteners failing at column base (back).
8.0	Sixth stud - top	Fasteners failing at stud/strap connection.
8.0	South column, upper corner	Top track tearing at column intersection.
8.0	North column, lower corner	Fastener failed at track. Uplift of track is causing tearing of bottom track flange. Total failure of column base weld. Multiple fastener failure at north end (back).
8.8	North column - exterior	Buckling of exterior face between knockouts.
8.8	Sixth stud – top	Fastener connecting strap failed (back).
8.8	North column, upper corner	Weld tearing at column/top track connection (exterior).
9.6	North column, upper corner	Tearing of weld at column/top track connection (back).
9.6	Front diagonal strap	Various fasteners shearing at stud connections.
9.6	North column, upper corner	Four fasteners have failed in shear at top track/column connection.
9.6	North column, lower corner	Almost all fasteners in column/bottom track have failed (front).
10.4	Third stud	Fasteners shearing at stud connections.
11.2	North column, upper corner	Fasteners failing at column connection to upper stud.
11.2	Sixth stud – bottom	Fasteners failing at bracing connections.
11.2	North column, upper corner	Weld at column/top track connection failing (still maintaining some load). Fastener failed in shear at column/top track connection.
11.2	Sixth stud – bottom	Fastener failed at strap connection.
11.2	South column, upper corner	Top track tearing at column intersection (back).
11.2	Interior studs	Fasteners failing (back).
11.2	South column, upper corner	Top track tearing at top (back).

Table B-7. Panel A2c cyclic observations.

Shear Deflection (in.)	Location	Failure or Other Observations
0.4	Diagonal straps	Straps yielding.
0.6	North column, upper corner	Exterior weld crack at column/top track connection.
0.6	South column, lower corner	Weld beginning to fail at column/bottom track connection at panel exterior.
0.6	South column, lower corner	Fastener at strap/column connection failure.
1.2	North column, upper corner	Exterior weld continues to crack at column/top track connection.
1.6	Sixth stud - top	Strap fastener shear (front and back).
1.6	South column, lower corner	Bottom track beginning to buckle upwards, followed by screw failure.
2.4	North column, lower corner	Weld fracture at column/base track connection.
2.4	Track	Fasteners pulling out (back).
2.4	South column, lower corner Exterior	Weld at column/bottom track connection failed.
3.2	North column, lower corner	Base track torn from corner to fastener. Track buckling out at column intersection at back face.
3.2	South column, upper corner	Screws sheared at column/top track connection.
4.0	Diagonal strap	Strap buckling (front).
4.0	South column	Top track beginning to tear at column connections. Top weld at upper track/column connection (exterior).
4.0	South column, lower corner	Weld failure along bottom track connection (interior). Entire bottom track failing along exterior column face.
4.0	North column, upper corner	Top track buckling at column. Top track tearing along fastener line.
4.0	North column, lower corner	Welds fracturing at base. Fasteners shearing at bottom of track at back face.
4.0	Upper/north lower corners	Bending of top track away from beam at top and bottom.
4.8	North column, lower corner	Brittle weld fracture along entire base. Bottom track torn along fastener line at back face.
4.8	Sixth stud - bottom	Strap fastener failing.
5.6	Second stud	Fastener failed at strap connection.
5.6	North column, lower corner	Bottom track pulling up from beam.
5.6	North column, upper corner	Weld failure along base (exterior).
5.6	Right column	Local buckling near knockouts.
5.6	North column, lower corner	Column tearing at base near exterior weld.
5.6	South column, lower corner	Bottom track shearing and weld failure through track.
6.4	South column, upper corner	Exterior weld at upper track/column connection failed completely.
6.4	South column, lower corner	Slight buckling of column near base. Bottom track has failed (Back)
6.4	North column, lower corner	Buckling of interior track/column connection.
6.4	North column, upper corner	Column tearing near weld (exterior).
6.4	Sixth stud - top	Stud fastener to top track sheared off. Fasteners have sheared at top track – front and back face.
7.2	South column, upper corner	Fasteners failing at column connection – back face
8.0	South column, lower corner	Track is beginning to uplift from beam.
8.0	Third stud	Fastener failure at strap connection.
8.0	North column, lower corner	Column buckling at track (exterior). Column starting to gap at base.

Shear Deflection (in.)	Location	Failure or Other Observations
8.0	North column, upper corner	Fasteners shearing at track/column connection.
8.8	Third stud – strap	Fasteners shearing at strap connection.
9.6	Third stud – strap	Fasteners shearing at strap connection.
9.6	North column, lower corner	Bottom track flange beginning to tear.
9.6	South column, lower corner	Fasteners at column/strap connection failing.
10.4	North column, lower corner	Bottom track at column base has sheared. Tear continuing along the bottom track.
11.2	First stud- top	Fasteners at strap connection shearing.
12.8	Interior studs - bottom	Studs fail along bottom track at screws.

Table B-8. Panel A3a monotonic observations.

Shear Deflection (in.)	Location	Failure or Other Observations
Loading to the South – Positive Direction on Data Plots		
1.3	South column, top corner	Screws failed between column and track.
2.8	South column, top corner	Major distortion of column.
3.5	South column, top corner	Column pulled away from anchor.
4.0	South column, top corner	Screws between column and strap failing.
5.0	South column, top corner	Strap failed.
Loading to the North – Negative Direction on Data Plots		
0.7	North column, top corner	Screws failed between column and track.
1.15	South column, bottom corner	Screws failed between column and track.
2.2	South column, bottom corner	Column pulling away from strong-tie.
2.8	South column, bottom corner	Column buckling around strong-tie.
5.9	Interior	Studs buckle.
6.3	South column, bottom corner	Column pulling away from strong-tie.
10.0	South column, bottom corner	Slow progression of crushing of double stud between anchors.

Table B-9. Panel A3b cyclic observations.

Shear Deflection (in.)	Location	Failure or Other Observations
0.45	South column, bottom corner	Screws failed between column and track.
0.9	North column, bottom corner	Screws failed between column and track.
1.2	South column, top corner	Strap pulling away from column.
1.2	North column, bottom corner	Bowing of column.
1.8	South column, top corner	Buckling of column.
1.8	South column, bottom corner	Strap pulling away from column.
2.4	South column, bottom corner	Buckling of column.
2.4	North column, top corner	Buckling of column.
3.6	South column, top corner	Screws fail between strap and column.
3.6	Interior	Buckling of interior channels and partial screw pullout.

Shear Deflection (in.)	Location	Failure or Other Observations
3.6	North column, bottom corner	Screws fail between strap and column. Major tearing of column away from anchor
4.8	North column, top corner	Crushing of column against anchor.
4.8	South column, top corner	Channels of column start pulling apart.
4.8	South column, bottom corner	Screws pull out.
6.0	South column, bottom corner	Strap failure by pullout.
6.0	North column, bottom corner	Strap failure by pullout.

Table B-10. Panel A3c cyclic observations.

Shear Deflection (in.)	Location	Failure or Other Observations
0.45	North column, bottom corner	Column flexing with strap tension.
0.6	North column, top corner	Screws failed between column and track.
0.9	South column, Top/bottom corner	Screws failed between column and track.
0.9	North column, top corner	Screws failed between column and track.
1.2	North column, top corner	As connection is stressed, back of column wraps back around anchor.
2.4	North column, top/bottom corner	Screws between column and strap nearly pulling out.
3.6	North column, bottom corner	Strap net area failure at connection.
4.8	North column, top corner	Screws between column and strap pull out.
6.0	South column, bottom corner	Lots of screws showing between strap and column.
7.2	Interior	Interior studs well buckled.

Table B-11. Panel C1a monotonic observations.

Shear Deflection (in.)	Location	Failure or Other Observations
0	Unknown	Weld between track and column failed at application of vertical load.
0.5	North column, top corner	Weld between track and column failed.
0.75	South column, top corner; North column, bottom corner	Major deflection of strap (compression).
2.25	South column, bottom corner	Tearing of the strap.
3.5	South column, bottom corner	Rear strap failed.

Table B-12. Panel C1b cyclic observations.

Shear Deflection (in.)	Location	Failure or Other Observations
0.6	North column, top corner	Weld crack.
0.8	North column, bottom corner	Weld cracked on both sides
1.2	North column, bottom corner	Small cracking at top of angle/column connection.

Shear Deflection (in.)	Location	Failure or Other Observations
1.6	North column, bottom corner	First three welds cracked.
1.6	South column, bottom corner	Weld failure.
2.4	North column, top corner; North column, bottom corner	Complete tear of strap.
3.2	North column, bottom corner	Angle splitting from column.
4.8	North column, bottom corner	Complete tear at angle/column connection.

Table B-13. Panel C1c cyclic observations.

Shear Deflection (in.)	Location	Failure or Other Observations
0.3	North column, top corner	Track weld failure (front).
0.4	North column, top corner	Track weld failure (back).
0.6	North column, bottom corner	Track weld failure (front/back).
1.6	South column, bottom corner	Track weld failure (back).

Table B-14. Panel D1a monotonic observations.

Shear Deflection (in.)	Location	Failure or Other Observations
0.95	Diagonal straps	Straps yielding.
1.0	South column, upper corner	Crack forming in weld at column/top track connection. (Exterior) Track bowing away from beam.
1.37	North column, lower corner	Track pulling up.
1.6	North column, lower corner	Welds fracture at nested studs.
2.1	North column, lower corner	Bottom track tearing at weld (back). Weld at base of column fracture at exterior face.
3.8	South column, upper corner	Top track bowing away from beam.
4.0	South column, upper corner	Welds at nested stud have failed.
4.0	North column, lower corner	Track torn through to base.
4.43	North column, lower corner	Track base tearing. Track flanges bowing out between welds.
6.7	South column, lower corner	Bottom track pulling away from beam.
8.0	South column, lower corner	Weld failing at nested stud/column connection.
8.0	South column, upper corner	Top Track beginning to tear. Buckling of top track is causing it to crush against tube column.
8.46	Sixth stud - straps	Strap exhibiting a hump between welds on same stud.
9.3	North column, lower corner	Nested stud flanges are buckling against tube.
10.2	North column, lower corner - Strap	Strap tearing on back face.
10.68	North column, lower corner – Strap	Strap tom through on back.
10.68	Interior studs - bottom	Weld at base of interior stud fail.
11.24	North column, lower corner-strap	Front strap torn through on front.

Shear Deflection (in.)	Location	Failure or Other Observations
11.24	North column, lower corner	Bottom track bowing up.
11.24	Third stud	Strap weld fails.
12.0	First stud - bottom	Weld failure at strap connection.
12.5	Fifth stud - bottom	Stud buckling at base.
13.14	North column, lower corner	Bottom track buckling at base.
13.6	Interior studs - bottom	Massive buckling at stud/bottom track connections.
14.0	North column, lower corner	Weld fracture/tearing through track.
14.45	Diagonal strap	Strap weld failures at stud connections.
14.45	Base beam	Dishing effects at bolts.

Table B-15. Panel D1b cyclic observations.

Shear Deflection (in.)	Location	Failure or Other Observations
0.4	Diagonal straps	Straps yielding.
0.6	North column, upper corner	Weld begins to fail at column/top track connection at exterior face.
1.2	North column, upper corner	Welds across flanges fail at nested studs.
1.2	South column, upper corner	Welds across flanges fail at nested studs.
1.6	South column, lower corner	Welds across flanges fail at nested studs.
2.4	South column, lower corner	Bottom track beginning to uplift under outside of column.
2.4	South column, upper track	Tear in top track beginning to propagate in track near column at exterior face.
3.2	North column, lower corner	Weld begins to fail at flange of nested stud. Bottom track lifting up.
3.2	Second stud - strap	Weld at strap connection begins to fail at front and back face.
3.2	Third stud - strap	Weld failure at strap connection at back face.
4.0	North column, lower corner	Track tearing near column connection at front face. Tearing of bottom track along side at front face.
4.0	Second stud - strap	Weld at strap connection fails at front face.
4.0	North column, upper corner	Top track tearing. Flange of nested stud beginning to buckle.
4.0	South column, upper corner	Tears forming at column/top track weld connection at front and back faces. Buckling of nested stud flange due to prying action against column.
4.8	Sixth stud - bottom	Weld failure at strap connection.
4.8	Diagonal straps	Straps bowing between welds of same stud.
4.8	Second stud - bottom	Weld at strap connection failed at front and back faces.
5.6	North column, lower corner	Bottom track buckling out at column.
5.6	Sixth strap - bottom	Weld beginning to fail at strap connection.
5.6	North column, upper corner	Top track pulling away from beam.
5.6	South column, lower corner	Weld failure of column/bottom track connection at exterior face.
6.4	South column, upper corner	Weld failure of column/bottom track connection at exterior face.
6.4	North column, lower corner	Sudden weld fracture at column/bottom track connection at exterior face. Strap/column connection beginning to fail at back face. Bottom track buckling out at back face.
7.2	North column, upper corner	Strap/column connection beginning to fail. Weld failure at column/top track connection at exterior face.
7.2	Sixth stud - bottom	Stud beginning to tear near bottom track. Stud buckling at base.

Shear Deflection (in.)	Location	Failure or Other Observations
7.2	Fifth stud - bottom	Weld fails around strap.
8.0	South column, upper corner	Top track flanges beginning to buckle near column/top track connection.
8.0	Interior studs	Welds at strap/stud connection fail. Studs tearing near bottom track.
9.6	North column, lower corner	Strap beginning to tear.
9.6	North column, upper corner	Weld failure at column/top track connection at exterior face.
10.4	North column, lower corner	Strap tearing near column in two places. Weld failure near tear column/strap connection.
11.2	North column, lower corner	Sudden failure of back strap.
11.2	North column, upper corner	Strap beginning to tear.
12.0	North column, upper corner	Strap beginning to tear on back near column.
13.6	Interior studs	Local buckling near knockouts.
13.6	Diagonal straps	Three straps have failed.

Table B-16. Panel D1c cyclic observations.

Shear Deflection (in.)	Location	Failure or Other Observations
0.4	Diagonal straps	Straps yielding.
0.8	South column, lower corner	Inside weld of nested stud beginning to fracture.
1.2	South column, upper corner	Weld on top of nested stud beginning to fracture.
1.6	South column, lower corner	Tearing of bottom track at column interior.
1.6	North column, upper corner	Crack in weld at column/nested stud connection at front face.
2.4	North column, Lower Column	Weld at column/bottom track failed. Tear forming across nested stud near column connection at exterior face. Buckling of bottom track away from the nested studs. Uplift of track at column (front).
2.4	First stud	Strap weld fracturing (back).
3.2	North column, lower corner	Tear at weld propagating into bottom track.
3.2	South column, upper corner	Top track beginning to tear (exterior).
4.0	First & second stud	Welds to strap beginning to fail (back).
4.0	Third stud	Weld to strap failed (front).
4.0	North column, lower corner	Large crack through weld at the top of Bottom track near column connection at exterior face.
4.0	North column, Upper Column	Tear forming in top track at column connection at exterior face.
4.8	South column, lower corner	Bottom track beginning to lift off beam. Bottom track beginning to tear near column interior face.
4.8	First stud - bottom	Weld to bottom track beginning to fail.
4.8	South column, lower corner	Buckling of track at base.
4.8	First stud - top	Strap weld fails at back face.
5.6	North column, upper corner	Weld beginning to tear at strap/column connection at back face.
5.6	South column, lower corner	Weld at column base continues to fail.
5.6	First stud - bottom	Strap weld failure (back).
5.6	Third stud	Strap weld failure (front).
6.4	Sixth stud - top	Weld failure at strap connection at front and back face.
6.4	Fifth stud - top	Top track beginning to tear and twist at top track/stud connection.

Shear Deflection (in.)	Location	Failure or Other Observations
6.4	South column, upper corner	Top track tearing around column interior. Buckling of top track around column interior.
6.4	South column, lower corner	Small weld fracture of column/strap connection (front).
7.2	South column, lower corner	Total weld failure of column to bottom track connection at back face.
7.2	North column, upper corner	Weld failure along column/top track connection at back face.
7.2	Fourth and fifth stud	Welds to strap fails.
8.0	First stud	Strap bowing between welds on same stud. Short panel welds fail. Short panel near stud is rotating down.
8.0	Interior studs - bottom	Studs buckling near bottom track.
8.0	Second stud - strap	Strap beginning to tear (back).
8.0	First stud - bottom	Stud tearing near bottom track.
8.0	Second stud - top	Weld failing at stud/top track connection.
8.0	Fourth stud - top	Stud tearing near top track (front).
8.0	First stud - top	Stud tearing near top track (front).
8.0	Fifth stud - bottom	Stud tearing at stud/bottom track connection.
8.0	Sixth stud - top	Weld at strap connection failed (back).
8.0	Diagonal strap at fifth stud	Strap beginning to tear at stud connection on front face.
8.8	Second and third stud – top	Weld beginning to fail (track/top track connection).
8.8	Interior studs	All studs tearing along bottom track.
8.8	Diagonal strap – north column, upper corner	Strap beginning to tear at column connection (front).
9.6	North column, upper corner	Welds at strap connections beginning to tear at front & back faces.
9.6	South column, upper corner	Sudden weld failure at column/top track connection.
9.6	Interior studs	All studs tearing along top track.
9.6	South column, upper corner	Top track pulling away from beam.
12.0	North column, upper corner	Strap beginning to tear near column at back and front face.
12.8	Sixth stud at strap	Tear is propagating at first stud weld.
13.6	North column, lower corner	Two tears forming in straps near column at front face.
13.6	First stud	Short panel weld fails causing panel to swing down.

Table B-17. Panel D2a monotonic observations.

Shear Deflection (in.)	Location	Failure or Other Observations
Loading to the North – Positive Direction on Data Plot		
0.7	South column, bottom corner	Track weld failure.
0.8	North column, top corner	Track weld failure.
1.7	North column, top corner	Brittle fracture of strap.
1.9	South column, bottom corner	Brittle fracture of strap (back side).
Loading to the South – Negative Direction on Data Plot		
0.5	South column, top corner	Track weld failure.
1.2	South column, top corner	Vibration noise.

Table B-18. Panel D2b cyclic observations.

Shear Deflection (in.)	Location	Failure or Other Observations
0.4	North column, bottom corner	Track welds failed (back – north side of column).
0.6	North column, top corner	Track welds failed (back).
0.8	North column, bottom corner	Track welds failed (back – south side of column).
2.4	South column, top corner	Back strap failed.
2.4	South column, bottom corner	Front strap broke.
4.0	Unknown	Last strap broke.

Table B-19. Panel D2c cyclic observations.

Shear Deflection (in.)	Location	Failure or Other Observations
0.3	North column, top/bottom corner	Track weld failure (front and back).
2.4	North column, bottom corner	Brittle tear of strap.

Appendix C: Prototype Shear Panels for Cold-Formed Steel Seismic Design

This appendix provides tabular data for the selection of possible prototype shear panels that may be used in the seismic design of cold-formed steel structures. These panels were developed for the example problem presented in Chapter 12, using the design recommendations presented in Chapter 11. Each shear panel given in Table C-1 is defined in Figure 12-9, Figure 12-11, Figure 12-13 and Figure 12-12, as indicated in Table C-1. The panel shown in Figure 12-14 was not selected for the example problem, but meets all the requirements of these design recommendations.

Definition of terms

The prototype shear panels given in Table C-1 shall be used based on the following definition of terms. For these panels, the values of GL_{max} and GL_{min} were defined at which the demand reached the capacity for one of the limiting equations given below.

$\varphi_t Q_{sy}$ = the lateral shear panel design strength that must exceed the maximum story shear per shear panel, including the effects of torsion, defined and limited by Equation 11-37.

GL_{max} = the maximum gravity load per shear panel, defined by Equation 11-18 and limited by Equations 11-55 or 11-56.

GL_{min} = the minimum gravity load per shear panel, defined by Equation 11-19 and limited by Equations 11-100, 11-108, 11-116, 11-117, 11-118, 11-120, or 11-122.

Prototype panel load table

Table C-1 provides the tabular data needed to select prototype shear panels.

Table C-1. Prototype shear panel load capacities.

Panel Figure	Lateral Design Strength $\phi_t Q_{sy}$ (kips)	Max Gravity Load/ Panel GL_{max} (kips)	Min Gravity Load/ Panel GL_{min} (kips)
Figure 12-9	8.1	35.2	-3
Figure 12-11	19.0	36.5	-4
Figure 12-13	24.2	88.5	10
Figure 12-14	24.2	224	5

Appendix D: Seismic Qualification Procedure and Acceptance Criteria for Other Shear Panel Configurations

This appendix presents the test procedure, acceptance criteria, and documentation requirements needed to demonstrate the acceptability of cold-formed steel shear panel configurations that are different from the specific system defined in Chapter 11. Acceptable configurations are limited to cold-formed steel shear panels that use diagonal straps or full panel sheets as the lateral-load-resisting elements. The columns shall be constructed with cold-formed or hot-rolled structural steel. This procedure applies to the qualification of a prototype of the specific panel that will be used in construction. Qualification requires the testing of three specimens. All panel tests shall represent full panel system tests of all the panel components including connections and anchors.

Coupon tests of all test panel materials

Coupon tests shall be performed on all materials that may contribute to the structural performance of the test panels. At least three coupons shall be tested from each lot of each type of material. Coupons shall be prepared and tested following the provisions of ASTM A370 (ASTM 2014b). Materials that contribute to the ductility of the shear panels shall have a total elongation of at least 10% for a 2 in. gage length. All coupon test results shall be plotted in a test report, in terms of stress versus strain. All coupon test results shall also be summarized in a table in the format shown in Table D-1. The data in this table shall be the average value of the three or more coupons of the particular component.

Table D-1. Tabular format for coupon test results.

Structural Component of Coupon	Design Yield Stress (MPa or ksi)	0.2% Offset Yield Strain* (mm/mm)	0.2% Offset Yield Stress* (MPa or ksi)	Maximum Load Strain (mm/mm)	Maximum Stress (MPa or ksi)	Max Stress 0.2% Offset Yield Stress
Component #1						
Component #2						

See Chapter 4 for the definitions of 0.2% offset yield strain and stress.

Coupon test of all field panel materials

Coupon tests shall be performed on all materials that contribute to the structural performance of the field panels. The field panels shall be identical to the prototype-tested panels. At least three coupons of each material shall be tested. Coupons shall be prepared and tested following the provisions of ASTM A370 (ASTM 2014b). Materials that contribute to the ductility of the shear panels shall have a total elongation of at least 10% for a 2 in. gage length. All coupon test results shall be plotted in a test report, in terms of stress versus strain. All coupon test results shall also be summarized in a table in the format shown in Table D-1. The data in this table shall be the average value of the three or more coupons of the particular component. The field diagonal straps or full panel sheets shall have a coupon yield stress (0.2% offset) not greater than 5% above or not less than 10% below the test panel coupon yield stress (0.2% offset). The field material coupons for all other structural elements shall have coupon yield stress (0.2% offset) not less than the test panel coupon yield stress (0.2% offset).

Test configuration

Full-scale test panels shall be tested with both monotonic (push-over in one direction) and cyclic loading. The panels shall be anchored to a base beam and top beam in a manner representative of the field installation. The base beam shall resist any slippage, out-of-plane movement or rotation in any direction. Vertical load shall be applied to the shear panel through the top beam, at a level representative of potential gravity loads in the field. The amount of vertical load applied should consider the worst-case condition for the most vulnerable panel components. For example, the minimal vertical load may provide the most severe loading for the anchors, while the maximum vertical would provide the worst-case loading for column buckling. This vertical load shall be held constant throughout each test. The top beam shall be held horizontal during all tests, as this represents the field conditions when the panel is assembled in a building. Figure D-1 shows the test configuration and instrumentation plan for shear panels tested at ERDC-CERL, to illustrate the load configuration. In the ERDC-CERL tests, stroke control was used to keep the two vertical actuators at the same length, which held the top beam horizontal. The combined vertical force was held constant by using the test control system (which was done manually for earlier tests).

Figure D-1. Schematic drawing showing sensor locations.

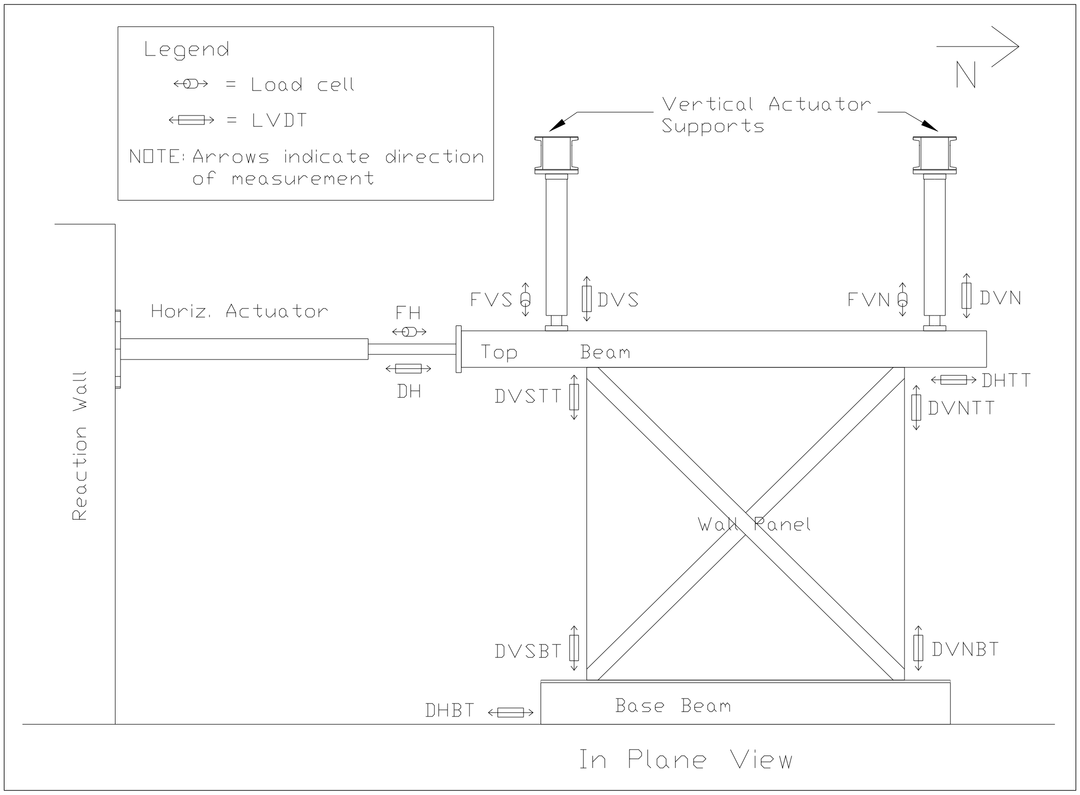

Instrumentation

Table D-2 defines the instrumentation required for all shear panel tests. Figure D-1 shows the location and orientation of all sensors, and Table D-2 describes the purpose of each sensor. The purpose of most gages is to ensure that no unwanted motion takes place and for test control. The only data used in reporting panel performance are the first, second, third, and fourth channels in Table D-2. The vertical actuator force measurements (FVS and FVN in Table D-2 and Figure D-1) are required to define total shear force when deflections reach large amplitudes, at which point the horizontal components of these forces become significant. This total shear force, TSF, is determined as follows:

$$TSF = FH - TVF\left\{sin\left[arctan\left(\frac{DH}{L}\right)\right]\right\} \quad \text{(Eq D1)}$$

where

FH = the measured horizontal actuator force (see Table D-2 or Figure D-1).

TVF = the total vertical actuator force, equal to FVS plus FVN (Table D-2 or Figure D-1).
DH = the measured horizontal displacement (Table D-2 or Figure D-1).
L = the length of the vertical actuators, with vertical load applied but no horizontal displacement.

Table D-2. Cold-formed steel shear panel instrumentation.

Channel #	Sensor Type	Measurement, Direction, Location and Symbol	Purpose
1	Load cell	Force Horizontal, FH	Horizontal actuator load measurement
2	LVDT	Deflection Horizontal, DH	Horizontal deflection, shear panel deformation
3	Load cell	Force Vertical South, FVS	Manual vertical load control (25k total load w/#5)
4	LVDT	Deflection Vertical South, DVS	Stroke (tied to #6)
5	Load cell	Force Vertical North, FVN	Load (summed with #3, for 25k total load)
6	LVDT	Deflection Vertical North, DVN	Controlled by #4 stroke feedback
7	LVDT	Defl Horiz Bot Track, DHBT	To ensure no slippage
8	LVDT	Defl Vert South Bot Track, DVSBT	To ensure no uplift
9	LVDT	Defl Vert North Bot Track, DVNBT	To ensure no uplift
10	LRDG* (20")	Defl Horiz Top Track, DHTT	Check for shear panel deformation - same as #2
11	LRDG (10")	Defl Vert South Top Track, DVSTT	Vertical panel/column deformation & rotation check
12	LRDG (10")	Defl Vert North Top Track, DVNTT	Vertical panel/column deformation & rotation check

*Linear resistance deflection gage, or cable-extension position transducer.

Test requirements

For each shear panel qualified, three specimens shall be fabricated and tested. This requirement assumes only minor variation in panel performance for a given shear panel. If large variations occur, more than three specimens shall be tested and a statistical evaluation of panel performance may be required. For panels with minor variation, one specimen shall be tested monotonically and two shall be tested cyclically, as defined below. All tests, both monotonic and cyclic, shall use stroke control, loading the panels laterally at a constant displacement per minute. The vertical load shall be held constant and the top beam shall be held horizontal throughout each test, as described previously under “Test Configuration.” Both monotonic and cyclic tests shall be conducted up to deflections that cause ultimate failure of the shear panels or reach the limits of the test equipment, but shall not be less than 10 times the lateral yield displacement of the test panel, δ_y. These deflections are very large (well beyond acceptable drift limits), but they are needed to ensure that brittle failures (sudden loss of lateral or vertical load-carrying capacity) do not occur near the useful deflection range of the panel.

Monotonic test protocol

A single specimen of each shear panel shall be loaded in one direction (monotonic) at a constant stroke rate that is slow enough to allow careful observation of panel performance and failure progression.[25] These observations shall include documentation of panel behavior through a log of observations with respect to displacement and photographs. Load versus deflection (TSF versus DH) shall be plotted to determine the measured lateral yield displacement, δ_y, and this value shall be used in defining the cyclic test protocol.

Cyclic test protocol

A minimum of two specimens of each panel configuration shall be loaded cyclically at a constant stroke rate that is slow enough to allow careful observation of panel performance and failure progression[26]. These observations shall include documentation of panel behavior through a log of observations with respect to displacement and photographs. Load versus deflection (TSF versus DH) shall be plotted to create load/deflection hysteretic envelopes. The cyclic load protocol follows a standard method, so that test results may be compared with cyclic test results of other systems. The protocol defined here is similar to SAC Phase 2 guidelines (SAC 1997) that have been modified to scale to the lateral yield deflection, as described in ATC-24 (ATC 1992). The SAC-recommended loading histories call for loading with a deformation parameter based on interstory drift angle, θ, defined as interstory displacement over interstory height. The commentary to SAC (1997) explains that the interstory drift angle of 0.005 radians corresponds to a conservative estimate of the value that would cause yield deformation. Therefore, the load protocol defined by SAC in terms of drift angle is scaled to the measured lateral yield deflection, δ_y, to define the cyclic test steps shown in Table D-3. This protocol calls for a set number of cycles at each of the deformation amplitudes shown in Table D-3. This protocol is illustrated by the deformation time history shown in Figure D-2, which is based on a lateral yield deflection, δ_y of 0.4 in. and stroke rate of 6 in. per minute.

[25] Monotonic tests reported in Chapter 7 used a stroke rate of 0.5 in. per minute.

[26] Cyclic tests reported in Chapter 7 used a stroke rate of 3 and 6 in. per minute. The faster stroke rate was used for panels tested cyclically beyond 10 in. (20 in. peak to peak).

Table D-3. Cyclic test load protocol.

Load Step #	SAC-2		Modified SAC Amplitude
	Number of Cycles, n	Peak Deformation, θ (radians)	
1	6	0.00375	$0.75\delta_y$
2	6	0.005	$1.0\delta_y$
3	6	0.0075	$1.5\delta_y$
4	4	0.01	$2\delta_y$
5	2	0.015	$3\delta_y$
6	2	0.02	$4\delta_y$
7	2	0.03	$6\delta_y$
8	2	0.04	$8\delta_y$
9	2	0.05	$10\delta_y$
10	2	0.06	$12\delta_y$
11	2	0.07	$14\delta_y$
12	2	0.08	$16\delta_y$
13	2	0.09	$18\delta_y$
14	2	0.10	$20\delta_y$
15	2	0.11	$22\delta_y$
16	2	0.12	$24\delta_y$
17	2	0.13	$26\delta_y$
18	2	0.14	$28\delta_y$
19	2	0.15	$30\delta_y$
20	2	0.16	$32\delta_y$

Shear panel performance documentation

Shear panel performance from both monotonic and cyclic tests shall be documented in terms of load versus deflection plots (TSF versus DH). Cyclic tests plot load versus deflection to define load-versus-deflection hysteretic envelopes. Observations of panel performance and failure progression with respect to lateral displacement shall be documented in a spreadsheet format. Photographs that document these observations shall be included in the test report. Test results for each specimen tested shall be summarized in the format shown in Table D-4. Repeatability of panel performance of a given configuration is critical so that if only two cyclic tests are conducted, the poorest performance of the two shall form the basis for design. Therefore, special consideration shall be given to large variations in panel performance, especially failure type or displacement amplitude of each type of failure. Test procedures and results shall be documented in a test report.

Figure D-2. Modified SAC cyclic test time history, with δ_y = 0.4 in. and 6 in./min stroke rate.

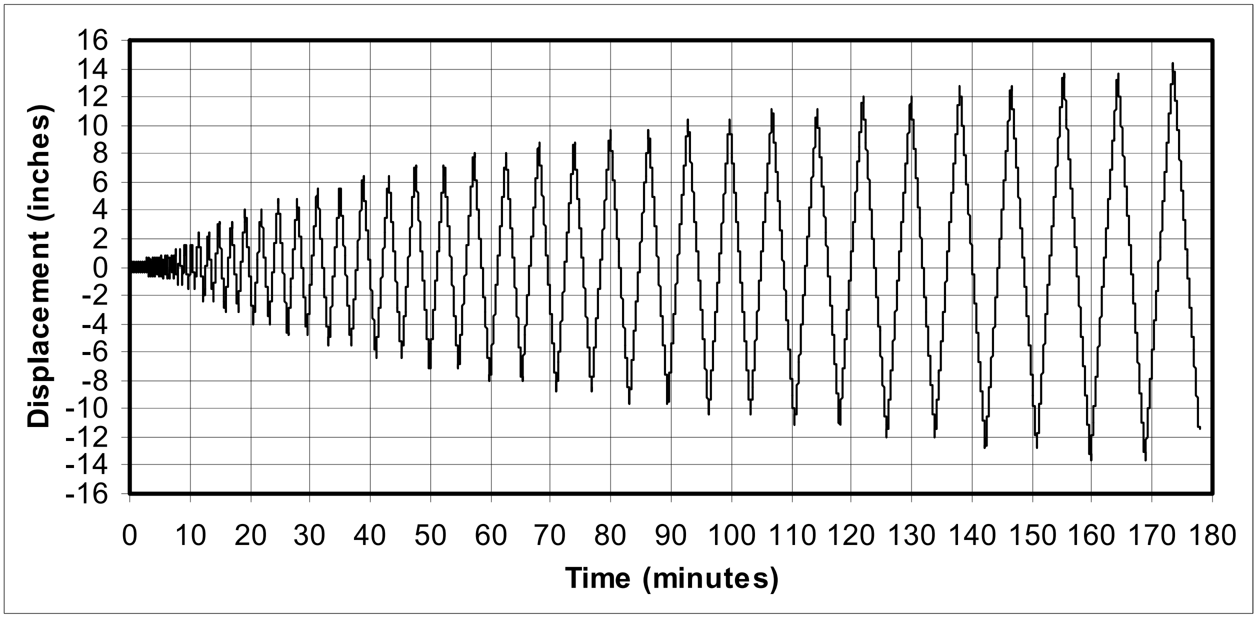

Table D-4. Summary of test panel performance (specified format).

Test Specimen	Load Type (Monotonic or Cyclic)	Load Rate (mm/min or in/min)	Linear Shear Stiffness (kN/mm) or (kips/in.)	Shear Load at δ_y Deflection (kip or kN)	Shear Deflection at Ultimate Shear Load (in. or mm)	Ultimate Shear Load (kip or kN)

Design recommendations

The measured load versus deflection data shall be used to define the design strength and stiffness of the shear panels. Resistance factors for each loading mechanism shall be defined that recognize the variation of the shear panel capacity. In other words, a panel shear capacity resistance factor, ϕ_v, shall reflect the variability of shear capacity of the tested panels. For example, ϕ_v = 0.9 if the strength variability is small and both mode and displacement of failures are consistent. The following criteria shall be defined from the shear panel cyclic test data:

1. The panel ductility, μ, the ultimate lateral deflection without loss of lateral or vertical load capacity, δ_u, over yield lateral deflection, δ_y, defined as follows:

$$\mu = \frac{\delta_u}{\delta_y} \quad \text{(Eq D2)}$$

2. The panel overstrength, Ω,[27] the maximum measured ultimate lateral panel capacity, Q_u, over the yield capacity, Q_y, defined as follows:

$$\Omega = \frac{Q_u}{Q_y} \quad \text{(Eq D3)}$$

3. The panel redundancy factor, ρ_1, of the individual shear panel tested[28]. This redundancy can be seen by comparing shear panel load/deflection data with coupon data, to determine if overstrength, Ω is due to strain hardening of the primary load-carrying element or due to the action of a secondary lateral load-resisting element. An example of this would be a panel with diagonal straps acting as the primary element with the columns effectively working to provide a significant moment frame. In this case the moment frame would provide redundancy for the shear panel. If the diagonal straps fail, this moment frame capacity would provide lateral resistance for the moment from the P-delta effect of the gravity load. This redundancy is critical to preventing building collapse for a structure whose lateral load-resisting system has failed. The panel redundancy factor, ρ_1 is calculated as follows:

$$\rho_1 = \frac{Q_u}{Q_p} = \frac{Q_p + Q_q}{Q_p} \quad \text{(Eq D4)}$$

where

Q_p = the portion of the shear panel ultimate lateral capacity carried by the primary lateral load-resisting element including the effects of strain hardening. For panels with full panel sheet(s), this contribution will increase with increasing deflection due to a widening of the panel tension field. This value can only be reasonably determined by measuring Q_c (as described below) and calculating Q_p as the difference between Q_u and Q_c.

Q_c = the portion of shear panel ultimate lateral capacity carried by the columns acting as moment frames. For panels with full

[27] This should not be confused with the system overstrength factor, Ω_0, as defined in ASCE 7-10 (ASCE 2010), Section 12.2.1.

[28] This should not be confused with the reliability factor, ρ or ρ_x, which is the extent of structural redundancy in the lateral-force-resisting system for an entire story of a building.

panel sheet(s), this value can only be obtained by testing the same exact panels with the full panel sheets removed. If these tests are not performed for full panel sheet shear panels, Q_c shall be set equal to zero.

4. The width of the cyclic test load/deflection hysteretic envelope. If the hysteretic envelope is significantly pinched (no or very little load resistance away from the peak excursions), much less energy is absorbed by the structural system so that building amplification grows. Pinched hysteretic envelopes occur when the primary lateral load-resisting element is stretched, and there is little redundant capacity from other elements to pick up load, so that little resistance is available away from the peak excursions of the load cycles. Panels with significantly pinched hysteretic envelopes, can experience high acceleration impact loading because the building will be free to sway with little resistance and then suddenly snap the lateral load-resisting element when another peak excursion is reached. This high acceleration snap can cause brittle failures. A shear panel with a great deal of redundancy within the panel, ρ_1 will tend to have a wide hysteretic envelope.

Table D-5 defines the acceptance criteria in terms of μ, Ω and ρ_1, based on data measured in the cyclic panel tests as defined by Equations D2 through D4.

Values for the system response modification coefficient, R; system overstrength factor, Ω_o; and deflection amplification factor, C_d, are defined in Table D-6. These values are used in the seismic design guidance defined in ASCE/SEI 7-10. Exceptions to these criteria shall require AISI approval or Corps of Engineers Headquarters (CEMP-ET) approval for Department of Defense construction.

Table D-5. Acceptance criteria for shear panels based on μ, Ω, and ρ_1.

Criteria	Acceptance Requirement
Panel ductility, μ	≥ 10
Panel overstrength, Ω	≥ 1.3
Panel redundancy factor, ρ_1	≥ 1.0
Hysteretic envelope width	Not required

Table D-6. Values for R, Ω_0, and C_d.

Factor	Value
System response modification coefficient, R	4
System overstrength factor, Ω_0	2
Deflection amplification factor, C_d	3.5